Rotational Properties of Two-Component Bose Gases

by

Marius Ladegård Meyer

Thesis submitted for the degree

Master of Science

Department of Physics
Faculty of Mathematics and Natural Sciences
University of Oslo

June 2013

Abstract

We study the rotational properties of a two-component Bose gas trapped in a rotating harmonic potential, effectively in two dimensions. We first consider a completely homogeneous interaction between particles, and assume the bosons to be in the lowest Landau level. We derive analytical expressions for some wave functions and energies at low angular momenta, and use these results together with exact numerical diagonalization results to test the applicability of composite fermion (CF) trial wave functions to the system. We find that a general procedure based on CF wave functions reproduces the exact ground states and many of the excited states for sufficiently low angular momenta, and give very good approximate results at angular momenta up to the two-component analogy of a single vortex. Additionally, we produce very simple CF states that have remarkably high overlaps with the lowest-lying states. Finally, we briefly discuss the case of inhomogeneous interactions, pointing out the difficulties arising from this generalization.

Acknowledgement

The thesis you are reading at this moment is the product of, like most master's theses, one year's worth of thinking, working, reading and writing. Of course, I have not travelled the road to a master's degree alone, and before we come to the interesting stuff (the physics) in this document, I would like to express my gratitude to the people that have made this year an interesting, stressful, funny and enjoyable one.

First of all, my heartfelt thanks to my supervisor and mentor Susanne Viefers. Your lectures in quantum physics in spring 2009 contributed immensely to both my knowledge of physics and my appetite for it. Having you as supervisor for the duration of my master's programme turned out to be one of the most positive factors in the year that has passed, and I have much enjoyed our numerous talks of academic as well as friendly nature. Also, the blazing speed at which you read and correct the drafts I send you is as impressive as it is helpful. Thank you for accepting me as your student. Secondly, I would like to thank Jainendra K Jain of Penn State University and Sreejith Ganesh Jaya of NORDITA, Stockholm for helping me with discussions and numerics. Our collaboration gave the project a great boost early on, and helped the work with this thesis take a fruitful direction. Sreejith's visit in November 2012 was particularly welcome. Thirdly, I am thankful for the helpful correspondence with Thomas Papenbrock, Uni. of Tennessee. Your swift and clear replies to e-mails from an unknown student are much appreciated. I would also like to thank the staff and my fellow students on the theoretical physics group, providing help in academic matters and frequents bouts of laughter during lunch breaks.

I must of course give a huge thank you to my best friends Simen L. Meyer, Pål Kvalnes and Alexander Hvaring, my mother Kirsten Ladegård and my father Morten L. Meyer and the rest of my very dear family. Thank you for the endless love, encouragement, patience and funny YouTube videos.

Most of all, a million thanks to my beautiful girlfriend and fiancée Anna Li. Your understanding, kindness, patience and love continues to overwhelm me. You are the love of my life.

Marius Ladegård Meyer, June 2013, Oslo.

Contents

Chapter 1

Introduction

In condensed matter physics, the classical objects of study are solids and liquids. The advent of quantum physics together with the marvelous technological progress in the 20th century has directed our attention to more exotic condensed states, such as superfluids, superconductors, Bose-Einstein condensates and low-dimensional electronic systems, to name a few. The building blocks of these systems are electrons, ions, atoms and "emergent particles" such as phonons and Cooper pairs. Particles in three dimensions can always be characterized by the fact that they are either fermions or bosons. Usually many-body systems of fermions have dramatically different behaviors than their bosonic counterparts, because of the Pauli principle. However, this is not always the case in low-dimensional systems. Some emergent particles are *anyons*, whose statistics are in a sense in between fermionic and bosonic statistics. Another fact of low-dimensional systems is that many-body systems of bosons and fermions don't necessarily behave so differently in all cases. We will point out an interesting connection between bosons rotating in a harmonic trap, and fermions moving in a magnetic field, when the two systems are confined to move in two dimensions. This connection has received much interest in the last two decades [1-4], both theoretically and experimentally. One of the main reasons why these are very interesting systems to study is that they show many exotic and fascinating phenomena that are inherently quantum-physical. Additionally, these phenomena are often either realizable in current experiments or foreseen to be realized in the near future, *and* there exist both approximate and even some exact analytical theoretical results.

One consequence of the quantum mechanical nature of rotating bosons in a trap is the formation of quantized vortices in the fluid [4-6]. The first experimental observation of a quantized vortex in a Bose-Einstein condensate occurred in 1999 at the JILA group [5], the same place where the first gaseous Bose-Einstein condensate was realized experimentally, in 1995 [7]. The vortex was produced in a system of ^{87}Rb, where two different internal spin states were manipulated to create the desired vortex wave function. In other words, the first vortex was observed in a *two-component system*. Such systems will be the topic of this thesis. The theoretical work treating rotating bosons has until now mostly dealt with a single species of bosons for simplicity. This topic will be covered in Chapter 2. We will then generalize some of these results, inspired by the recent paper [8], in Chapter 3.

In this thesis we will study the system of two-component rotating bosons by three means: analytical calculations, exact numerical diagonalization and by using trial wave functions. An emphasis will be put on the comparison of exact analytical results and the trial wave functions: the reason is that we will employ a method of constructing trial wave functions

that *a priori* was not designed to apply to bosons. Instead, the trial wave functions we will use are *composite fermion trial wave functions* [9,10], developed by Jainendra Jain to understand the (fractional) quantum Hall effect. We give an introduction to this topic in Chapter 4. As mentioned above, it may seem strange to use trial wave functions tailored for fermions when studying rotating bosons. Additionally, we will focus on rotation at low angular momenta, whereas the fermions in the quantum Hall regime typically have high angular momenta because of a strong external magnetic field. Recent work [11-14] has shown that, despite the arguments just presented, the composite fermion wave functions give faithful representations of the exact states for rotating *one-component* bosons at both high and low angular momenta. We want to analyze their applicability to the two-component case: this is done in Chapter 5 for a homogeneous interaction between bosons. By homogeneous we mean that inter- and intra-species interactions are equal in strength. Finally, we give a brief discussion on inhomogeneous interactions in Chapter 6.

While completing the work presented in this document we became aware of a very recent manuscript [29] applying CF wave functions to two-component rotating bosons in the high angular momenta (fractional quantum Hall) regime. To the best of our knowledge these are the first two times that CF has ever been used to study two-component rotating bosons.

Chapter 2

Non-interacting Bose gas

The purpose of this thesis is as stated earlier to study two species of bosons interacting with each other in a trap. However, much of the language, notation and concepts needed for a fruitful study of such a system is most easily attained by first concentrating on a *one-species gas*, where all the particles in the gas are of the same type. In this chapter we will study such a one-species gas of particles. We will present some basics concerning the statistics of bosons leading to the prediction of Bose-Einstein condensation. We will derive the many-body wave functions for a non-interacting, rotating Bose-Einstein condensate confined in a harmonic trap, where the motion becomes essentially two-dimensional. Finally we discuss the *yrast* states of the condensate.

2.1 Bose-Einstein statistics

In quantum mechanics, the concept of truly *identical* particles appears when one tries to construct many-body wave functions from single-particle ones. A two-body wave function describing identical particles must have the property that

$$|\Psi(\mathbf{r}_1, \chi_1, \mathbf{r}_2, \chi_2)|^2 = |\Psi(\mathbf{r}_2, \chi_2, \mathbf{r}_1, \chi_1)|^2 \tag{2.1.1}$$

i.e. the property that an exchange of the two particles (positions and spins) does not change probability amplitudes. In three-dimensional space, this means that the wave function itself must either be fully symmetric or fully anti-symmetric with respect to particle interchange [15]. Particles of the first kind are bosons, and particles of the second kind are fermions. In addition, the spin-statistics theorem of relativistic quantum field theory tells us that bosons are particles with integer spins, while fermions have half-integer spins. Because of the antisymmetry of wave functions describing fermions, we have the Pauli exclusion principle: No two fermions can occupy the same single-particle state. However, there is no such restriction for bosons: there can be any number n of bosons occupying a single-particle state. Normally, this makes systems of bosons behave very differently from systems of fermions under similar conditions.

From statistical mechanics, we know that a system of quantum particles in thermal equilibrium can be described by the grand partition function Ξ of its available states. For a system of bosons, each with single-particle states of energy ϵ_ν available, the grand partition function is [16]

$$\Xi = \sum_{n=0}^{\infty} e^{-n\beta(\epsilon_\nu - \mu)} = \frac{1}{1 - e^{-\beta(\epsilon_\nu - \mu)}} \tag{2.1.2}$$

Here, $\beta = 1/kT$ is the well-known factor containing the temperature dependence, μ is the chemical potential, and we have used the fact that the series must converge in order to have well-defined occupational probabilities. The average number of particles in the state with energy ϵ_ν is

$$\bar{n} = \sum_{n=0}^{\infty} n e^{-n\beta(\epsilon_\nu - \mu)} = \sum_{n=0}^{\infty} n e^{-nx} = -\frac{1}{\Xi}\frac{\partial \Xi}{\partial x} = \frac{1}{e^{-\beta(\epsilon_\nu - \mu)} - 1} \tag{2.1.3}$$

Now, let the lowest energy state have energy ϵ_0. The convergence of the series in (2.1.2) means that we must have $\epsilon_0 > \mu$. Thus, an excited single-particle state at energy ϵ_ν can at most have mean occupation

$$\bar{n}_{max} = \frac{1}{e^{\beta(\epsilon_\nu - \epsilon_0)} - 1} \tag{2.1.4}$$

while the ground state can accommodate arbitrarily many bosons. Typically μ increases as T decreases, so at a certain temperature T_c the temperature will be so low that μ is very close to ϵ_0, and only a few bosons occupy the excited states: the rest have condensed to the lowest-lying state. In this case, we speak of a Bose-Einstein condensate.

It can be shown [17] that the critical temperature T_c at which the free non-interacting Bose gas condenses is zero if the gas is two-dimensional. However, when the gas is trapped in a harmonic oscillator potential, T_c is finite and non-zero, but usually very small. In the next section I will discuss the behavior of a rotating Bose gas in such a potential. We will not consider the effects of finite temperature in this thesis, but focus on the many-body quantum eigenstates of the system themselves.

2.2 Rotating trapped Bose gas

Let's first define the trap in which our bosons will be placed. A *harmonic trap* is a trap subjecting the particles in it to a potential of the form

$$V(\mathbf{r}) = \frac{1}{2}M(\omega_1^2 x^2 + \omega_2^2 y^2 + \omega_3^2 z^2) \tag{2.2.1}$$

where M is the mass of the particles and the ω_i are the classical oscillator frequencies in the three spatial directions defined by a Cartesian coordinate system. Imagine now N spinless bosons of mass M in such a harmonic trap. Further, assume $\omega_1 = \omega_2 = \omega_3 = \omega$. Then, the Hamiltonian for the system would be

$$H = \sum_{i=1}^{N} \left(\frac{\mathbf{p}_i^2}{2M} + \frac{1}{2}M\omega^2 \mathbf{r}_i^2 \right) \tag{2.2.2}$$

Now, we will rotate the trap around the z-axis at angular frequency Ω. In a rotating reference frame following the trap, the Hamiltonian would now be

$$H = \sum_{i=1}^{N} \left(\frac{\mathbf{p}_i^2}{2M} + \frac{1}{2}M\omega^2 \mathbf{r}_i^2 - \Omega(L_z)_i \right) = \sum_{i=1}^{N} H_i \tag{2.2.3}$$

Here $\sum_{i=1}^{N}(L_z)_i = \sum_{i=1}^{N} xp_y - yp_x$ is the total angular momentum operator in the z direction. Since the particles are (for now) non-interacting, we consider the single-particle

Hamiltonian H_i in the following. It can be rewritten as follows:

$$\begin{aligned} H_i &= \left(\frac{\mathbf{p}_i^2}{2M} + \frac{1}{2}M\omega^2\mathbf{r}_i^2 - \Omega L_z\right) \\ &= \frac{1}{2M}\Big(p_x^2 + (M\omega)^2x^2 - 2M\omega x p_y + 2M\omega x p_y \\ &\quad + p_y^2 + (M\omega)^2y^2 - 2M\omega y p_x + 2M\omega y p_x + p_z^2 + (M\omega)^2z^2 - 2M\Omega L_z\Big) \\ &= \frac{1}{2M}\Big(p_x^2 + 2M\omega y p_x + (M\omega)^2y^2 + p_y^2 - 2M\omega x p_y + (M\omega)^2x^2 \\ &\quad + 2M\omega(x p_y - y p_x) + p_z^2 + (M\omega)^2z^2 - 2M\Omega L_z\Big) \end{aligned} \tag{2.2.4}$$

where $x, y, z, p_x, p_y, p_z, L_z$ all refer to particle i. Now let $A_x = -M\omega y$, $A_y = M\omega x$, so that

$$\begin{aligned} H_i &= \frac{1}{2M}\left[(p_x - A_x)^2 + (p_y - A_y)^2\right] + \left[\frac{p_z^2}{2M} + \frac{1}{2}M\omega^2z^2\right] + \omega L_z - \Omega L_z \\ &= H_\parallel + H_z + H_\Omega \end{aligned} \tag{2.2.5}$$

The first part of the Hamiltonian,

$$H_\parallel = \frac{1}{2M}\left[(p_x - A_x)^2 + (p_y - A_y)^2\right] = \frac{1}{2M}(\mathbf{p} - \mathbf{A})_\parallel^2 \tag{2.2.6}$$

should be familiar from classical mechanics; it resembles the Hamiltonian of a charged particle moving in a magnetic field $\mathbf{B} = \nabla \times \mathbf{A} = 2M\omega\mathbf{z}$ where $\mathbf{z}$ is a unit vector in the z direction. Classically, $\mathbf{B}$ is the observable field and $\mathbf{A}$ is a handy mathematical quantity in calculations. We know that the condition $\mathbf{B} = \nabla \times \mathbf{A}$ does not uniquely determine $\mathbf{A}$ for a given $\mathbf{B}$; we can choose a *gauge* of our liking. Our choice of $\mathbf{A} = (-M\omega y, M\omega x)$ is known as the symmetric gauge. However, note that $H_\parallel$ contains only the coordinates x and y and thus is equal to a Hamiltonian describing a charged particle *in two dimensions.* It is this Hamiltonian, along with a term describing interactions, that lies at the core of the quantum Hall effect. This similarity will be of high importance in the subsequent chapters. The one-body energy spectrum of $H_\parallel$ is well known [1,9]: the energies form so-called *Landau levels* with energies

$$E_n = (n + \frac{1}{2})2\hbar\omega \tag{2.2.7}$$

where $n \in \{0, 1, 2, ...\}$ is known as the Landau level index. The H_z part is on the other hand just a one-dimensional harmonic oscillator Hamiltonian in the z direction, and the last part is

$$H_\Omega = (\omega - \Omega)L_z \tag{2.2.8}$$

Since the problem involves a harmonic oscillator potential, it is natural to define two operators conjugate to each other, $a, a^\dagger$, that act as lowering and raising operators between Landau levels. Let $\boldsymbol{\pi} = (\mathbf{p} - \mathbf{A})_\parallel$ such that

$$H_\parallel = \frac{\boldsymbol{\pi}^2}{2M} \tag{2.2.9}$$

is the one-particle Landau part of the Hamiltonian. Taking inspiration from the one-dimensional harmonic oscillator, we want to arrive at the form

$$H_\parallel = \left(a^\dagger a + \frac{1}{2}\right)\hbar\omega_0 \tag{2.2.10}$$

and the operators

$$a = C(\pi_x + i\pi_y) \qquad a^\dagger = C(\pi_x - i\pi_y) \tag{2.2.11}$$

can be seen to accomplish this for a certain value of C. It is easiest to calculate C from the well known commutation relation $[a, a^\dagger] = 1$:

$$\begin{aligned}
[a, a^\dagger] &= C^2[\pi_x + i\pi_y, \pi_x - i\pi_y] \\
&= -2iC^2[\pi_x, \pi_y] \\
&= -2iC^2[p_x + M\omega y, p_y - M\omega x] \\
&= -2iC^2(2M\omega i\hbar)
\end{aligned} \tag{2.2.12}$$

The last step follows the canonical commutation relations $[x, p_x] = [y, p_y] = i\hbar$. We find

$$[a, a^\dagger] = 1 \quad \Longrightarrow \quad C = (4M\omega\hbar)^{-1/2} \tag{2.2.13}$$

Inserting this back into (2.2.10) gives

$$\begin{aligned}
H &= \left(C^2(\pi_x - i\pi_y)(\pi_x + i\pi_y) + \frac{1}{2}\right)\hbar\omega_0 \\
&= \left(C^2(\pi_x^2 + \pi_y^2 + i[\pi_x, \pi_y] + \frac{1}{2}\right)\hbar\omega_0 \\
&= \left(C^2\boldsymbol{\pi}^2 + \frac{-2M\omega\hbar}{4M\omega\hbar} + \frac{1}{2}\right)\hbar\omega_0 \\
&= \frac{\boldsymbol{\pi}^2\hbar\omega_0}{4M\omega\hbar} \\
&= \frac{\boldsymbol{\pi}^2}{2M}
\end{aligned} \tag{2.2.14}$$

thus we must have $\omega_0 = 2\omega$. The lowest energy state $|n = 0\rangle$ is found by the requirement $a\,|0\rangle = 0$. The energy is $E_0 = \hbar\omega$ because

$$H_\parallel\,|0\rangle = 2\hbar\omega\left(a^\dagger a\,|0\rangle + \frac{1}{2}\,|0\rangle\right) = 2\hbar\omega\left(0 + \frac{1}{2}\,|0\rangle\right) = \hbar\omega\,|0\rangle \tag{2.2.15}$$

The other energies are found by applying $H_\parallel$ to states raised from $|0\rangle$ by the raising operator $a^\dagger$. The energy spectrum one gets in this fashion confirms (2.2.7).

2.3 The lowest Landau level

Our goal will be to find the lowest-lying states for any given total angular momentum. Another way of saying this is to find the states of maximum total angular momentum for a given energy: these are termed the *yrast states* after the Swedish word meaning "dizziest". Thus, we will assume that the particles are in a state that minimizes the energy contributions from both the oscillator in the z direction, and the Landau part of the Hamiltonian. The harmonic oscillator term in the z direction reduces to an unimportant constant which we will ignore, and the full Hamiltonian now only contains the x and y coordinates: the problem has become two-dimensional. Experimentally, this can also be achieved by increasing the oscillator frequency in the z direction, w_3, to a much larger

value, making excitations in the z direction prohibitively expensive. From now on we will take the one-particle Hamiltonian to be

$$H_i = H_{\parallel} + H_{\Omega} = \left(a^{\dagger}a + \frac{1}{2}\right) 2\hbar\omega + (\omega - \Omega)L_z \tag{2.3.1}$$

and we seek the eigenfunctions and eigenvalues of this operator.

In dealing with two-dimensional quantum systems it is often useful to work with a pair of complex conjugate coordinates instead of Cartesian ones. Since we don't need the Cartesian z component any longer, we redefine z to mean

$$z = x + iy \tag{2.3.2}$$

and work with this and its complex conjugate $\bar{z} = x - iy$ in place of x and y. We will continue to use L_z for the angular momentum in the direction of the rotational axis of the trap, since we don't foresee any confusion arising from this. We thus need the replacements

$$x = \frac{1}{2}(z + \bar{z}) \qquad y = \frac{1}{2i}(z - \bar{z}) \tag{2.3.3}$$

$$p_x = -i\hbar\frac{\partial}{\partial x} = -i\hbar\left(\frac{\partial z}{\partial x}\frac{\partial}{\partial z} + \frac{\partial \bar{z}}{\partial x}\frac{\partial}{\partial \bar{z}}\right) = -i\hbar\left(\frac{\partial}{\partial z} + \frac{\partial}{\partial \bar{z}}\right) \tag{2.3.4}$$

$$p_y = -i\hbar\frac{\partial}{\partial y} = -i\hbar\left(\frac{\partial z}{\partial y}\frac{\partial}{\partial z} + \frac{\partial \bar{z}}{\partial y}\frac{\partial}{\partial \bar{z}}\right) = \hbar\left(\frac{\partial}{\partial z} - \frac{\partial}{\partial \bar{z}}\right) \tag{2.3.5}$$

We can now work out the operators a and L_z as follows:

$$\begin{aligned} a &= C(\pi_x + i\pi_y) \\ &= C\left(p_x + M\omega y + i(p_y - M\omega x)\right) \\ &= -iC\left(2\hbar\frac{\partial}{\partial \bar{z}} + M\omega z\right) \end{aligned} \tag{2.3.6}$$

$$\begin{aligned} L_z &= xp_y - yp_x \\ &= \frac{1}{2}(z + \bar{z})\hbar\left(\frac{\partial}{\partial z} - \frac{\partial}{\partial \bar{z}}\right) + \frac{1}{2i}(z - \bar{z})(-i\hbar)\left(\frac{\partial}{\partial z} + \frac{\partial}{\partial \bar{z}}\right) \\ &= \hbar\left(z\frac{\partial}{\partial z} - \bar{z}\frac{\partial}{\partial \bar{z}}\right) \end{aligned} \tag{2.3.7}$$

To study the yrast states, we now impose the restriction that the particle wave functions live in the lowest Landau level, hereby denoted the LLL. This means that, for a wave function in coordinate basis:

$$\begin{aligned} a\psi(z, \bar{z}) &= 0 \\ -iC\left(2\hbar\frac{\partial}{\partial \bar{z}} + M\omega z\right)\psi(z, \bar{z}) &= 0 \end{aligned} \tag{2.3.8}$$

If we make the ansatz

$$\psi(z, \bar{z}) = \phi(z, \bar{z})\exp(-\frac{M\omega}{2\hbar}z\bar{z}) \tag{2.3.9}$$

then we see that the LLL requirement reduces to

$$\begin{aligned} \left(2\hbar\frac{\partial\phi}{\partial \bar{z}}\exp(-\frac{M\omega}{2\hbar}z\bar{z}) - M\omega z\phi(z, \bar{z})\exp(-\frac{M\omega}{2\hbar}z\bar{z})\right) \\ +M\omega z\phi(z, \bar{z})\exp(-\frac{M\omega}{2\hbar}z\bar{z}) = 0 \end{aligned} \tag{2.3.10}$$

or simply put

$$\frac{\partial}{\partial \bar{z}}\phi(z,\bar{z}) = 0 \tag{2.3.11}$$

This is the condition of analyticity of complex functions, equivalent to the Cauchy-Riemann equations. It means that we can think of ϕ as a function of only one variable z, instead of two variables x *and* y or z *and* $\bar{z}$.

Now that we have found the condition ψ must satisfy in order to live in the LLL, we turn to the other part of (2.3.1): the angular momentum part. The important fact is that the first and second parts of the Hamiltonian (2.3.1) commute. To see this, remember that

$$H_{\parallel} = \frac{\boldsymbol{\pi}^2}{2M} = \frac{1}{2M}(\pi_x^2 + \pi_y^2) \tag{2.3.12}$$

From this and the replacement rules (2.3.3-2.3.7) we get

$$[\pi_x, L_z] = -i\hbar\pi_y \qquad [\pi_y, L_z] = i\hbar\pi_x \tag{2.3.13}$$

$$\begin{aligned}[\pi_x^2, L_z] &= \pi_x[\pi_x, L_z] + [\pi_x, L_z]\pi_x \\ &= \frac{1}{i\hbar}[\pi_y, L_z](-i\hbar\pi_y) + (-i\hbar\pi_y)\frac{1}{i\hbar}[\pi_y, L_z] \\ &= -[\pi_y^2, L_z]\end{aligned} \tag{2.3.14}$$

$$\begin{aligned}[H_{\parallel}, H_{\Omega}] &= \frac{\omega - \Omega}{2M}[\pi_x^2 + \pi_y^2, L_z] \\ &\propto [\pi_x^2, L_z] + [\pi_y^2, L_z] \\ &= 0\end{aligned} \tag{2.3.15}$$

We can therefore conclude that there exist simultaneous eigenstates of the two parts of the Hamiltonian! Now we can simply look for the eigenstates of L_z within the LLL. We combine (2.3.7) and (2.3.9) to get

$$\begin{aligned}L_z\phi(z)\exp(-\frac{M\omega}{2\hbar}z\bar{z}) &= \hbar\left(z\frac{\partial}{\partial z} - \bar{z}\frac{\partial}{\partial \bar{z}}\right)\phi(z)\exp(-\frac{M\omega}{2\hbar}z\bar{z}) \\ &= \hbar\left(z\frac{\partial\phi}{\partial z} - \frac{M\omega}{2\hbar}z\bar{z}\phi\right)\exp(-\frac{M\omega}{2\hbar}z\bar{z}) \\ &- \hbar\left(\bar{z}\frac{\partial\phi}{\partial \bar{z}} - \frac{M\omega}{2\hbar}z\bar{z}\phi\right)\exp(-\frac{M\omega}{2\hbar}z\bar{z}) \\ &= \hbar\left(z\frac{\partial\phi}{\partial z} - \bar{z}\frac{\partial\phi}{\partial \bar{z}}\right)\exp(-\frac{M\omega}{2\hbar}z\bar{z}) \\ &= \exp(-\frac{M\omega}{2\hbar}z\bar{z})L_z\phi(z)\end{aligned} \tag{2.3.16}$$

An important observation to make here is the fact that L_z does not "see" the exponential part of ψ. The LLL requirement was that

$$\frac{\partial}{\partial \bar{z}}\phi(z,\bar{z}) = 0 \tag{2.3.17}$$

The two last lines of (2.3.16) then leave us with

$$L_z\phi = \hbar z\frac{\partial}{\partial z}\phi \tag{2.3.18}$$

The unnormalized eigenfunctions in this equation are clearly powers of z:

$$\phi_m(z) = z^m \tag{2.3.19}$$

and we get

$$L_z\phi_m = L_z z^m = \hbar z m z^{m-1} = \hbar m z^m \tag{2.3.20}$$

where we from now on use the conventional notation m as the quantum number for L_z.

In summary, we have found that the single-particle eigenstates of the Hamiltonian (2.3.1) with good angular momentum $\hbar m$ in the LLL are

$$\psi_m(z,\bar{z}) = N_m z^m \exp(-\frac{M\omega}{2\hbar} z\bar{z}) \tag{2.3.21}$$

where N_m is a normalization factor that we will give minimal attention in this thesis: we will mostly be working with unnormalized wave functions throughout. By applying the raising operator $a^\dagger$ to such a state, one can see that the power m is shifted by 1: evidently $m \in \mathbb{Z}$. Since negative m would give a non-normalizable wave function, the possible values for m are $m = 0, 1, 2, \ldots$ The many-body wave function of N bosons at total angular momentum $\sum_i (L_z)_i = \hbar \sum_i m_i \equiv \hbar L$ is then a homogeneous, symmetric polynomial of total degree L in the particle coordinates z_i times the exponential factor $\exp(-\frac{M\omega}{2\hbar}\sum_{i=1}^N z_i\bar{z}_i)$. These are the kind of wave functions we will be studying for the majority of this thesis. We will normally drop the factor $\hbar$ in the eigenvalues of $\sum_i (L_z)_i$ and simply talk of angular momentum as the dimensionless number L.

There exist analytical expressions for the states in higher Landau levels as well; we will see in Chapter 4 that we need them in order to construct trial wave functions with the correct angular momentum. These can be found either by using the ladder operators (2.2.11), or by solving the Schrödinger equation directly. We will only quote the result [1,9] here:

$$\psi_{n,m}(z,\bar{z}) = N_{n,m} z^m L_n^m\left(\frac{M\omega}{\hbar} z\bar{z}\right) \exp(-\frac{M\omega}{2\hbar} z\bar{z}) \tag{2.3.22}$$

where L_n^m is the associated Laguerre polynomial

$$L_n^m(x) = \sum_{k=0}^{n} (-1)^k \binom{n+m}{n-k} \frac{x^k}{k!} \tag{2.3.23}$$

and $n = 0, 1, \ldots$ is the Landau level index. The possible values of the quantum number m are $m = -n, -n+1, \ldots$ in the n'th Landau level. The possible single particle states can be visualized using the following diagram

	3	–	–	–	–	–	–
	2		–	–	–	–	–
n	1			–	–	–	–
	0				–	–	–
		−3	−2	−1	0	1	2
				m			

(2.3.24)

The dashes signify possible single particle states. For instance, the state $\psi_{2,-1}(z,\bar{z})$ corresponds to the diagram

	3	–	–	–	–	–	–
	2		–	♦	–	–	–
n	1			–	–	–	–
	0				–	–	–
		−3	−2	−1	0	1	2
				m			

(2.3.25)

2.4 The filling factor

How many single-particle states are there in a given area of the plane? If we write

$$|\psi_m(z,\bar{z})|^2 = \overline{\psi_m}\psi_m = |N_m|^2(z\bar{z})^m \exp(-\frac{2M\omega}{2\hbar}z\bar{z}) = |N_m|^2 r^{2m}\exp(-\frac{M\omega}{\hbar}r^2) \quad (2.4.1)$$

then we can take the value of r that maximizes this distribution as a crude estimate for the radius of the circular area in which the LLL states live. We find

$$\begin{aligned}
\frac{\partial}{\partial r}\left(|\psi_m(r)|^2\right) &= 0 \\
\frac{\partial}{\partial r}\left(N_m^2 r^{2m}\exp(-\frac{M\omega}{\hbar}r^2)\right) &= 0 \\
\left(2mr^{2m-1} - r^{2m}2\frac{M\omega}{\hbar}r\right)\exp(-\frac{M\omega}{\hbar}r^2) &= 0 \\
mr^{2m-1} &= \frac{M\omega}{\hbar}r^{2m+1} \\
\frac{\hbar m}{M\omega} &= r^2 \\
r &= \sqrt{\frac{\hbar m}{M\omega}}
\end{aligned}$$

Using this estimate, the increase in area going from the state ψ_m to the state ψ_{m+1} is

$$\Delta A = \pi\left(\frac{\hbar(m+1)}{M\omega} - \frac{\hbar m}{M\omega}\right) = \frac{2\pi\hbar}{2M\omega} = \frac{h}{2M\omega} \quad (2.4.2)$$

Equivalently, we say that the density of states per area is

$$n_s = \frac{2M\omega}{h} \quad (2.4.3)$$

A related quantity, which will be crucial in the discussions of the Chapter 4, is known as the *filling factor*. It is defined as the number density n of the particles of the sample, divided by the density of states per area:

$$\nu = \frac{n}{n_s} = \frac{nh}{2M\omega} \quad (2.4.4)$$

2.5 The road ahead

So far we have treated a single species of bosons that rotate while trapped in a harmonic oscillator potential. We have completely neglected interactions between the bosons, and found that their kinetic energy is quantized into Landau levels. This is the case also for fermions in two dimensions when they are subjected to an external magnetic field, which is one of the main things we will exploit in this thesis. Our task now will be to address two issues: the first is the fact that N bosons in a trap are rarely non-interacting. The second issue is that the goal of this thesis is to study how *two types of bosons* behave when trapped and rotated. In the next chapter, we will follow the work of Papenbrock, Reimann & Kavoulakis [8,18] to derive analytical expressions for some of the low-lying wave functions and energies when a two-species Bose gas is *weakly interacting*.

Chapter 3

Interacting two-species Bose gas

This chapter will be devoted to deriving exact, analytical expressions for wave functions and energies of some of the low-lying states of a *two-species* Bose gas. The two species of the gas could be different kinds of atoms, different isotopes of the same atom, or they could be different internal states of the condensate, like particles of different spin. We will incorporate weak, repulsive two-body interactions into the Hamiltonian describing the system, and end up with the ground states and some of the excited states of the gas. This chapter is mainly a presentation of the results that T. Papenbrock, S. M. Reimann and G. M. Kavoulakis published in the 2012 paper *Condensates of p-wave pairs are exact solutions for rotating two-component Bose gases* [8]. However, I will more closely follow the presentation as it appeared in the first version of the paper [18].

3.1 Model for the interaction

Let us clarify at once the assumptions that we will make and the restrictions they will place on the states that we will discuss in this chapter. We will study a harmonically trapped two-component Bose gas. There will be N bosons of a first species and M bosons of a second species, where $N \leq M$. Their positions will be described by the complex numbers $z = x + iy$ for the first species and $w = u + iv$ for the second. We will assume that the gas is sufficiently dilute to be confined to the lowest Landau level at all total angular momenta $L = \sum_i m_i = 0, \ldots, N+M$ even in the presence of interactions; in other words, the bosons will be *weakly interacting*. This range of low angular momenta has been quite extensively studied for one species, see for instance [12,13,19]. In this literature, the ground state for $L = N$ is called the *single vortex state*. We will be studying angular momentum up to the two-species analogue of the "single vortex" $L = N+M$. Note that the assumption that all particles are in the LLL might not be valid in present day experiments at the low angular momenta discussed here: for the gas to become dilute enough for the assumption to hold, the rotational frequency of the trap Ω must be extremely close to the deconfinement limit of the trap. [1] cites that the entrance to the LLL regime typically occurs at $\Omega \simeq 0.98\omega$. If we think of Ω as fixed instead of L, which is a more natural view to take in an experimental setting, then the total angular momentum will typically be higher than the range considered here. However, recent experimental work [20] claims to achieve LLL for as few as 4 particles in our angular momentum range, giving hope to the realizability of the theory presented here. For simplicity, we will simply take the LLL-assumption as a prerequisite in this thesis.

When the bosons satisfy the above criteria, the many-body wave functions will be of the form found in the last chapter:

$$\Psi = F(z,w)\exp\left(-\frac{M\omega}{2\hbar}\left(\sum_{i=1}^{N}|z_i|^2+\sum_{j=1}^{M}|w_j|^2\right)\right) \tag{3.1.1}$$

where $F(z,w) = F(z_1, z_2, \ldots, z_N, w_1, w_2, \ldots, w_M)$ is a homogeneous symmetric polynomial in all the coordinates z and w. To be sure that we can indeed talk about a sharp total angular momentum L, we need to check that the interaction energy operator commutes with the angular momentum. In this thesis we will mostly be interested in the contact interaction between pairs of bosons, modeled by a delta-function potential. In [19], the authors show that interactions of the form

$$V = g\sum_{m=0}^{\infty} v_m V_m = g\sum_{m=0}^{\infty} v_m (z_i - z_j)^m (\partial_{z_i} - \partial_{z_j})^m \tag{3.1.2}$$

represent a quite large class of two-body interactions for one-species gases, with different interactions having different v_m. The energy scale of the interaction is g, and $\partial_{z_i} = \frac{\partial}{\partial z_i}$. By comparing matrix elements with the usual representation of delta-function interaction

$$V = 2\pi g\delta(\mathbf{r}_i - \mathbf{r}_j) \tag{3.1.3}$$

they find

$$v_m = \frac{(-1/2)^m}{m!} \tag{3.1.4}$$

It can be shown that Coloumb interaction and repulsive dipole interaction are also of the form (3.1.2).

Generalizing the interaction (3.1.2) to the two-component gas is straightforward: we will use

$$V = \sum_{m=0}^{L} v_m V_m = \sum_{m=0}^{L} v_m (A_m + B_m + C_m) \tag{3.1.5}$$

with

$$\begin{aligned} A_m &= \sum_{1\le i<j\le N} (z_i - z_j)^m (\partial_{z_i} - \partial_{z_j})^m \\ B_m &= \sum_{1\le i<j\le M} (w_i - w_j)^m (\partial_{w_i} - \partial_{w_j})^m \\ C_m &= \sum_{1\le i\le N}\sum_{1\le j\le M} (z_i - w_j)^m (\partial_{z_i} - \partial_{w_j})^m \end{aligned} \tag{3.1.6}$$

being the interactions between pairs of the first species, second species, and inter-species respectively. Notice that we have set the unit of energy equal to the interaction energy scale, $g = 1$, and also assumed *equal interaction strength* between all particle pairs, inter- and intra-species. We will use the term *homogeneous interaction* for the case of equal interaction strength in this thesis. We only need $m \le L$ in the sum, because we will only be acting on homogeneous polynomials F of degree L: the operators (3.1.6) act on pairs of particles x_i, x_j, and the highest powers a pair of coordinates in a term in F can have are $x_i^\lambda x_j^{L-\lambda}$. The operators (3.1.6) clearly annihilate such terms and terms of lower single-particle angular momenta when $m > L$.

The reasons for writing the interaction on the form (3.1.5-3.1.6) can now be seen. Firstly, the interaction indeed commutes with the total angular momentum. This is because the parts (3.1.6) preserve the angular momentum (total degree) of whatever polynomial it acts on, meaning that a polynomial eigenfunction of L turns into another polynomial with the same eigenvalue of L. Thus we can conclude that the degree of F still gives the total angular momentum L, just like in the last chapter. Secondly, the interaction is *translationally invariant*, because only differences between coordinates and derivatives appear. This will give us a simplifying condition for the trial wave functions in the next chapter. Thirdly, we can discard the exponential part of (3.1.1) in the following discussion and only consider the polynomial part $F(z, w)$. This follows from the observation we made in Section 2.3, that the angular momentum operators do not act on the exponentials on the wave functions in the LLL. In other words, the exponentials are fixed solely by the Landau level quantization. The chapter will thus be devoted to finding homogeneous polynomials $F(z, w)$ that are eigenfunctions of (3.1.5).

3.2 A basis for $F(z, w)$

To proceed, we want a basis in which we can express the solutions $F(z, w)$. A naive choice is the set of all monomials $\{\prod_{i=1}^{N}\prod_{j=1}^{M} z_i^{p_i} w_j^{q_j}\}$ one could use to construct a polynomial of the correct total degree $\sum_{i,j} p_i + q_j = L$. However, a much more clever choice would incorporate the fact that we are dealing with bosons: $F(z, w)$ needs to be totally symmetric when two particles of type z or two particles of type w are interchanged. One such type of function that is symmetric with respect to any interchange of its arguments is known as *elementary symmetric polynomials* [8,11,21]. They are given by

$$e_\lambda(x) \equiv e_\lambda(x_1, x_2, \ldots, x_n) = \sum_{1 \le i_1 < \ldots < i_\lambda \le n} x_{i_1} x_{i_2} \cdots x_{i_\lambda} \tag{3.2.1}$$

for $1 \le \lambda \le n$. We define $e_0(x) = 1$. For example, the symmetric polynomial of degree three in $\{z\} = z_1, z_2, z_3, z_4$ is

$$e_3(z) = z_1 z_2 z_3 + z_1 z_2 z_4 + z_1 z_3 z_4 + z_2 z_3 z_4 \tag{3.2.2}$$

It obviously has the desired symmetry, is homogeneous and only contains evenly distributed powers of variables. There is also a very powerful theorem [21] that states that any homogeneous symmetric polynomial can be written as a polynomial in elementary symmetric polynomials. It is in this sense that the elementary symmetric polynomials can be seen as a basis for all symmetric polynomials. An important example is the *center of mass* for the two-component gas:

$$R = \frac{1}{N+M}\left(z_1 + \ldots + z_N + w_1 + \ldots + w_M\right) = \frac{1}{A}\left(e_1(z) + e_1(w)\right) \tag{3.2.3}$$

where $A = N + M$ is the total number of bosons in the trap.

It turns out [8,21] that the set of all products

$$e_{\lambda_1}(z) e_{\lambda_2}(z) \cdots e_{\lambda_k}(z) e_{\mu_1}(w) e_{\mu_2}(w) \cdots e_{\mu_l}(w) \tag{3.2.4}$$

of elementary symmetric polynomials with $\sum_i^k \lambda_i + \sum_j^l \mu_j = L$ forms a non-orthogonal basis for the Hilbert space of $N + M$ bosons at angular momentum $L \le M$. For the rest

of this chapter, we will limit ourselves to this range of angular momenta. The functions in (3.2.4) will be very convenient both for the analytical derivations in this chapter, and also as a basis for exact numerical diagonalization of the interaction in a later discussion. Note that the possible sets of values of the λ_i and μ_j are equal to the possible ways of dividing L into sums of integers. We call this the *integer partitions* of L. For example, the integer partitions of 4 are $\{4\}, \{3,1\}, \{2,2\}, \{2,1,1\}, \{1,1,1,1\}$.

3.3 An invariant subspace of Hilbert space

Numerical studies of the two-species system that we are describing here have previously shown [6,22] that, for $L \leq N$, the ground states only contains single-particle angular momenta $l = 0$ or $l = 1$. Candidates for such functions can be written in terms of some of the simplest functions in our basis (3.2.4), namely the ones where only one symmetric polynomial in each set of variables are multiplied together:

$$e_\lambda(z)e_{L-\lambda}(w) \tag{3.3.1}$$

for some $0 \leq \lambda \leq \min(N, L)$. The degree of the two polynomials secure that the total angular momentum is L. Because of this discovery, we would like to see how the interaction we are studying (3.1.5) acts on such a function. But first, notice a few very simplifying facts. Since each term in $e_\lambda(z)$ only contains at most one power of any variable in the set $\{z\} = z_1, \ldots, z_N$, any attempt to differentiate $e_\lambda(z)$ twice or more with respect to any of its variables must vanish. That is:

$$\partial_{z_i}^m e_\lambda(z) = 0 \qquad m \geq 2 \tag{3.3.2}$$

This means that

$$\begin{aligned} A_m e_\lambda(z) = B_m e_\mu(w) &= 0 \qquad m \geq 3 \\ C_m e_\lambda(z) e_\mu(w) &= 0 \qquad m \geq 3 \end{aligned} \tag{3.3.3}$$

because the lowest power of a differential operator equals or exceeds 2 for these m. We also see that

$$A_m R = B_m R = C_m R = 0 \qquad m \geq 1 \tag{3.3.4}$$

because pairs of variables of power one in the e_1 get differentiated to 1's that cancel because of the minus in the operators (for $m = 1$), or they vanish directly ($m > 1$). We are now ready to let the interaction (3.1.5) act on (3.3.1). The simplifying conditions tells us that we only need to consider $m = 0, 1, 2$. We get [18]

$$\begin{aligned} V_0 e_\lambda(z)e_{L-\lambda}(w) &= \left(\binom{N}{2} + \binom{M}{2} + NM\right) e_\lambda(z)e_{L-\lambda}(w) \\ &= \left(\frac{1}{2}N(N-1) + \frac{1}{2}M(M-1) + NM\right) e_\lambda(z)e_{L-\lambda}(w) \\ &= \frac{1}{2}A(A-1)e_\lambda(z)e_{L-\lambda}(w) \end{aligned} \tag{3.3.5}$$

$$\begin{aligned} V_1 e_\lambda(z)e_{L-\lambda}(w) = {} & ALe_\lambda(z)e_{L-\lambda}(w) - A(N-\lambda+1)e_{\lambda-1}(z)e_{L-\lambda}(w)R \\ & - A(M-L+\lambda+1)e_\lambda(z)e_{L-\lambda-1}(w)R \end{aligned} \tag{3.3.6}$$

$$\begin{aligned} V_2 e_\lambda(z) e_{L-\lambda}(w) = {} & 2\left(N\lambda + M(L-\lambda) + 2\lambda(L-\lambda)\right) e_\lambda(z) e_{L-\lambda}(w) \\ & + 2(N-\lambda+1)(L-\lambda+1) e_{\lambda-1}(z) e_{L-\lambda+1}(w) \\ & + 2(M-L+\lambda+1)(\lambda+1) e_{\lambda+1}(z) e_{L-\lambda-1}(w) \\ & - 2A(N-\lambda+1) e_{\lambda-1}(z) e_{L-\lambda}(w) R \\ & - 2A(M-L+\lambda+1) e_\lambda(z) e_{L-\lambda-1}(w) R \end{aligned} \tag{3.3.7}$$

These three expressions show that the subspace

$$\mathcal{M} = \{R^n e_\lambda(z) e_{L-\lambda-n}(w)\} \tag{3.3.8}$$

where $0 \leq \lambda \leq \min(N, L)$ and $0 \leq n \leq L-\lambda$, is invariant under the action of the interaction operator (3.1.5). We can thus start looking for eigenfunctions of the interaction within this subspace, and hope that we find the lowest-lying states.

3.4 Eigenfunctions of the interaction within $\mathcal{M}$

We will now solve the eigenstate equation

$$VF(z,w) = EF(z,w) \tag{3.4.1}$$

in the subspace $\mathcal{M}$. To do this, we want to write an ansatz to $F(z,w)$ that is manifestly in this subspace. Since we are mainly looking for the ground states of the system, the appearance of R^n in the spanning functions for $\mathcal{M}$ may trouble us, because it suggests that the interaction induces center-of-mass excitations: that is, if ψ_L is a wave function with angular momentum L, then $R^l\psi_L$ is a wave function with angular momentum $L+l$, l of it in the center of mass. However, we see that there are $\min(N,L)+1$ spanning functions that have $n=0$, i.e. no power of R. We therefore model our ansatz wave function as such a state, and explicitly translate the ansatz to the center of mass so that center-of-mass excitations are avoided. The ansatz is therefore

$$F(z,w) = P_0 \Psi_{L,n}(z,w) \tag{3.4.2}$$

with

$$\Psi_{L,n} = \sum_{\lambda=0}^{\min(N,L)} c_\lambda^{(n)} e_L(z) e_{L-\lambda}(w) \tag{3.4.3}$$

and $P_0 : P_0\Psi(z,w) = \Psi(z-R, w-R)$ is the operator that translates to the center of mass. The label n distinguishes between the $\min(N,L)+1$ wave functions with zero angular momentum in the center of mass. The neat expansion

$$e_\lambda(z_1 - R, \ldots, z_N - R) = \sum_{\nu=0}^{\lambda} \binom{N-\nu}{\lambda-\nu} (-R)^{\lambda-\nu} e_\nu(z_1, \ldots, z_N) \tag{3.4.4}$$

(and similarly for $e_{L-\lambda}(w-R)$) taken from [19] shows explicitly that the ansatz (3.4.2) is in the subspace $\mathcal{M}$.

The next step should now be to insert the ansatz wave function (3.4.2) with (3.4.3) into the eigenvalue equation (3.4.1), utilize (3.3.5-3.3.7) to expand the left hand side, and solve for the coefficients $c_\lambda^{(n)}$. The full equation one would arrive at in this manner is a rather lengthy expression and thus difficult to display here. The important feature of the expression

is that the products of elementary symmetric polynomials that appear in (3.3.5-3.3.7) were part of the basis for the Hilbert space, so they must be linearly independent. This means that we can compare coefficients for different combinations $e_i(z)e_j(w)$ independently, without tackling the full expression in one step. If we look for every occurrence of the form $e_i(z)e_{L-i}(w)$ in (3.3.5-3.3.7), we get *five* contributions: one from each of the first terms in the three right hand sides for $i = \lambda$, and two from the second and third line in (3.3.7) for $i = \lambda+1$ and $i = \lambda-1$ respectively. Since our ansatz contains a sum over λ, all five of these will appear in the eigenvalue equation. Equating the coefficients of $e_\lambda(z-R)e_{L-\lambda}(w-R)$ on the left and right hand sides of the eigenvalue equation gives us:

$$\begin{aligned} &\frac{1}{2}v_0A(A-1)c_\lambda^{(n)} + v_1ALc_\lambda^{(n)} \\ &+ 2v_2\left(N\lambda + M(L-\lambda) + 2\lambda(L-\lambda)\right)c_\lambda^{(n)} \\ &+ 2v_2(N-(\lambda+1)+1)(L-(\lambda+1)+1)c_{\lambda+1}^{(n)} \\ &+ 2v_2(M-L+(\lambda-1)+1)((\lambda-1)+1)c_{\lambda-1}^{(n)} = E_nc_\lambda^{(n)} \end{aligned} \tag{3.4.5}$$

With no loss of generality we now rewrite the energy as

$$E_n = \frac{1}{2}v_0A(A-1) + v_1AL + 2v_2\varepsilon_n \tag{3.4.6}$$

where ε_n is to be determined by the equation above. This simplifies the equation above to:

$$\begin{aligned} 2v_2\left(N\lambda + M(L-\lambda) + 2\lambda(L-\lambda)\right)c_\lambda^{(n)} \\ + 2v_2(N-\lambda)(L-\lambda)c_{\lambda+1}^{(n)} \\ + 2v_2(M-L+\lambda)\lambda c_{\lambda-1}^{(n)} = 2v_2\varepsilon_nc_\lambda^{(n)} \end{aligned} \tag{3.4.7}$$

$$\begin{aligned} &\left(N\lambda + M(L-\lambda) + 2\lambda(L-\lambda) - \varepsilon_n\right)c_\lambda^{(n)} \\ &+(N-\lambda)(L-\lambda)c_{\lambda+1}^{(n)} + \lambda(M-L+\lambda)c_{\lambda-1}^{(n)} = 0 \end{aligned} \tag{3.4.8}$$

This recurrence relation must now be solved for the coefficients $c_\lambda^{(n)}$. The authors of [18] make an interesting note at this point, namely the fact that the equation determining the coefficients is independent of the matrix elements of the interaction, as long as it is of the form (3.1.5). This is a consequence of the homogeneous interaction, and it would not be the case if, for instance, the inter-species interaction was weaker than the intra-species. We will return to such *inhomogeneous interaction* in Chapter 6.

To solve (3.4.8), we assume that the coefficients can be written as power series in the summation index λ:

$$c_\lambda^{(n)} = \sum_{k=0}^{n}\beta_k\lambda^k \tag{3.4.9}$$

Inserting this into (3.4.8) allows us to compare coefficients for each power of λ. The largest power is λ^{n+2}, and the coefficients must fulfill

$$-2\beta_n + \beta_n + \beta_n = 0 \tag{3.4.10}$$

i.e. β_n is undetermined by the equation. The second largest power is λ^{n+1}, and the coefficients must satisfy

$$\begin{aligned} &(N-M+2L)\beta_n - 2\beta_{n-1} \\ &+\left(n-(N+L)\right)\beta_n + \beta_{n-1} \\ &+\left((M-L)-n\right)\beta_n + \beta_{n-1} = 0 \end{aligned} \tag{3.4.11}$$

which also reduces to $0 = 0$, i.e. both β_n and β_{n-1} are still undetermined. The next step resolves the problem: comparing coefficients of λ^n gives

$$\begin{aligned}(LM - \varepsilon_n)\beta_n + (N - M + 2L)\beta_{n-1} - 2\beta_{n-2} \\ + \left(NL - (N+L)n + \frac{1}{2}n(n-1)\right)\beta_n + (n - 1 - (N+L))\beta_{n-1} \\ + \beta_{n-2} + (\frac{1}{2}n(n-1) - n(M-L))\beta_n + (M - L - (n-1)\beta_{n-1} \\ + \beta_{n-2} = 0\end{aligned} \tag{3.4.12}$$

This reduces beautifully: both β_{n-1} and β_{n-2} vanish, and we are left with

$$\beta_n(n(n-1) + (N+M)L - (N+M)n - \varepsilon_n) = 0 \tag{3.4.13}$$

The solutions are $\beta_n = 0$ and

$$\varepsilon_n = n(n-1) + AL - An \tag{3.4.14}$$

If we continue in this fashion, comparing coefficients of different powers of λ, we will see that the β_i, $i < n$ are determined recursively in terms of β_n. The choice $\beta_n = 0$ can be seen to give $\beta_i = 0\ \forall i$, which gives us a vanishing wave function. We reject $\beta_n = 0$ for this reason, and by accepting the solution (3.4.14), have solved the eigenvalue problem. The eigenenergies of the interactions are

$$E_n = \frac{1}{2}v_0 A(A-1) + v_1 AL + 2v_2(n(n-1) + A(L-n)) \tag{3.4.15}$$

The lowest energy is obtained for $n = \min(N, L)$, with lower n producing monotonically higher energy. What about the undetermined β_n? It simply shows up as an overall factor in the wave function (3.4.3), and should be determined by normalization. This completes the derivations of eigenfunctions in $\mathcal{M}$.

3.5 Properties of the eigenstates

We start the discussion of the acquired results by showing a typical interaction energy plot for the system in question. A plot of the eigenenergies for $N = 3$, $M = 5$ particles is shown for $0 \leq L \leq 8$ in Fig. (3.5.1). The spectrum was produced by exact diagonalization of the contact interaction given by (3.1.4); the method that was used will be discussed in Appendix A. We have also removed center-of-mass excitations from the plot, that is, states Ψ_L of a given angular momentum L which equal a state Ψ_l of a lower angular momentum l times a center-of-mass factor R^{L-l}. The energies (3.4.15) have been highlighted in the plot. Note that, since we have been working in the subspace $\mathcal{M}$, we have not found *all* the eigenstates and -energies. But as is visible in the plot, we have indeed found the ground states for all $L \leq M$, which was the primary goal.

We also see certain excited states in this plot, and they all lie on lines $E_n(L)$ for the different n. We notice the lack of an excited state at $L = 1$ though, and this is the only case where the formula (3.4.15) might fool us: the state corresponding to this missing energy in the spectrum is $P_0\Psi_{1,0} = P_0(e_1(z) + e_1(w)) = P_0 AR = 0$, because P_0 projects away the center of mass R. Therefore the energy $E_0(L = 1)$ is in fact not an eigenvalue of the interaction.

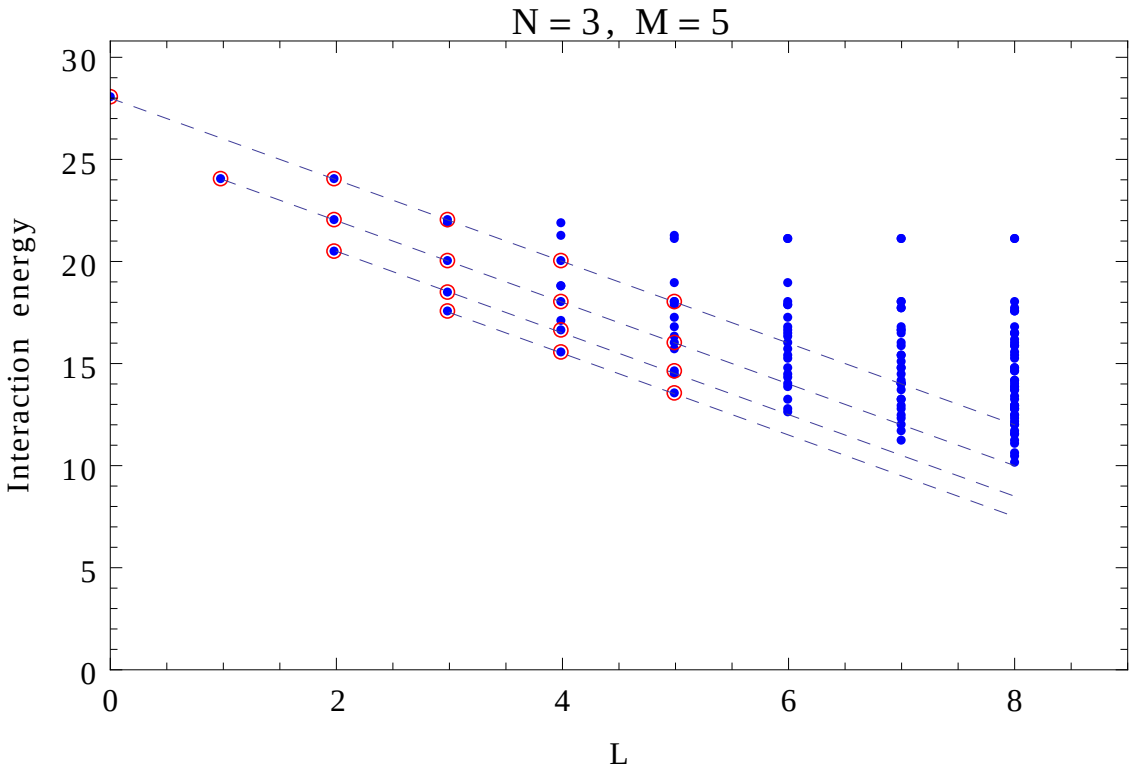

Figure 3.5.1: Interaction energy vs. angular momentum. Blue dots are energies from exact diagonalization, red circles are eigenenergies in the subspace $\mathcal{M}$.

We will now comment on some of the more interesting features of the states and energies that we have found. For example, we have found that the ground state energies are very simple functions of L. Another very interesting fact is that, if we compute the ground state wave functions for $L \leq N$ by first calculating the β-coefficients, from them the $c_\lambda^{(L)}$ and insert into (3.4.3), we find that applying the operator P_0 does not change the result at all, i.e. $P_0\Psi_{L,L} = \Psi_{L,L}$ for $L \leq N$. Since the wave function $\Psi_{L,L}$ is just a sum of two elementary symmetric polynomials multiplied together, this means that the wave function only contains single particle angular momenta $l = 0, l = 1$. This agrees with the numerical work mentioned earlier, [6,22]. This very simple form of the ground state wave function will be a motivation for the use of trial wave functions in Chapter 5. In this lowest angular momentum regime, one can even find the coefficients $c_\lambda^{(L)}$ *without* first computing the β-coefficients: the result is [18]

$$c_\lambda^{(L)} = (-1)^\lambda \frac{(M-N+\lambda)!(N-\lambda)!}{(M-L)!N!} c_0^{(L)} \tag{3.5.1}$$

where $c_0^{(L)} = \beta_0$ is still an overall, unimportant factor that should be determined (if necessary) by normalizing the wave function. Finally, the ground state energies at a given particle number $A = N + M$ with $M - N > 1$ reappear as *excited* states at all other system configurations $0 \leq M' - N' < M - N$ with the same total number of particles, $N' + M' = A$. This is because the energies (3.4.15) depend only on A and the quantum number n, not independently on N or M. We will later see how to utilize this fact to generate excited states from ground states.

3.6 Pseudospin formulation

Since we are studying a gas of *two* species of bosons, a suitable language to describe them is the familiar spin 1/2 language: in this case we will call it pseudospin, because our treatment allows the two species to be for instance two different kinds of spin 0-atoms, with no real spin. This is the view taken in the final version of the paper, [8]. If we associate the species of coordinates z_i with pseudospin down, and the species of coordinates w_k with pseudospin up, we can choose a number representation basis instead of the coordinate basis-projected states we have been using until now. We will keep naming the two species z's and w's. Let the state

$$\left| \begin{array}{cc} n_L & m_L \\ n_{L-1} & m_{L-1} \\ \vdots & \vdots \\ n_0 & m_0 \end{array} \right\rangle \tag{3.6.1}$$

be a state with n_0 pseudospin-down bosons at single-particle angular momentum $l = 0$, n_1 pseudospin-down bosons at $l = 1$ and so on, and similarly for the other species. Since we always consider a definite L, we only need $i, k \leq L$. The sums $\sum_i n_i$, $\sum_k m_k$ must of course give the total number of each species, N, M, and we must have $\sum_i n_i i + \sum_k m_k k = L$. The many-particle state composed of such kets are always symmetrized with respect to all z_i and all w_k when projected onto a coordinate basis. This means for instance that

$$\left| \begin{array}{cc} 2 & 1 \\ 0 & 1 \\ 1 & 2 \end{array} \right\rangle \Leftrightarrow z_1^2 z_2^2 z_3^0 \cdot w_1^2 w_2^1 w_3^0 w_4^0 + \cdots \tag{3.6.2}$$

where the dots mean all such terms where indices on z's and on w's are permuted. On the other hand, projection onto the basis of products of elementary symmetric polynomials (3.2.4) also yields a non-trivial result, namely

$$\begin{aligned} \left| \begin{array}{cc} 2 & 1 \\ 0 & 1 \\ 1 & 2 \end{array} \right\rangle \Leftrightarrow & -2e_1(z)e_3(z)e_1(w)e_2(w) + 6e_1(z)e_3(z)e_3(w) \\ & + e_2(z)^2 e_1(w)e_2(w) - 3e_2(z)^2 e_3(w) \end{aligned} \tag{3.6.3}$$

This result suggests that a general conversion matrix between the two bases is not straightforwardly attainable. But this is not a problem for us, as we are mainly interested in the insights offered by the pseudospin formalism, namely the meaning of the associated spin quantum numbers.

We define single-particle creation and annihilation operators in the usual way:

$$\begin{aligned}
b_{z,l}\left|\begin{matrix}\vdots & \vdots\\ n_l & m_l\\ \vdots & \vdots\end{matrix}\right\rangle &= \sqrt{n_l}\left|\begin{matrix}\vdots & \vdots\\ n_l-1 & m_l\\ \vdots & \vdots\end{matrix}\right\rangle\\
b_{w,l}\left|\begin{matrix}\vdots & \vdots\\ n_l & m_l\\ \vdots & \vdots\end{matrix}\right\rangle &= \sqrt{m_l}\left|\begin{matrix}\vdots & \vdots\\ n_l & m_l-1\\ \vdots & \vdots\end{matrix}\right\rangle\\
b^\dagger_{z,l}\left|\begin{matrix}\vdots & \vdots\\ n_l & m_l\\ \vdots & \vdots\end{matrix}\right\rangle &= \sqrt{n_l+1}\left|\begin{matrix}\vdots & \vdots\\ n_l+1 & m_l\\ \vdots & \vdots\end{matrix}\right\rangle\\
b^\dagger_{w,l}\left|\begin{matrix}\vdots & \vdots\\ n_l & m_l\\ \vdots & \vdots\end{matrix}\right\rangle &= \sqrt{m_l+1}\left|\begin{matrix}\vdots & \vdots\\ n_l & m_l+1\\ \vdots & \vdots\end{matrix}\right\rangle
\end{aligned} \tag{3.6.4}$$

They obey the standard commutation relations for bosons, the only non-commuting ones being

$$[b_{z,l}, b^\dagger_{z,l'}] = [b_{w,l}, b^\dagger_{w,l'}] = \delta_{l,l'} \tag{3.6.5}$$

The interaction operator (3.1.5) is certainly pseudospin independent: any particle interchange $z_i \leftrightarrow z_j,\ w_k \leftrightarrow w_l,\ z_i \leftrightarrow w_k$ leaves the interaction invariant. Since the interaction is independent of species, the interaction commutes with the total pseudospin operators $\mathbf{S}^2$ and S_z. We express $\mathbf{S}^2$ in terms of S_z and the pseudospin lowering operator S_-, given by

$$\begin{aligned}
S_z &= \frac{1}{2}\sum_{l=0}^{\infty} b^\dagger_{w,l}b_{w,l} - b^\dagger_{z,l}b_{z,l}\\
S_- &= \sum_{l=0}^{\infty} b^\dagger_{z,l}b_{w,l}
\end{aligned} \tag{3.6.6}$$

such that

$$\mathbf{S}^2 = S_-S_-^\dagger + S_z(S_z+1) \tag{3.6.7}$$

We see that S_z is composed of single-particle number operators only, so S_z basically counts how many bosons we have of each species. That is, the eigenvalues of S_z are simply

$$\mathcal{S}_z = \frac{1}{2}(M-N) \tag{3.6.8}$$

We write the eigenvalues of $\mathbf{S}^2$ in the customary way

$$\mathbf{S}^2\left|\Psi\right\rangle = \mathcal{S}(\mathcal{S}+1)\left|\Psi\right\rangle \tag{3.6.9}$$

We know that the eigenstates we have derived in this chapter are sums of products of elementary symmetric polynomials, $e_\lambda(z)e_{L-\lambda}(w)$, before projection. These represent λ pseudospin-down bosons with single-particle angular momentum $l = 1$ and $\min(N, L) - \lambda$ with $l = 0$, and equivalently for the spin-up bosons. These can be seen to be linear combinations of states $|\chi_\tau\rangle$that have a certain form. The states $|\chi_\tau\rangle$ are generated from

pseudospin singlet pairs with $L = 1$ in the following way: one defines the singlet creation operator

$$B^\dagger = \frac{1}{\sqrt{2}}\left(b^\dagger_{z,1}b^\dagger_{w,0} - b^\dagger_{z,0}b^\dagger_{w,1}\right) \tag{3.6.10}$$

Let us say we make $\tau \leq \min(N, L)$ of these pairs, by acting τ times with $B^\dagger$ on the vacuum state $|0\rangle$. Then, we create the remaining $A - \tau$ bosons along with the correct angular momentum by applying $b^\dagger_{w,1}$ and $b^\dagger_{w,0}$ the appropriate amount of times. This generally leaves us with too many w's, so finally we ensure the correct number of bosons of each species by applying the pseudospin lowering operator. The result is summed up in [18]:

$$|\chi_\tau\rangle = (S_-)^{N-\tau}(b^\dagger_{z,0})^{A-L-\tau}(b^\dagger_{w,1})^{L-\tau}(B^\dagger)^\tau\,|0\rangle \tag{3.6.11}$$

This state has pseudospin quantum number $\mathcal{S} = A/2-\tau$. The conclusion is that projecting linear combinations of these kets onto the subspace of states with zero angular momentum in the center of mass gives the eigenstates we have derived in this chapter. The number of singlets τ is the same as the quantum number n used in the eigenfunctions (3.4.3).

We can use the pseudospin lowering operator to get from a state of the form (3.6.11) at a given N, M to a state at $N+1, M-1$ and the same energy. This is useful because we have seen that ground states for some N, M are excited states for other N', M'. For example, the first excited state (among those covered in this chapter) at $N' = 3, M' = 5, L = 4$ has the same energy as the second excited state at $N = M = L = 4$. The former can be found from the latter as follows: the latter is

$$|\chi_n\rangle = (S_-)^{4-2}(b^\dagger_{z,0})^{8-4-2}(b^\dagger_{w,1})^{4-2}(B^\dagger)^2\,|0\rangle \tag{3.6.12}$$

because the second excited state has $n = \min(N, L) - 2 = 4 - 2 = 2$. The former state has $n' = \min(N', L) - 1 = 3 - 1 = 2$ and looks like

$$|\chi_{n'}\rangle = (S_-)^{3-2}(b^\dagger_{z,0})^{8-4-2}(b^\dagger_{w,1})^{4-2}(B^\dagger)^2\,|0\rangle \tag{3.6.13}$$

giving

$$\begin{aligned} |\chi_n\rangle &= (S_-)^{4-2}(b^\dagger_{z,0})^{8-4-2}(b^\dagger_{w,1})^{4-2}(B^\dagger)^2\,|0\rangle \\ &= (S_-)(S_-)^{3-2}(b^\dagger_{z,0})^{8-4-2}(b^\dagger_{w,1})^{4-2}(B^\dagger)^2\,|0\rangle \\ &= S_-\,|\chi_{n'}\rangle \end{aligned} \tag{3.6.14}$$

Note however that the *coefficients* in the linear combinations that give the eigenstates for the interaction still need to be determined, similarly to how we found $c^{(n)}_\lambda$. We can further appreciate the non-triviality of the results in this chapter by computing the action of the operators in (3.6.11) on the vacuum, and expressing the answer in the number basis of states (3.6.1). A little combinatorics along with the operator identities (3.6.4) yields

$$|\chi_\tau\rangle = \frac{\tau!}{\sqrt{2^\tau}}(S_-)^{N-\tau}\sum_{k=0}^{\tau} C_k(-1)^k \left|\begin{bmatrix} \tau-k \\ k \end{bmatrix}\begin{bmatrix} k+L-\tau \\ A-L-k \end{bmatrix}\right\rangle \tag{3.6.15}$$

where the parentheses around the spin-down and spin-up parts have been added for readability, and

$$C_k = \sqrt{\frac{(k+L-\tau)!}{k!}\frac{(A-L-k)!}{(\tau-k)!}} \tag{3.6.16}$$

Notice that we have neither applied the spin lowering operator nor projected out the center of mass, because the form would become even more complicated. Because of this, we prefer working in the coordinate basis used in the other sections of this chapter, keeping in mind the essentials from this pseudospin perspective, namely the facts that $\mathcal{S}_z = (M - N)/2$ and $\mathcal{S} = A/2 - \tau = A/2 - n$. The ground states with $\tau = n = N$ (that is, $N \leq L \leq M$) will be especially interesting later, because these are states with $\mathcal{S} = (M+N)/2 - N = \mathcal{S}_z$, called *highest weight states*.

3.7 Beyond the subspace $\mathcal{M}$

The results that we have arrived at in this chapter thanks to Papenbrock, Reimann and Kavoulakis gives us a good deal of insight into the behavior of the two-component rotating system of bosons. However, there are certain pieces missing. Firstly, while we would like to know the states and energies for all L in the range $0 \leq L \leq N + M = A$, we have only found expressions for energies and wave functions up to $L \leq M$. Moreover, we have assumed a completely homogeneous interaction. As mentioned, $\mathcal{M}$ would not be an invariant subspace if the interaction was inhomogeneous, and this is often the case for real mixtures of gases. The ultimate goal of this thesis is to investigate whether or not a systematic use of certain trial wave functions can overcome these limitations, and/or add to the understanding of the physics that these wave functions and energies represent. The next chapter will therefore be a presentation of these trial wave functions.

Chapter 4

Composite Fermion approach

We saw in the last chapter how one can find certain eigenstates for the two-species rotating Bose gas in a trap. We restricted ourselves to angular momenta $0 \leq L \leq M$ and found the ground states and some excited states, which were polynomial wave functions with algebraic coefficients, multiplied with an exponential function determined by the Landau level quantization. What we would like to do in this chapter, is present another way of approaching a description of our system. To this end we will introduce the idea of composite fermions. First, we will give some very basic background information about the classical and quantum Hall phenomena, the latter being what the composite fermion (CF) model was invented to understand. Then, we explain how trial wave functions for bosons are generated in the composite fermion formalism, and we also discuss how to incorporate the two-component nature of our bosonic system in a natural way.

4.1 Why composite fermions?

It might seem strange that we plan to use the composite fermion wave functions in our study of a many-body system of bosons. Firstly, we are studying bosons and not fermions. Secondly, the CF formalism was designed to deal with electrons in high magnetic fields, classically corresponding to high angular momentum. On the other hand, we are studying the lowest angular momenta up to the "single vortex" $L = N+M$. However, two arguments make the use of CF wave functions more plausible. As we have already seen, the Hamiltonians of the two systems are basically equal under the circumstances detailed in Chapter 2. This suggests that the many-particle wave functions might be similar. Moreover, quite recent studies [12,13] of *single-species* rotating bosons at low angular momenta $L \sim N$ show that the CF formalism gives surprisingly good overlaps with the known eigenstates. It is our hope that something similar will happen for two species of bosons. The CF wave functions might enable us to better understand the yrast spectra because many results are already available for two-species composite fermions. Also, we would like to know whether or not it is possible to find relatively simple approximate wave functions for the states at higher angular momenta, $M < L \leq N + M$. The first goal will be to determine the suitability and accuracy of the CF wave functions in describing the states we obtained in Chapter 3. The second goal will be to extend the angular momenta we consider all the way up to $L = N + M$. In Chapter 5 we will do this by calculating overlaps with the known exact states obtained in Chapter 3, and with exact diagonalization results. In Chapter 6

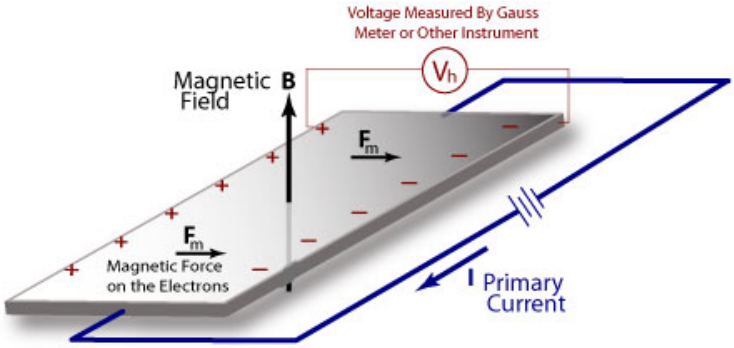

Figure 4.2.1: Illustration of the classical Hall effect. The figure was downloaded from http://www.ndt-ed.org/.

we will consider inhomogeneous interaction, where no analytical results are known except in two limits.

4.2 The classical Hall effect

The classical Hall effect was discovered by Edwin H. Hall in 1879 [9]. In essence, the Hall effect is the appearance of an electric potential *transverse to* an applied electric current across a piece of conductor, when the conductor is placed in a magnetic field. The phenomenon can be understood by considering the following idealized situation: Let's assume for simplicity that a conductor, shaped as a rectangular parallelepiped, is placed in a uniform magnetic field that points in the positive z direction. If a constant electric current is passed through the conductor along the positive x direction, the charge carriers (which are normally electrons) will be affected by a force, given by Lorentz' law (in SI units):

$$\mathbf{F} = q\ \mathbf{v} \times \mathbf{B} \tag{4.2.1}$$

Here q is the charge of the carriers, $\mathbf{v} = v_x\mathbf{x}$ is the drift velocity of the carriers and $\mathbf{B} = B\mathbf{z}$ is the magnetic field. From the right hand rule of vector multiplication, we immediately see that this force will push the charge carriers to one side of the conductor. Thus, there will be a net charge difference between the two sides of the conductor, which sets up a voltage V_y. In other words, the external magnetic field will cause the charge carriers to diverge from the straight path they would have taken if there were no magnetic field. This voltage V_y will continue to increase as more and more charge carriers accumulate at the side(s) of the conductor. At some point, however, the Coulomb force exerted on the incoming charge carriers of the current by the charges on the sides will balance the Lorentz force, and the voltage V_y will attain a fixed value V_H, known as the Hall voltage. Since the sum of the forces in the y direction now equal zero, the carriers of the applied current will attain a drift velocity purely in the x direction. Figure 4.2.1 illustrates the situation.

The ratio of the electric field E_y associated with the Hall voltage V_H to the applied current density j_x is known as the Hall resistivity,

$$\rho_H = \frac{E_y}{j_x} = \frac{|\mathbf{F}/q|}{nqv_x} = \frac{v_xB}{nqv_x} = \frac{B}{nq} \tag{4.2.2}$$

where n is the charge carrier density of the current. Note that, in two dimensions under disorder-free conditions, this would equal the resist*ance* R_H simply because resistance and resistivity have the same units in two dimensions. Since we will be discussing two-dimensional systems in the following, we write

$$R_H = \frac{B}{nq} \tag{4.2.3}$$

4.3 The quantum Hall effect

When treating electrons confined to two dimension moving in an external magnetic field in quantum mechanics, the simplest situation is to image the electrons to be non-interacting. The Hamiltonian for such a system of N electrons is

$$H = \sum_{i=1}^{N} \frac{1}{2M_e} \left(\mathbf{p}_i - q\mathbf{A}\right)^2 \tag{4.3.1}$$

We recognize this form of H from Section 2.2, reminding us of the mathematical connection between the electrons in a magnetic field an the bosons in a rotating trap. The electron eigenenergies form Landau levels, and the eigenstates have the same form as those found in Chapter 2.

In the 1970's, a group of Japanese physicists studied the theoretical quantization of conductivity in two-dimensional electronic systems. In 1975, Ando, Matsumoto and Uemura [23] predicted a quantization of the Hall resistance R_H when the charge carriers were subjected to strong magnetic fields at low temperatures. However, their analysis was based on Born approximations, and it was uncertain how or if the quantization would be observable in the laboratory. In 1980, Klaus von Klitzing and collaborators discovered this quantization in experiments [24], and the astonishing fact was that the resistance was *exactly* quantized! The Hall resistance took values

$$R_H = \frac{h}{iq^2} \tag{4.3.2}$$

where $i \in \mathbb{Z}$ and h is Planck's constant, and the results were in good agreement with the theoretical predictions. The appearance of h leaves little doubt as to the quantum mechanical origin of the phenomenon. Figure 4.3.1 shows the quantization of the Hall resistance as a function of the external magnetic field.

This phenomenon is known as the integer quantum Hall effect, or IQHE. It is a very special result, because it is universal, in the sense that it is largely independent of sample geometry and material parameters. Also, the quantization is insensitive to variation in parameters such as temperature and sample disorder, as long as the variations are small.

This exact quantization was relatively quickly understood. If one calculates the filling factor for the electrons in the same manner as we did for bosons in Section 2.4, one finds

$$\nu = \frac{nh}{qB} \tag{4.3.3}$$

that is, the role of qB in the quantum Hall system is equivalent to the role of $2M\omega$ for rotating bosons. We see that if the filling factor is an *integer* i, then

$$\nu = \frac{nh}{qB} = i \quad \Rightarrow \quad \frac{n}{qB} = \frac{i}{h} \tag{4.3.4}$$

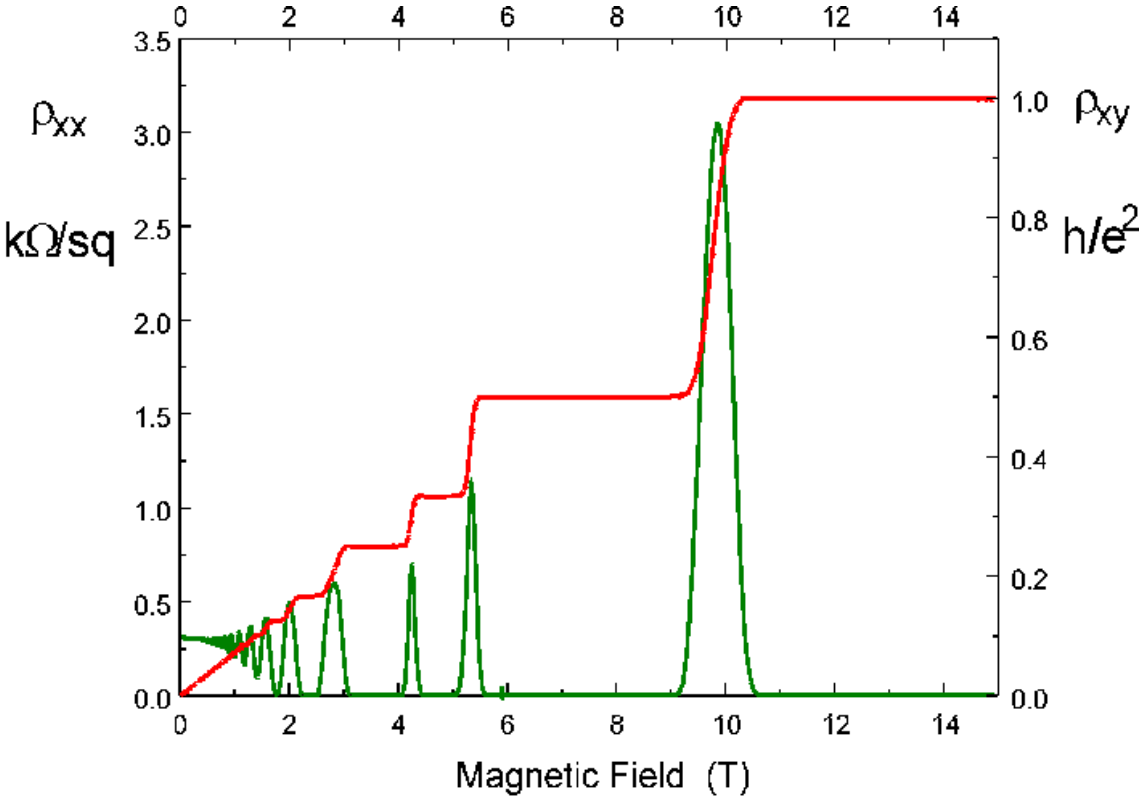

Figure 4.3.1: Quantization of Hall resistance in the IQHE. Figure retrieved from the homepage of David Leadley, University of Warwick.

---

gives

$$R_H = \frac{B}{nq} = \frac{h}{iq^2} \tag{4.3.5}$$

directly from the classical expression for the Hall resistance. This is the reason why the filling factor is such an important parameter in quantum Hall physics. The expression for R_H is not the whole story though: we need to explain how the plateaus in Figure 4.3.1 emerge.

The IQHE stems directly from the known single-particle Landau level quantization that we saw in Chapter 2, combined with the effect of interactions and material impurities [9]. We will give a short qualitative explanation here. When interactions and impurities are present, the Landau levels cease to be sharp lines in the energy spectrum, and in general the energy gaps disappear. However, it can be shown that the states with energy close to the unperturbed Landau level energies, and the states with energy in between two unperturbed levels are different: they are called extended states and localized states respectively [9] and an important distinction between the two is that localized states do not contribute to electric transport. If the Fermi energy lies inside a range of localized states, then a hypothetical addition of one fermion would not change the resistance because the new electron would not contribute to the transport. Another way of saying this is that the resistance will remain a constant function of the filling factor as long as the Fermi energy lies within the localized states. This explains the formation of plateaus. Note that the IQHE can be understood, at least qualitatively, in terms of *single-particle* states. We now move on to another, perhaps more mysterious side to the quantum Hall effect.

The next step on the way to a thorough understanding of quantum Hall physics came in 1982. Experiments by Tsui, Stormer and Gossard [25] showed that the quantized Hall resistance could, in addition to the values (4.3.2) also take on values

$$R_H = \frac{h}{fq^2} \tag{4.3.6}$$

with f taking on certain *fractional* values. That is, one observed plateaus in the Hall resistance also for the fractional filling factor $\nu = \frac{1}{3}$. In later experiments, other fractions were observed as well, such as $\nu = \frac{1}{5}, \frac{1}{7}, \ldots \frac{2}{5}, \frac{3}{7}, \ldots$ This appearance of plateaus at fractional filling factors is known as the fractional quantum Hall effect, FQHE. The quantization at fractional filling factors had not been predicted by theory, and was soon found to stem from the collective many-body behavior of the electrons due to interactions. In the simplest case, one assumes that all the electrons are confined to the LLL and that their internal degrees of freedom (i.e. spin) are frozen out. The non-constant contribution to the Hamiltonian of the system is therefore only the interaction term: in the case of Coloumb interaction one has

$$H = \mathcal{P}_{LLL} \sum_{i<j} \frac{1}{|\mathbf{r}_i - \mathbf{r}_j|} \mathcal{P}_{LLL} \tag{4.3.7}$$

where suitable units of length and energy have been chosen, and $\mathcal{P}_{LLL}$ projects solutions of the eigenvalue equation to the LLL [9]. We do not know the exact many-body solutions to the eigenvalue equation

$$H\Psi = E\Psi \tag{4.3.8}$$

for this Hamiltonian. To make matters worse, the lack of any small parameter in (4.3.7) eliminates the perturbative approach one would usually take in this case. Therefore, one can either try to find another, approximate Hamiltonian of the system and find the eigenstates exactly, or one can construct a wave function based on some principal knowledge of the system and hope to model the important physics in this way. Such wave functions are often called ansatz wave functions. A very successful and celebrated ansatz for the FQHE states was found by Robert Laughlin in 1983 [26]. It has the form

$$\Psi_{Laughlin}(z) = \prod_{i<j} (z_i - z_j)^m \exp\left(-\frac{1}{4}\sum_i |z_i|^2\right) \tag{4.3.9}$$

where the unit of length has been set to $l = \sqrt{\hbar/qB} = 1$ and m is an odd integer. It turns out that this wave function gives a very good description of the states at filling factors $1/m$. Its success was a very important step in understanding the FQHE in particular, but it was also important for condensed matter physics in general because it proves that it is not impossible to find very good descriptions of the physics one is studying despite that the exact states are impossible to find analytically, and extremely complicated when found numerically. However, this is not to say that good trial wave functions exist for a large number of quantum many-body systems: the fractional quantum Hall effect is special because it is the result of a very robust *topological quantum phase*.

4.4 The composite fermion idea

Even though the Laughlin wave function successfully described the states at filling factors $1/m$, plateaus were observed at many fractions not of this form. To attempt to explain

these other fractions, as well as gain some systematic way of obtaining trial wave functions, Jain [9,10] proposed the idea of *composite fermions*. The idea is in essence to imagine that, when the strongly interacting electrons (or generally, fermions) are subjected to a strong magnetic field B, each of the fermions attach to themselves an even number of magnetic "flux quanta" $\phi_0 = h/q$ opposite to the external magnetic field. This definition of flux quantum is borrowed from the field of superconductivity, where the magnetic field inside a loop carrying a supercurrent is actually quantized; there is no quantization of the magnetic field in our case. In a moment we will show that the attachment of an *even* number of flux quanta gives us a composite particle which is also a fermion. In this picture, the composite fermions do not experience the (strong) magnetic field B, but instead a weaker field $B^* = B - 2pn_f\phi_0$ because of the attached flux quanta. We assume that the flux quanta are smeared out such that the field B^* is approximately uniform. Here n_f is the number density of fermions and $2p$ is the number of attached flux quanta per fermion. The fermion filling factor was

$$\nu = \frac{n_f h}{qB} = \frac{n_f \phi_0}{B} \tag{4.4.1}$$

which leads to the composite fermion filling factor

$$\nu^* = \frac{n_f \phi_0}{|B^*|} = \frac{n_f \phi_0}{2pn_f\phi_0 \pm B} = \frac{\nu}{2p\nu \pm 1} \tag{4.4.2}$$

The $\pm$ takes care of the fact that B^* may point antiparallel to B.

Is this picture of flux attachment sufficient for a good description of the physics we are studying here? After all, the "attachment" of magnetic flux quanta to fermions is clearly an oversimplification of the actual, collective behavior of the fermion quantum fluid. Indeed, Jain originally imagined attaching quantized unit vortices to the fermions, and not flux quanta [9]. This distinction turns out not to matter for the CF predictions, because the Aharonov-Bohm phase associated with any closed loop around $2p$ flux quanta is $2\pi\phi/\phi_0 = 4\pi p$. The phase picked up by following a closed loop around around one unit vortex is by definition 2π, thus a closed loop around $2p$ such vortices is naturally $4\pi p$. Moreover, the phase factor on the wave function is $e^{4\pi pi} = 1$, so the attachment of either flux quanta or vortices is not observable in experiments [10]. So, for convenience, one can in fact use the image of either vortex or flux attachment to visualize the physics of the FQHE to some extent.

So what good is it then, to think about composite fermions in an effective magnetic field B^* instead of regular fermions in the field B? Consider the case of all electrons in the LLL, $\nu \leq 1$. Here, the many-particle ground state is highly degenerate in absence of interaction because *all* LLL configurations have the same energy, as we saw in Section 2.2. But at $\nu \leq 1$, there will always exist a choice of p such that $\nu^* > 1$. If we assume that the composite fermions are *non-interacting*, they will form Landau-like levels called Λ-levels [9]. The ground state of the composite fermions at $\nu^* > 1$ must necessarily be a less degenerate state, as more Λ-levels are occupied. In fact, when

$$\nu^* = \frac{\nu}{2p\nu \pm 1} = i \in \mathbb{Z} \tag{4.4.3}$$

the ground state is non-degenerate. This indicates that the composite fermions can be treated as independent to a decent approximation, like we assumed. A consequence is that we can write the many-body CF wave function as an antisymmetric combination of single-CF eigenstates $\eta_i(z, \bar{z})$. For ordinary fermions at filling factor ν, this is commonly

accomplished by writing down a determinant of states known as a Slater determinant. It has the form

$$\Phi_{z,\bar{z}}(\nu) = \begin{vmatrix} \eta_1(z_1,\bar{z}_1) & \eta_1(z_2,\bar{z}_2) & \cdots & \eta_1(z_N,\bar{z}_N) \\ \eta_2(z_1,\bar{z}_1) & \eta_2(z_2,\bar{z}_2) & \cdots & \eta_2(z_N,\bar{z}_N) \\ \vdots & \vdots & \ddots & \vdots \\ \eta_N(z_1,\bar{z}_1) & \eta_N(z_2,\bar{z}_2) & \cdots & \eta_N(z_N,\bar{z}_N) \end{vmatrix} \tag{4.4.4}$$

The concept of flux attachment to turn an ordinary fermion into a composite fermion now attains its quantitative meaning: the CF wave function ansatz is written as a Slater determinant at CF filling factor ν^* times a factor $J_{N,p}$ representing the attached flux quanta, projected into the LLL:

$$\Psi(z) = \mathcal{P}_{LLL}\left(\Phi_{z,\bar{z}}(\nu^*)J_{N,p}\right) \tag{4.4.5}$$

The factor $J_{N,p}$ is known as a Jastrow factor. It is defined as

$$J_{N,p} = \prod_{1\leq i<j\leq N} (z_i - z_j)^{2p} \tag{4.4.6}$$

We can now see how the flux attachment helps the composite fermions become more independent: the factor $\Phi_{z,\bar{z}}(\nu)$ typically goes to zero as r^2 when two particles get within a distance r of each other. Clearly $J_{N,p}$ goes to zero as r^{2p}, which is much faster than the Pauli principle demands even for $p = 1$. And when the particles are kept further apart, the repulsive interactions we consider become weaker. The flux attachment therefore helps screen the composite fermions, leading to a lower total interaction energy. Another very interesting conclusion we can draw from this argument is that the fractional filling factors that were observed in experiments can be seen to correspond to *integer* CF filling factors! For example $\nu = \frac{2}{5}$ corresponds to the CF filling factor

$$\nu = \frac{2}{5} = \frac{\nu^*}{2p\nu^* \pm 1} \tag{4.4.7}$$

that is, composite fermions with $2p = 2$ flux quanta each at filling factor $\nu^* = 2$. The Laughlin states are simply the states where the composite fermions fill the LLL, $\nu^* = 1$. This means that one can think of the FQHE of fermions simply as the IQHE of the composite fermions. The fermions attach to vortices in order to minimize the interaction energy.

4.5 CF wave functions for one-component Bose gas

The quantum Hall effect is truly a fascinating phenomenon to study, and important advances and additions to the understanding of the phenomenon are made even today. However, our present goal is to use this CF formalism to obtain approximations to the eigenstates of the two-species rotating Bose gas. Therefore, we take a more pragmatic stance and view the CF wave functions as trial wave functions to be tested agains exact results (and/or experiments). The main idea is to adapt the CF formalism to bosons by reconsidering the vortex attachment defined by the Jastrow factor (4.4.6): we must attach and *odd* number of vortices to each boson to end up with a composite *fermion*; we work out the details in the following. The subtle conceptual and theoretical consequences of using the CF formalism this way are mostly beyond the scope of this thesis; some discussions are included in the concluding chapters.

To apply the CF formalism to our bosonic gas, let us first consider a gas of one species, such as was studied in Chapter 2. The Jastrow factor is the part of the ansatz that attaches vortices to the particles of the original problem. In FQHE studies, the basic particles are fermions, and we argued that an even number of vortices gave a composite particle that was also a fermion. Now, the basic particles are *bosons*, and we must therefore attach an *odd* number of vortices to each boson in order to turn them into composite fermions. The simplest case is one vortex per boson, giving the Jastrow factor

$$J_N = \prod_{1\leq i<j\leq N} (z_i - z_j) \tag{4.5.1}$$

This is the Jastrow factor we will be using in this thesis, and it contains the essential difference between the CF wave functions for fermions and bosons. Thus, the CF candidate wave functions become

$$\Psi_{CF} = \mathcal{P}_{LLL}\left(\Phi_{z,\bar{z}}(\nu^*)J_N\right) \tag{4.5.2}$$

We know the single-particle eigenstates that go in the Slater determinants, namely the eigenstates we found in Chapter 2:

$$\psi_{n,m}(z,\bar{z}) = N_{n,m} z^m L_n^m\left(\frac{M\omega}{\hbar} z\bar{z}\right)\exp(-\frac{M\omega}{2\hbar} z\bar{z}) \tag{4.5.3}$$

Setting the unit of length to $l = \sqrt{\hbar/2M\omega} = 1$ and dropping the normalization factor, we get

$$\psi_{n,m}(z,\bar{z}) = z^m L_n^m\left(\frac{z\bar{z}}{2}\right)\exp\left(-\frac{z\bar{z}}{4}\right) \tag{4.5.4}$$

These are the η_i that go into the Slater determinant. Note that (4.5.4) contains powers of both z and $\bar{z}$. When these are projected into the LLL by the operator $\mathcal{P}_{LLL}$, the result must be a wave function where the $\bar{z}$ have vanished: remember that the polynomial parts of the states in the LLL were analytic functions. A typical term in (4.5.4) has the form

$$\begin{aligned} & z^m(-1)^k\binom{n+m}{n-k}\frac{(z\bar{z})^k}{(2)^k k!}\exp(-\frac{z\bar{z}}{4}) \\ \propto & \bar{z}^k z^{m+k}\exp(-\frac{z\bar{z}}{4}) \\ \equiv & f(z,\bar{z}) \end{aligned} \tag{4.5.5}$$

If we project this onto an LLL wave function, we get

$$\begin{aligned} \left\langle \psi_{0,m'} \,\middle|\, f(z,\bar{z})\right\rangle &= \int_{\mathbb{C}} \bar{z}^{m'}\bar{z}^k z^{m+k}\exp(-\frac{z\bar{z}}{2})\; d^2\mathbf{r} \\ &= \int_{\mathbb{C}} \bar{z}^{m'} z^{m+k}\left(-2\frac{\partial}{\partial z}\right)^k \exp(-\frac{z\bar{z}}{2})\; d^2\mathbf{r} \\ &= 0 + \int_{\mathbb{C}} \exp(-\frac{z\bar{z}}{2})\left(2\frac{\partial}{\partial z}\right)^k \bar{z}^{m'} z^{m+k}\; d^2\mathbf{r} \\ &= \int_{\mathbb{C}} \bar{z}^{m'}\left[\left(2\frac{\partial}{\partial z}\right)^k z^{m+k}\right]\exp(-\frac{z\bar{z}}{2})\; d^2\mathbf{r} \\ &= \left\langle \psi_{0,m'} \,\middle|\, f(z,2\partial_z)\right\rangle \end{aligned} \tag{4.5.6}$$

We have used integration by parts k times to get from line 2 to line 3, where all boundary terms vanish. The equation means that the action of the projection operator $\mathcal{P}_{LLL}$ is

equivalent to the replacement $\bar{z} \to 2\frac{\partial}{\partial z} = 2\partial_z$ after moving all the $\bar{z}$ to the left of all the z; this is called normal ordering. The exponential is unaffected by the action of this operator, just as it was unaffected by the angular momentum operator in Section 2.3. As a convention for the rest of this thesis, the exponentials are not acted upon by differential operators unless explicitly stated. Therefore we will omit them in most cases. To sum things up, the many-body CF wave functions, adapted for bosons, are

$$\Psi_{CF} = \Phi_{z,2\partial_z}(\nu^*) J_N \tag{4.5.7}$$

where $\Phi_{z,2\partial_z}$ is the projected Slater determinant.

We seek a CF candidate wave function that describes the ground state of the rotating Bose gas at total angular momentum L for a given number of particles N. We know that the degree of the polynomial part of the wave function determines the angular momentum. By counting factors in the expression for J_N, one finds that the degree of the Jastrow factor J_N is

$$L_J = \frac{1}{2}N(N-1) \tag{4.5.8}$$

Thus it is up to us to choose the single-particle wave functions in the Slater determinant that give the correct angular momentum L when acting on the Jastrow factor. We make an important note at this point. The Jastrow factor adds $\frac{1}{2}N(N-1) \sim N^2$ angular momentum to the wave function. The CF formalism is usually applied to electrons in strong magnetic fields, where the angular momentum is typically in this range or even higher. But let us see what happens when we try to create a CF candidate for a system in the low angular momentum regime $L \leq N$. For example, one CF candidate for $N = 4$ bosons at angular momentum $L = 4$ is

$$\Psi_{CF} = \mathcal{P}_{LLL} \begin{vmatrix} z_1 & z_2 & z_3 & z_4 \\ 1 & 1 & 1 & 1 \\ \bar{z}_1 & \bar{z}_2 & \bar{z}_3 & \bar{z}_4 \\ \bar{z}_1^2 & \bar{z}_2^2 & \bar{z}_3^2 & \bar{z}_4^2 \end{vmatrix} \prod_{1 \leq i < j \leq 4} (z_i - z_j) \tag{4.5.9}$$

We see that after projection, the $\bar{z}$ will differentiate the Jastrow factor 3 times, lowering the angular momentum from $1/2 \cdot 4 \cdot 3 = 6$ to 3, and the multiplication of a z will raise it again to 4, giving the correct angular momentum. The single-state diagram for this many-particle state would be

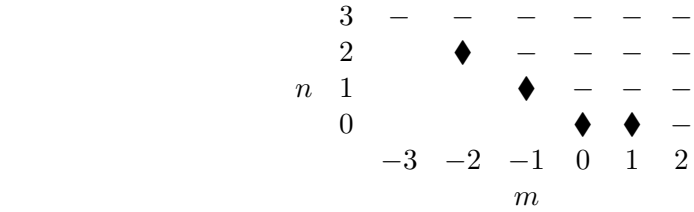

(4.5.10)

where a ♦ signifies an occupied state. But the Jastrow factor was responsible for the favorable screening of bosons from one another: if we differentiate this factor, we might very well destroy the good correlations it provided. This is one of the main points that make the success of CF trial wave functions in this low angular momentum regime (mentioned above) surprising.

At this point there seem to be many, many ways of choosing single-particle states in the Slater determinant if the only constraint is that the total angular momentum should come out correct: the state (4.5.9) was simply one possible choice. These different Slater

determinants are in general not the same wave functions. We will discuss two important constraints on the CF trial wave functions in a later section. For now, we will generalize the CF construction to the main object of study, the two-species Bose gas.

4.6 Two species and pseudospin

As we did in Section 3.6, we take the pseudospin perspective into account, and see which insights it may give. We remember that the building blocks of the eigenstates, $|\chi_\tau\rangle$, were quite complicated when expressed in the number representation. Because of this, we will continue to write the CF functions in coordinate basis. We have N bosons of the first species, which will take the role of pseudospin down, and $M \geq N$ bosons of the second species, representing spin up. We have

$$\begin{aligned} S^2\Psi &= \mathcal{S}(\mathcal{S}+1)\Psi \\ S_z\Psi &= \mathcal{S}_z\Psi \end{aligned} \tag{4.6.1}$$

for eigenfunctions Ψ of the interaction. If Ψ is a CF wave function, the act of pseudospin lowering will correspond to turning a single-particle CF state of the spin-up species into the same state for the spin-down species. Physically, the number of particles of the two species cannot change, of course, since the interaction conserves the particle numbers of each species. That is, we cannot physically talk of turning a particle of one species into a particle of the other species. However, for a given total number of particles $N + M$ and angular momentum L, the pseudospin language makes it natural to define a pseudospin multiplet consisting of all the states at different $M - N$. The quantum number $\mathcal{S}$ of a state Ψ can then be found by counting the number of states in the multiplet with the same energy as Ψ: this number will equal $2\mathcal{S} + 1$. Spin raising/lowering a state thus corresponds to finding a state for a different set of N and M but with the same energy and total spin quantum number. When counting states of equal energy, we have to remember that we have taken $N \leq M$ as a starting point for the theory in this thesis, meaning that we only count "half" of the systems in a multiplet, namely $M - N \geq 0$. This must be considered when calculating $\mathcal{S}$. For example, if there exist states of energy E at $L = 2$ for $(N, M) = (4, 4), (3, 5), (2, 6)$ then we would also find such states at $(5, 3), (6, 2)$ if we allowed the two species to switch roles. So

$$2\mathcal{S} + 1 = 5 \quad \Rightarrow \quad \mathcal{S} = 2 \tag{4.6.2}$$

On the other hand, $\mathcal{S}_z$ is always given by

$$\mathcal{S}_z = \frac{M - N}{2} \tag{4.6.3}$$

It can be shown [9] that the CF construction, taking us from an antisymmetric wave function $\Phi_{z,\bar{z},w,\bar{w}}$ to a symmetric wave function Ψ_{CF} through multiplication by a Jastrow factor and projection to the LLL, commutes with the pseudospin operators as well. Therefore, our CF candidates are eigenfunctions of the pseudospin operators. In Section 4.8 we will see what this entails. The function $\Phi_{z,\bar{z},w,\bar{w}}$ will for our purposes be a simple product of two single-particle Slater determinants, because the interaction does not mix the two species. That is

$$\Phi_{z,\bar{z},w,\bar{w}} = \Phi_{z,\bar{z}}\Phi_{w,\bar{w}} \tag{4.6.4}$$

and we place single-particle wave functions in these Slaters as before. The Jastrow factor attaches one vortex to each boson; in other words, the Jastrow factor makes every boson see a vortex on every other boson, regardless of species. Therefore, the Jastrow factor now becomes

$$J_{N,M} = \prod_{1\le i<j\le N} (z_i - z_j) \prod_{1\le k<l\le M} (w_k - w_l) \prod_{1\le i\le N} \prod_{1\le k\le M} (z_i - w_k) \tag{4.6.5}$$

Counting the number of parentheses gives us the angular momentum of the Jastrow factor: it is

$$L_J = \frac{1}{2}N(N-1) + \frac{1}{2}M(M-1) + NM = \frac{1}{2}A(A-1) \tag{4.6.6}$$

where $A = N + M$ as before. The projection is done the same way as in the single species case, i.e. $\bar{z} \to 2\partial_z$ and $\bar{w} \to 2\partial_w$ after normal ordering. To sum this up, the CF candidates for the two-species Bose gas will look like

$$\Psi_{CF} = \mathcal{P}_{LLL} \left(\Phi_{z,\bar{z}} \Phi_{w,\bar{w}} J_{N,M} \right) \tag{4.6.7}$$

4.7 Compact states

We now discuss the constraints we should place on our trial wave functions to avoid considering all of the very many choices of single particle states one could put in the two Slater determinants. The first constraint we place on our CF candidates is concerned with the fact that the states we found in the previous chapter are translationally invariant. There are certain CF wave functions called *compact states*, that by construction are always translationally invariant [9]. A compact state is a state where a given Λ-level is filled from the lowest value of m without any "holes". Also, an occupied single-particle state at a given n and m must also have all the states for lower n and same m occupied. The following diagrams should make the distinction clear. The state given by the diagram

	3	♦	♦	–	–	–	–
	2		♦	–	–	–	–
n	1			–	–	–	–
	0				♦	♦	–
		−3	−2	−1	0	1	2
				m			

(4.7.1)

is a compact single-species state, because in any Λ-level the states are filled from the left without vacancies. The fact that the $n = 1$ Λ-level is empty is perfectly all right. Also note that there are no vacancies directly underneath any occupied state. On the other hand the state

	3	–	–	–	–	–	–
	2		♦	♦	–	–	–
n	1			♦	–	♦	–
	0				♦	–	–
		−3	−2	−1	0	1	2
				m			

(4.7.2)

is certainly not compact: the state at $(n, m) = (1, 1)$ is missing states to the left of and below it. We verify, using the CF generation code in Appendix A, that the latter is not translationally invariant.

The fact that we only consider compact states makes it possible to simplify the Slater determinants to a great extent. We will show the procedure for the specific case (4.7.1) and argue that it holds in general for compact states. The Slater determinant for this one-species state is

$$\Phi_{z,\bar{z}} = \begin{vmatrix} \psi_{0,0}(z_1,\bar{z}_1) & \cdots & \psi_{0,0}(z_5,\bar{z}_5) \\ \psi_{0,1}(z_1,\bar{z}_1) & \cdots & \vdots \\ \psi_{2,-2}(z_1,\bar{z}_1) & \cdots & \vdots \\ \psi_{3,-3}(z_1,\bar{z}_1) & \cdots & \vdots \\ \psi_{3,-2}(z_1,\bar{z}_1) & \cdots & \vdots \end{vmatrix} \tag{4.7.3}$$

We consider only the first column, drop the index 1 on the coordinates, and use the series expansion of the Laguerre polynomials to get:

$$\Phi_{z,\bar{z}} = \begin{vmatrix} 1 \\ z \\ \frac{1}{2}\bar{z}^2 \\ -\frac{1}{6}\bar{z}^3 \\ \frac{1}{2}\bar{z}^2 - \frac{1}{6}\bar{z}^3 z \end{vmatrix} \tag{4.7.4}$$

Now we remember that row operations only changes an overall factor of the determinant. That does not matter here because we are not working with normalized wave functions to begin with; the equalities will hold up to an unimportant overall factor. We see that we can subtract row number three from row number five, and also multiply each row with their denominators and signs giving

$$\Phi_{z,\bar{z}} = \begin{vmatrix} 1 \\ z \\ \bar{z}^2 \\ \bar{z}^3 \\ \bar{z}^3 z \end{vmatrix} \tag{4.7.5}$$

We realize that such elimination of terms from a given row would not be possible if states are allowed to have vacancies "below" them; this is the structure of Laguerre polynomials. In our example, the state at $(n,m) = (2,-2)$ below $(3,-2)$ allowed the simplification.

The next step is to consider projection. We make the replacement $\bar{z} \to 2\partial_z$ and forget about the factors of 2, giving rows of the form $\partial_z^n z^{n+m}$. By acting on a test function $f(z)$ we see that

$$\partial_z^n \left(z^{n+m} f(z) \right) = \partial_z^{n-1} \left[(n+m) z^{n+m-1} f(z) + z^{n+m} \partial_z f(z) \right] \tag{4.7.6}$$

that is,

$$\partial_z^n z^{n+m} = (n+m)\partial_z^{n-1} z^{n+m-1} + \partial_z^{n-1} z^{n+m} \partial_z \tag{4.7.7}$$

The point is that the first term on the right hand side of this equation can be found in the state "below" as well! For instance, row number five becomes

$$\partial_z^3 z = \partial_z^2 + \partial_z^2 z \partial_z \tag{4.7.8}$$

and the first term on the right hand side can be eliminated by subtracting the third row, corresponding to the state "below". The result of this was that we were able to move one

differential to the right of the coordinate z in the last term. If we repeat this procedure we get

$$\partial_z^2 z \partial_z = \partial_z^2 + \partial_z z \partial_z^2 \tag{4.7.9}$$

which can again be eliminated. The end result is that we are able to move all the derivatives to the right, that is

$$\Phi_{z,\bar{z}} = \begin{vmatrix} 1 & \cdots & 1 \\ z_1 & \cdots & z_5 \\ \partial_{z_1}^2 & \cdots & \partial_{z_5}^2 \\ \partial_{z_1}^3 & \cdots & \partial_{z_5}^3 \\ z_1\partial_{z_1}^3 & \cdots & z_5\partial_{z_5}^3 \end{vmatrix} \tag{4.7.10}$$

We see that we no longer need to compute the single-particle states at all: a particle in the state $\psi_{n,m}$ simply means a row of the form $z_i^{n+m}\partial_{z_i}^n$ in the Slater determinant. A special case appears when we only put one CF in each Λ-level: then all the states are of the form $\psi_{n,-n}$, and the Slater determinants contain only differentials. To summarize, compact states ensure two things: translational invariance, because states are filled "from the left", and simplified Slater determinants, because they are filled "from below".

4.8 The Fock condition

The constraint that we only consider compact states as our CF candidates greatly reduces the number of possible Slater determinants. However, we can do even better. As we have pointed out, the states Ψ we are trying to model are eigenstates of the pseudospin operator S^2. In many cases where a CF candidate is a good approximation to the exact ground state of a system, the ground state is a so-called *highest weight* state. This means that the total pseudospin is purely in the "z direction", that is,

$$\mathcal{S} = \mathcal{S}_z \tag{4.8.1}$$

This is a consequence of the famous Hund's first rule, applied to bosons in our case: minimizing repulsive interaction by selecting an antisymmetric spatial part of the wave function leads to an antisymmetric pseudospin part as well, i.e. the lowest possible value of $\mathcal{S}$ [8]. We saw in Section 3.6 that the ground states satisfy (4.8.1) when $N \leq L \leq M$. It can be shown [9] that a CF state has $\mathcal{S} = \mathcal{S}_z$ if and only if it satisfies what is known as *Fock's cyclical condition*, or simply, the Fock condition. The condition is that any attempt to antisymmetrize a pseudospin down coordinate with respect to the pseudospin up coordinates gives a vanishing pair of Slater determinants. That is,

$$\left(I - \sum_{k=1}^{M} P_{\leftrightarrow}(z_i, w_k) \right) \Phi_{\{z_i, w_k\}} = 0 \quad \forall\ i \tag{4.8.2}$$

where I is the identity operator and $P_{\leftrightarrow}$ is the exchange operator, exchanging the two arguments it is given in the function it acts on. The simplest case, and the case we will study most of the time, is when $\Phi_{\{z_i,w_k\}}$ is a product of two Slater determinants. This allows us to reformulate the Fock condition: the single-particle states that are occupied in $\Phi_{z,\bar{z}}$ *must also be occupied in* $\Phi_{w,\bar{w}}$. In a more general case, $\Phi_{\{z_j,w_k\}}$ can be a linear superposition of pairs of Slater determinants. We will use the term Fock states to mean sets of Slater determinants satisfying the Fock condition in this thesis. The Fock states will play an essential role in understanding the eigenstates in the next chapter. The revelation is that *all* ground states can be approximated by states that are either Fock states, or states that are obtained from Fock states by pseudospin lowering.

Chapter 5

Comparing CF states with exact states

All the preliminaries are now in place for us to begin applying the CF scheme to our system of rotating bosons. In this chapter we will only consider homogeneous interaction; Chapter 6 gives a few first steps into the landscape of inhomogeneous interactions. To give a quantitative measure of the comparison of CF wave functions with exact ones, we calculate the *overlap* between them:

$$O = \langle \Psi_{CF} \,|\, \Psi_{exact} \rangle \tag{5.0.1}$$

that is, the inner product of the two wave functions after normalization (see Appendix A for details). First, we create CF candidate wave functions for the states in the subspace $\mathcal{M}$ of Hilbert space that we defined in Chapter 3. We will show that in many cases we get *exact states* using very simple CF wave functions. In those cases where we don't, we will show that it's possible to create CF wave functions with very high overlap against the exact states, focusing on ground states. Then we create CF candidates for angular momentum in the range $M < L \leq N + M$. Since we don't have any analytical results to compare to in this parameter range, we turn to exact numerical diagonalization to get the eigenstates and -energies. We will show that the CF wave functions fare remarkably well also in this regime. The mathematical derivations as well as the Mathematica code used to calculate overlaps and perform the exact diagonalization in this chapter and the next can be found in Appendix A. The results are discussed in the final section of this chapter, and in the Conclusions.

5.1 Notation

We would like to be able to state what single-particle wave functions we put in the Slater determinants of the CF trial wave functions without having to write them out in matrix form. We will employ two kinds of notations in the following. In the general case we need to specify the single particle wave functions $\psi_{n,m}$ that we place in the two determinants. Since the states are uniquely characterized by the two quantum numbers n, m, we will simply define lists of the form

$$\{\{n_1, m_1\}, \{n_2, m_2\}, \ldots, \{n_N, m_N\}\} \tag{5.1.1}$$

to mean the determinant

$$\begin{vmatrix} \psi_{n_1,m_1}(z_1) & \cdots & \psi_{n_1,m_1}(z_N) \\ \vdots & \vdots & \vdots \\ \psi_{n_N,m_N}(z_1) & \cdots & \psi_{n_N,m_N}(z_N) \end{vmatrix} \tag{5.1.2}$$

and equally for w. We call this the *explicit notation* for the determinants.

As we will see in a moment, we will give special attention to states where every Λ-level contains at most one composite fermion. This means that the projected Slater determinants will only consist of powers of differential operators, see Section 4.7. We define the *exponent notation* corresponding to such a Slater determinant in the following way: the tuple $[p_1, p_2, \ldots, p_N]$, $p_i \in \{0, 1, 2, \ldots\}$ symbolizes the Slater determinant

$$\begin{vmatrix} \partial_{z_1}^{p_1} & \partial_{z_2}^{p_1} & \cdots & \partial_{z_N}^{p_1} \\ \partial_{z_1}^{p_2} & \partial_{z_2}^{p_2} & \cdots & \partial_{z_N}^{p_2} \\ \vdots & \vdots & \ddots & \vdots \\ \partial_{z_1}^{p_N} & \partial_{z_2}^{p_N} & \cdots & \partial_{z_N}^{p_N} \end{vmatrix} \tag{5.1.3}$$

and equally for w. Notice that the numbers in the exponent notation directly tells us which Λ-levels are occupied. Equations of the form $[\Phi_z] = [\Phi_w]$ mean that the two determinants have equal exponent notations, even though they concern different species.

5.2 The simple case $N = M = L$

The starting point for our trials with the CF wave functions were the exact ground states for the very special cases $N = M = L$. We will here take an intuitive approach to finding a trial wave function, and argue for the validity of the approach in the next sections. Because the states at $N = M = L$ satisfy $L \leq N$, we know from Chapter 3 that they only contain single particle angular momenta $l = 0$ and $l = 1$. From the last chapter we remember that the Jastrow factor has angular momentum $L_J = \frac{1}{2}A(A-1)$. Thus, to end up with a polynomial that has $L = N = M$ angular momentum, we need to differentiate a total of

$$\begin{aligned} L_S = L_J - L &= \frac{1}{2}(N+M)(N+M-1) - L \\ &= \frac{1}{2}(2L(2L-1) - 2L) \\ &= 2L(L-1) \end{aligned} \tag{5.2.1}$$

times with respect to certain combinations of the variables z and w. Well, since $N = M$, the two Slater determinants should intuitively have identical forms because the interaction treats the two types of particles completely identically in this case. Therefore we let the two Slater determinants differentiate the Jastrow factor $L(L-1)$ times each. $L(L-1)$ happens to be equal to the sum of all even numbers up to the $(L-1)$'th, that is, up to $2(L-1)$. As a first trial wave function, we thus propose the projected Slater determinants

$[0, 2, 4, \ldots, 2(L-1)]$, i.e.

$$\begin{aligned}
\Phi_z &= \begin{vmatrix} 1 & 1 & \cdots & 1 \\ \partial_{z_1}^2 & \partial_{z_2}^2 & \cdots & \partial_{z_N}^2 \\ \vdots & \vdots & \vdots & \vdots \\ \partial_{z_1}^{2(L-1)} & \partial_{z_2}^{2(L-1)} & \cdots & \partial_{z_N}^{2(L-1)} \end{vmatrix} \\
\Phi_w &= \begin{vmatrix} 1 & 1 & \cdots & 1 \\ \partial_{w_1}^2 & \partial_{w_2}^2 & \cdots & \partial_{w_N}^2 \\ \vdots & \vdots & \vdots & \vdots \\ \partial_{w_1}^{2(L-1)} & \partial_{w_2}^{2(L-1)} & \cdots & \partial_{w_N}^{2(L-1)} \end{vmatrix}
\end{aligned} \tag{5.2.2}$$

in the CF trial wave function

$$\Psi_{CF} = \Phi_z \Phi_w J_{L,L} \tag{5.2.3}$$

Let's see how a product of Slater determinants such as $\Phi_z\Phi_w$ acts on the Jastrow factor $J_{L,L}$. The Jastrow factor $J_{L,L}$ contains all possible terms of the form

$$x^0 x^1 x^2 \cdots x^{A-1} \tag{5.2.4}$$

where the x are either z_i or w_k, with no coordinate appearing twice. A symbolic way of writing a term in $\Phi_z\Phi_w$ acting on a term in $J_{L,L}$ is

$$(1 \cdot \partial_z^2 \cdot \partial_z^4 \cdots \partial_z^{2L-2})(1 \cdot \partial_w^2 \cdot \partial_w^4 \cdots \partial_w^{2L-2})(x^0 x^1 x^2 \cdots x^{A-1}) \tag{5.2.5}$$

To see what can come out of this, let's look at an example, say, $N = M = L = 4$. Then we have

$$(1 \cdot \partial_z^2 \cdot \partial_z^4 \cdot \partial_z^6)(1 \cdot \partial_w^2 \cdot \partial_w^4 \cdot \partial_w^6)(x^0 x^1 x^2 x^3 x^4 x^5 x^6 x^7) \tag{5.2.6}$$

It is now clear that the only way this will *not* vanish is if both differential operators of power 6 differentiate with respect to the variables that are raised to the 6th and 7th power, the operators of power 4 differentiate with respect to the variables of power 4 and 5 and so on. And because the operators always act on a variable of the same power or one higher, we are left with only variables of power 0 or 1 after the differentiation: in other words, only $l = 0$ and $l = 1$! This is exactly the sort of ground states we found in Chapter 3, so it might seem like we are on the right track. Moreover, this argument holds for all systems with $N = M = L$. One could ask if there are other ways of distributing the $L(L-1)$ differentiations in the Slater determinants that still treat the two species identically (meaning $[\Phi_z] = [\Phi_w]$). Since the Jastrow factor vanishes when differentiated more than $A - 1$ times with respect to one variable, the other possibilities for $[\Phi_z] = [\Phi_w]$ with $L = 4$ are, in exponent notation

$$[0,1,4,7] \quad [0,1,5,6] \quad [0,2,3,7] \quad [0,3,4,5] \quad [1,2,3,6] \quad [1,2,4,5] \tag{5.2.7}$$

By calculating the CF wave functions of these candidates with Mathematica, or by analyzing the action of the determinants on the Jastrow factor similarly to what we just did, we can compare the CF wave functions with the known ground state. It turns out that the CF state represented by the Slater determinants [0,2,4,6] is *exactly equal* to the ground state given by the expressions in Chapter 3! Another very interesting fact is that all the other six choices of Slater determinants give a vanishing wave function. This is a surprising result for many reasons. Normally one would expect some vanishing CF candidates and

some candidates with varying overlaps. We suspected that the overlaps should be good given previous work on one-component Bose gases (see e.g. [12,13]), but here we get either a vanishing candidate or the exact ground state.

In fact, it is known that for a *one-component gas*, the CF prescription trivially gives the exact ground state for $N = L = 2$ and $N = L = 3$ because of translational symmetry [11]. However, there does not seem to be any triviality of that type connected with the two-species case $N = M = L = 4$. We have found that the CF wave functions resulting from the Slater determinants (5.2.2) give the exact ground states in the cases $N = M = L = 2, 3, 4, 5$ using the Mathematica code in Appendix A, and we believe that this holds *for all* $N = M = L$.

5.3 General CF state diagonalization

We now turn to the other states where exact solutions were given in Chapter 3, namely the ground states and some excited states for all angular momenta $0 \leq L \leq M$ for given N and M. We will primarily be interested in finding ground states, because as we know from Section 3.5, the excited states in $\mathcal{M}$ are related to these. As argued in Chapters 3 and 4, the system can be described in pseudospin language, where the N particles of the first type correspond to pseudospin down, and the M particles of the second type correspond to pseudospin up. When viewed this way, all N and M for a given $N + M$ and L are part of the same pseudospin multiplet, and should be treated together. We remember that the total pseudospin eigenvalue is $\mathcal{S}$ and the "z-component" is $\mathcal{S}_z = \frac{M-N}{2}$.

The general way to make CF predictions for the states in a multiplet of a given $N + M$ will be:

1. Consider the angular momenta $N \leq L \leq M$, where $\min(N, L) = N$. The ground states will then have $\mathcal{S} = A/2 - N = \mathcal{S}_z$, i.e. they are highest weight states (see Section 3.6). This limits us to look at states satisfying the Fock condition.

2. Determine all pairs of Slater determinants that satisfy the Fock condition and give the correct angular momentum L when acting on the Jastrow factor.

3. Compute the CF wave functions for all these pairs of determinants. Generally, there will be some vanishing wave functions, and some Slaters producing equal wave functions.

4. Keep only the unique, non-zero wave functions. This set of wave functions $\{\Psi_{CF}\}$ may or may not be a linearly independent set. If desirable, reduce to a linearly independent set.

5. Diagonalize the interaction operator within the space spanned by $\{\Psi_{CF}\}$. If we are primarily interested in finding ground states, it is sufficient to compute the linear combination of the wave functions $\{\Psi_{CF}\}$ that minimizes the interaction energy, i.e. no diagonalization is necessary.

6. Use pseudospin lowering to find non-Fock states, including ground state candidates at $L < N$ and some excited states at $N \leq L \leq M$.

Let us look at some numbers to get a feel for the computations required to go through the steps outlined above. For $N = 2$, $M = 6$, $L = 8$ the dimension of Hilbert space is 111. The number of possible pairs of Slater determinants that are compact, obey the Fock condition and occupy Λ-levels lower than $n = A$ is 260. We ignore states where Λ-level A or higher is occupied because the Jastrow factor can only take at most $A - 1$ differentiations with respect to one coordinate without vanishing. Even though the 260 candidates are in fact more numerous than the dimension of Hilbert space, only 46 of these are unique and non-zero. Since the time complexity for numerical diagonalization of $n \times n$ matrices is typically $\mathcal{O}(n^3)$ [27], we see that step 5 will be roughly $\left(\frac{111}{46}\right)^3 \approx 2^3 = 8$ times faster than a diagonalization on the full Hilbert space basis. The problem is that we need to compute and store the CF wave functions of *all* the 260 candidates in order to obtain the 46 unique functions. This illustrates the general problem: the number of unique, non-zero CF wave functions will usually be much smaller than the dimension of Hilbert space, often between half as big to about an order of magnitude smaller. But there will be many, many candidates, with number increasing both with system size and angular momentum, which we have little control over until we compute their wave functions. In Appendix A, we discuss a method that reduces the number of candidates by eliminating those that we know will vanish before acting on the Jastrow. This reduces the number of candidate Fock states here from 260 to 90, which is indeed a significant reduction. However, evaluating 90 CF wave functions is still a demanding task for a computer if $N + M$ is larger than, say, 10.

5.4 Primary results, need for simplification

In some cases where both $N + M$ and L are sufficiently small, it is possible to do the computations without overstepping the computer memory, even though the computation of the very many CF candidates in step 3 above takes a lot of time. Our calculations show that, for $N + M = 8$, the states we derived in Chapter 3 can all be reproduced *exactly* by the above procedure. This is one of the main results we have produced. Let us look at the highest weigh-states ($\mathcal{S} = \mathcal{S}_z$) first. In fact, the diagonalization of the interaction operator within the CF subspace gives us *more* than the results we found in Chapter 3: we are able to find excited states with larger energies than those in the subspace $\mathcal{M}$, and these states also have complete overlaps with states from the full diagonalization. We suspect that the few excited states that are not reproduced with the CF diagonalization are not highest weight-states, so it is no surprise that our CF wave functions, bound by the Fock condition, do not reproduce these. We have plotted the exact eigenstates together with those found from CF diagonalization for $N = 1$, $M = 7$, $L = 6$ in Figure 5.4.1. As we claimed, almost all states are captured by the CF diagonalization. The plot has been rotated relative to other energy plots in this thesis for improved visualization of the results.

As stated in step 6 in the procedure, we find states at $\mathcal{S} > \mathcal{S}_z$ by lowering the pseudospin of the highest weight states found in steps 1-5. Generally we will have a linear combination of Fock states, and it is not obvious how to lower them, because there are generally many ways of moving a single-particle state in Φ_w to the same (vacant) state in Φ_z. We therefore make a new set $\{\Psi_{CF}\}_{low}$ of candidate states by taking all possible pseudospin lowered versions of all the states in the set $\{\Psi_{CF}\}$. For example, if a state in $\{\Psi_{CF}\}$ has explicit notation

$$\{\{0,0\}\} \times \{\{0,0\},\{0,1\},\{2,-2\},\{3,-3\}\} \tag{5.4.1}$$

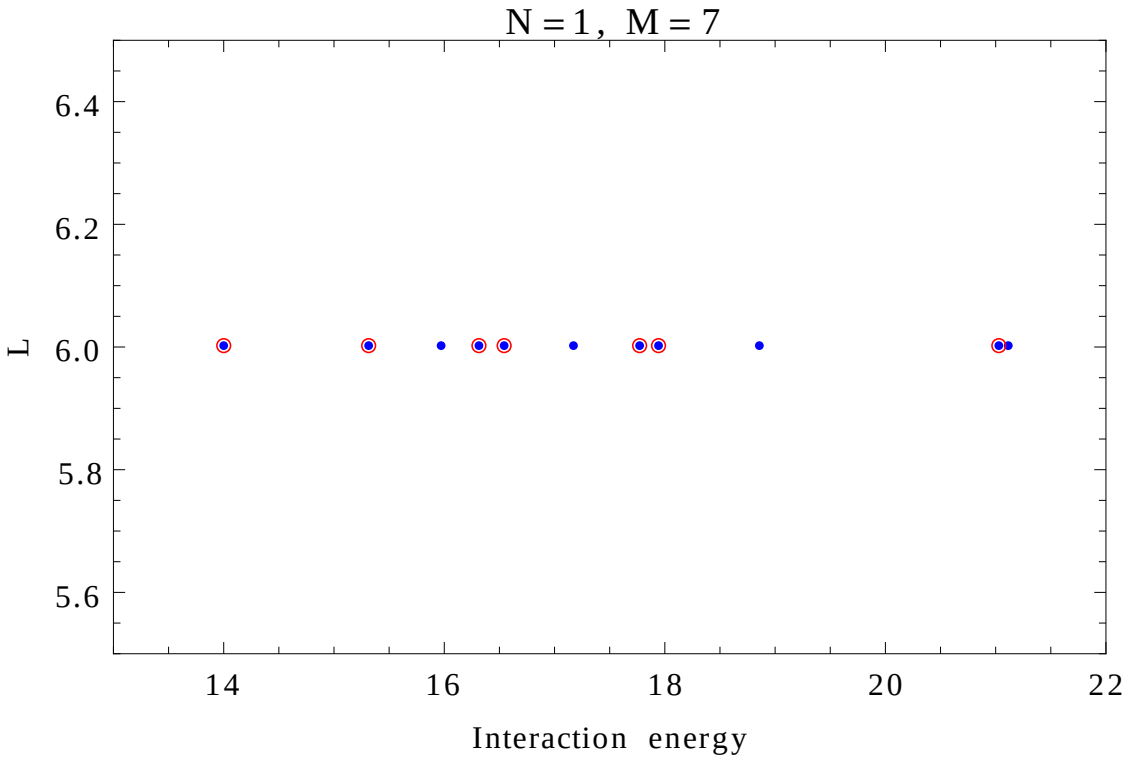

Figure 5.4.1: Comparison of full diagonalization and CF diagonalization. The blue disks are energies from full diagonalization. The red rings are CF diagonalization energies. All CF states are eigenstates of the interaction.

---

then the contributions to the set $\{\Psi_{CF}\}_{low}$ from this state are the states

$$\begin{aligned} &\{\{0,0\},\{0,1\}\} \times \{\{0,0\},\{2,-2\},\{3,-3\}\} \\ &\{\{0,0\},\{2,-2\}\} \times \{\{0,0\},\{0,1\},\{3,-3\}\} \\ &\{\{0,0\},\{3,-3\}\} \times \{\{0,0\},\{0,1\},\{2,-2\}\} \end{aligned} \tag{5.4.2}$$

A very important thing to note here is the fact that pseudospin lowering in this manner may yield states that are not compact. We also note that this new set will be larger than the set $\{\Psi_{CF}\}$. After generating the set $\{\Psi_{CF}\}_{low}$, we go through the steps 3-5 in the procedure again, reducing $\{\Psi_{CF}\}_{low}$ to a set of unique functions and performing the CF diagonalization. Again, we find that the exact states are linear combinations of the unique CF states, this time in the set $\{\Psi_{CF}\}_{low}$.

Complete overlap between CF wave functions and exact states are quite rare, and the fact that it happens in our situation is a manifestation of the simplicity of Hilbert space at $L \leq M$. The states in the subspace $\mathcal{M}$ are particularly simple and we have seen that the general CF procedure reproduces them faithfully. We will see in a later section that complete overlaps are not possible for $L > M$. And while achieving complete overlaps is both a significant feat in itself and also a sign that it may be possible to get good overlaps at higher L, there are some problems with the applicability of the above procedure.

The foremost problem is the huge number of possible pairs of Slater determinants. Whether we only want a specific wave function, for instance the ground state, or the full spectrum produced by CF diagonalization, we need to compute all these candidate wave functions.

```
N=1, M=7, L=7 : CF=[0][0,1,2,3,4,5,6] : OVERLAP = 0.99869
N=1, M=7, L=6 : CF=[0][0,1,2,3,4,5,7] : OVERLAP = 0.995116
N=1, M=7, L=5 : CF=[0][0,1,2,3,4,6,7] : OVERLAP = 0.986095
N=1, M=7, L=4 : CF=[0][0,1,2,3,5,6,7] : OVERLAP = 0.978955
N=1, M=7, L=3 : CF=[0][0,1,2,4,5,6,7] : OVERLAP = 0.916579
N=1, M=7, L=2 : CF=[0][0,1,3,4,5,6,7] : OVERLAP = 1.
N=1, M=7, L=1 : CF=[0][0,2,3,4,5,6,7] : OVERLAP = 1.
N=1, M=7, L=0 : CF=[0][1,2,3,4,5,6,7] : OVERLAP = 1
```

Table 5.1: Overlaps of selected CF candidates and exact ground states, 1+7 particles.

This will in general be almost as challenging or in fact even more challenging (computationally) than doing a full exact diagonalization, because the evaluation of a CF wave function requires a large number of differentiations on a huge polynomial (the Jastrow factor). In addition, the size of the set $\{\Psi_{CF}\}_{low}$, needed to compute the CF prediction for all states with $\mathcal{S} > \mathcal{S}_z$, is usually almost as large or equally large as the set of basis states for the full Hilbert space. Because of this, the usage of full CF diagonalization loses some of its appeal. Is it perhaps possible to remedy this situation? We will give a detailed description of how we find simple CF candidates for ground states in Section 5.5, and a summary of the results in Section 5.6.

5.5 Simple trial wave functions

The fact that (5.2.2) gave us the exact ground state for $N = M = L$ inspires us to look for the other ground states using the same type of CF candidate. Indeed the ground state was a "highest weight" state, clearly visible from the fact that the Slater determinants (5.2.2) satisfy the Fock condition. Another interesting fact is that these Slaters have no two CFs in the same Λ-level. Note that states with more than one CF in each Λ-level are perfectly reasonable states, and *a priori* there are no reasons why we should not consider them, except for the computational issues presented in Section 5.4. As we shall see below, we are actually able to get *very good* overlaps without including them. Therefore we restrict our choice of CF candidates to compact states that have no two composite fermions in the same Λ-level in the following. The Slater determinants will for this reason be expressed in exponent notation. We will call such states *simple states*.

To make the following discussion as concrete and clear as possible, we study the case $N + M = 8$, $0 \leq L \leq M$. As far as possible we will try to keep the arguments valid for the general case. The starting point should perhaps be the $N = 0$, $M = 8$ set of states, as this corresponds to all particles having the same pseudospin, being a simplifying condition. However, $N = 0$ is clearly not a two-species system per se, which is what we are interested in in this thesis. Additionally, such single-species systems have been thoroughly studied in the literature. Therefore we will not consider systems where $N = 0$ in the following, and we begin by computing all the possible CF constructions of the type we are working with for $N = 1$, $M = 7$ particles, and their overlaps with the exact ground states. A selection from this computation can be seen in Table 5.1.

There are three remarkable things about the results of the computation. The first is that, amazingly, all the possible simple states for a given L in fact reduce to the same wave

```
N=2, M=6, L=6 : CF=[0,2][0,2,3,4,5,6] : OVERLAP = 0.997821
N=2, M=6, L=6 : CF=[0,6][0,1,2,3,4,6] : OVERLAP = 0.997821
N=2, M=6, L=6 : CF=[0,3][0,1,3,4,5,6] : OVERLAP = 0.993041
N=2, M=6, L=6 : CF=[0,5][0,1,2,3,5,6] : OVERLAP = 0.993041
N=2, M=6, L=6 : CF=[0,4][0,1,2,4,5,6] : OVERLAP = 0.992753
N=2, M=6, L=6 : CF=[0,1][0,1,3,4,6,7] : OVERLAP = 0.0125939
N=2, M=6, L=6 : CF=[0,3][0,1,2,3,6,7] : OVERLAP = 0.0125939
N=2, M=6, L=6 : CF=[1,2][0,1,2,4,5,7] : OVERLAP = 0.0125939
N=2, M=6, L=6 : CF=[1,4][0,1,2,3,4,7] : OVERLAP = 0.0125939
N=2, M=6, L=6 : CF=[2,3][0,1,2,3,5,6] : OVERLAP = 0.0125939
N=2, M=6, L=6 : CF=[2,5][0,1,2,3,4,5] : OVERLAP = 0.0125939
N=2, M=6, L=6 : CF=[0,2][0,1,2,4,6,7] : OVERLAP = 0.0113219
N=2, M=6, L=6 : CF=[1,3][0,1,2,3,5,7] : OVERLAP = 0.0113219
N=2, M=6, L=6 : CF=[2,4][0,1,2,3,4,6] : OVERLAP = 0.0113219
N=2, M=6, L=6 : CF=[0,1][0,1,2,5,6,7] : OVERLAP = 0.00254563
N=2, M=6, L=6 : CF=[1,2][0,1,2,3,6,7] : OVERLAP = 0.00254563
N=2, M=6, L=6 : CF=[2,3][0,1,2,3,4,7] : OVERLAP = 0.00254563
N=2, M=6, L=6 : CF=[3,4][0,1,2,3,4,5] : OVERLAP = 0.00254563
```

Table 5.2: Overlaps of simple states and exact ground state, 2+6 particles, $L = 6$.

function! This is the reason why we have only included one candidate per L in Table 5.1. The second remarkable thing is that, for $L \leq 2$, the CF wave function *equals the ground state* for that L. That is, as we lower L, the simple state suddenly equals the exact ground state. The third remarkable thing is that all the overlaps are reasonably good. The overlaps for $L = 3$ are maybe not extraordinary, but for higher L the result is rather astonishing in my opinion.

The next step in understanding these pseudospin multiplets is to "flip one spin", i.e. consider the case $N = 2$, $M = 6$, $0 \leq L \leq 6$. When it is possible to construct Slater determinants that satisfy the Fock condition, we know that the states they represent must have $\mathcal{S} = \mathcal{S}_z$. From Table 5.1 we see that these candidates have a good chance of obtaining the highest possible overlap with the exact ground state. There are now many more ways of constructing simple states for a given L: for example, for $L = 6$, there are 18 simple Slater-pairs. However, we know that seemingly different Fock states might produce the same wave function. To investigate whether this was something unique to the case $N = 1$, $M = 7$ or a more general fact, we calculate the overlaps between all the 18 possible simple states and the exact ground state for $L = 6$. The result can be found in Table 5.2. The list has been sorted with highest overlap appearing first.

The new feature of Table 5.2 compared to the $N = 1$, $M = 7$ case is that not all simple states give the same wave function. In fact, we now have six distinct wave functions (six unique overlaps) and neither of them is by itself the exact ground state. We also see a very prominent distinction between two classes of simple states, where three of the distinct states have overlap larger than 99%, while the other three states have less than 2%. The latter may in fact be excited states, but we choose to focus on ground states for now. We find that taking a linear combination of these six distinct states can give us as much as 99.92% overlap for a certain set of coefficient in the linear combination. This occurred for

coefficients

$$\begin{bmatrix} -0.818291 \\ 0.539426 \\ 0.056109 \\ 0.096208 \\ 0.078756 \\ -0.144265 \end{bmatrix} \tag{5.5.1}$$

corresponding to the six distinct wave functions in Table 5.2, sorted in that order. However, one may argue that the improvement from 99.78% to 99.92% overlap is not such a significant improvement, and that one may as well use only the one wave function with the highest overlap as the approximate wave function instead of doing the linear combination. For example, the expectation value of the energy of the state $[0,2] \times [0,2,3,4,5,6]$ is approximately 12.5039. Compared to the exact ground state energy 12.5, the relative error is $3.12 \cdot 10^{-4}$. The linear combination has energy expectation value equal to 12.5 to computer precision, which is about 15 decimal digits. Another point to consider is that, because we have restricted ourselves to look at simple states, we see that there is a finite and relatively small set of possible wave functions that we must calculate for a given system size. For instance, the dimension of Hilbert space for $N = 2$, $M = L = 6$ is 47, while the possible CF candidates we have allowed only counts 18, and the set of *unique* states counts only 6.

For $L = 5$ and $L = 4$ we obtain the same kind of result as for $L = 6$. A relatively large set of Slater determinant pairs are simple states, but they result in only a few unique wave functions, where some have very good overlaps and some have terrible overlaps with the known exact ground state. None are exactly equal to the real ground state. Because of the similarity to $L = 6$, we do not post the lists of overlaps here: they can be reproduced using the code in Appendix A if needed. This trend ends abruptly at $L = 3$: there are 26 different combinations of simple Slater determinants, but the wave functions they result in *are either zero or equal to the exact ground state.* The proof is in Table 5.3. This is found to hold true for $0 \leq L \leq 3$. For $L = 0$ and $L = 1$ the outcome was somewhat special: all candidate wave functions vanished. We will see how to deal with this in a later paragraph.

Table 5.4 shows some results for the rest of the pseudospin multiplet. The full lists of overlaps follow the same pattern that was seen for $N = 2$, $M = 6$ and so we only include the simple states with the highest overlap for a given L. We are now almost in a position where we can summarize the results so far, but first we need to deal with the cases where the CF prescription seems to fail. These are the cases where either all simple states give a vanishing wave function, or it is not possible to create Slater determinants that satisfy the Fock condition at all. An example of the latter is the case $N = M = 4$, $L = 3$. The fact that we cannot make a Fock state must mean that the ground state is not a $\mathcal{S} = \mathcal{S}_z$ state, and we have to create a trial wave function that is not bound by the Fock criterion. When seen this way, it looks like we need to abandon the Fock states and compute *all* the CF candidates for the given N, M and L without knowing which will be good candidates for the ground state. Luckily, this is not the case. The pseudospin analogy tells us that there is *some* N and M in the multiplet $N + M = 8$, $L = 3$ that has $\mathcal{S} = \mathcal{S}_z$, i.e. that satisfies the Fock condition. By looking at the other combinations in the multiplet, $(N, M) = (3,5), (2,6)$ and $(1,7)$, we find that the CF state

$$[0,2,4] \times [0,2,4,6,7] \tag{5.5.2}$$

satisfies the Fock condition, is a simple state, and gives the exact ground state wave function for $L = 3$. Since it is a Fock state, it must have $\mathcal{S} = \frac{M-N}{2} = 1$. By spin lowering this

```
N=2, M=6, L=3 : CF=[0,2][0,2,3,5,6,7] : OVERLAP = 1.
N=2, M=6, L=3 : CF=[0,3][0,1,3,5,6,7] : OVERLAP = 1.
N=2, M=6, L=3 : CF=[0,3][0,2,3,4,6,7] : OVERLAP = 1.
N=2, M=6, L=3 : CF=[0,4][0,1,3,4,6,7] : OVERLAP = 1.
N=2, M=6, L=3 : CF=[0,4][0,2,3,4,5,7] : OVERLAP = 1.
N=2, M=6, L=3 : CF=[0,5][0,1,3,4,5,7] : OVERLAP = 1.
N=2, M=6, L=3 : CF=[0,5][0,2,3,4,5,6] : OVERLAP = 1.
N=2, M=6, L=3 : CF=[0,6][0,1,2,3,6,7] : OVERLAP = 0
N=2, M=6, L=3 : CF=[0,6][0,1,3,4,5,6] : OVERLAP = 1.
N=2, M=6, L=3 : CF=[0,7][0,1,2,3,5,7] : OVERLAP = 0
N=2, M=6, L=3 : CF=[1,2][1,2,3,4,5,7] : OVERLAP = 0
N=2, M=6, L=3 : CF=[1,3][0,1,3,4,6,7] : OVERLAP = 1.
N=2, M=6, L=3 : CF=[1,3][1,2,3,4,5,6] : OVERLAP = 0
N=2, M=6, L=3 : CF=[1,4][0,1,2,4,6,7] : OVERLAP = 1.
N=2, M=6, L=3 : CF=[1,4][0,1,3,4,5,7] : OVERLAP = 1.
N=2, M=6, L=3 : CF=[1,5][0,1,2,4,5,7] : OVERLAP = 1.
N=2, M=6, L=3 : CF=[1,5][0,1,3,4,5,6] : OVERLAP = 1.
N=2, M=6, L=3 : CF=[1,6][0,1,2,4,5,6] : OVERLAP = 1.
N=2, M=6, L=3 : CF=[1,7][0,1,2,3,4,7] : OVERLAP = 0
N=2, M=6, L=3 : CF=[2,3][0,2,3,4,5,6] : OVERLAP = 0
N=2, M=6, L=3 : CF=[2,4][0,1,2,4,5,7] : OVERLAP = 1.
N=2, M=6, L=3 : CF=[2,5][0,1,2,3,5,7] : OVERLAP = 1.
N=2, M=6, L=3 : CF=[2,5][0,1,2,4,5,6] : OVERLAP = 1.
N=2, M=6, L=3 : CF=[2,6][0,1,2,3,5,6] : OVERLAP = 1.
N=2, M=6, L=3 : CF=[3,5][0,1,2,3,5,6] : OVERLAP = 1.
N=2, M=6, L=3 : CF=[3,6][0,1,2,3,4,6] : OVERLAP = 1.
```

Table 5.3: Overlaps of all simple states at 2+6 particles, $L = 3$.

state, we see that we can make the state

$$[0, 2, 4, 7] \times [0, 2, 4, 6] \tag{5.5.3}$$

that has $N = M = 4$, $L = 3$. This state has $\mathcal{S} = 1$ and $\mathcal{S}_z = 0$ because we lowered the spin. The amazing fact is that this state is *exactly equal to the ground state*! So not only have we found a CF candidate that exactly equals the ground state of the system, but we have also learned that, for this L, the ground state is an $\mathcal{S} = 1$ state, and not a highest weight state as the other states have been. We now clearly see the advantage of the pseudospin perspective we have taken. We also realize that generally, given a Fock state at some L, we can use spin lowering on this state to create states with the same energy at other values of N and M in the multiplet. Spin raising a Fock state does not work, because all the pseudospin down-states are already occupied by the pseudospin up-states. Working this way, we can save all the cases where the CF recipe seemed to fail before. For example, the ground state candidate of $N = M = 4$, $L = 1$ (see Tables 5.1 & 5.4) is lowered three times from

$$[0] \times [0, 2, 3, 4, 5, 6, 7] \tag{5.5.4}$$

giving for instance

$$[0, 2, 4, 6] \times [0, 3, 5, 7] \tag{5.5.5}$$

The wave function has complete overlap with the exact ground state. Notice that we could have flipped the spins in lots of different ways here: the reason we chose exactly this form will become clear in a moment.

```
N=3, M=5, L=5 : CF=[0,2,4][0,2,4,5,6] : OVERLAP = 0.993761
N=3, M=5, L=4 : CF=[0,2,4][0,2,4,5,7] : OVERLAP = 1.
N=3, M=5, L=3 : CF=[0,2,4][0,2,4,6,7] : OVERLAP = 1.
N=3, M=5, L=2 : CF=[0,2,6][0,2,3,6,7] : OVERLAP = 0
N=3, M=5, L=1 : CF=[0,2,5][0,2,5,6,7] : OVERLAP = 0
N=3, M=5, L=0 : CF=[0,2,6][0,2,5,6,7] : OVERLAP = 0
```

```
N=4, M=4, L=4 : CF=[0,2,4,6][0,2,4,6] : OVERLAP = 1.
N=4, M=4, L=3 : NO FOCK STATE
N=4, M=4, L=2 : CF=[0,2,4,7][0,2,4,7] : OVERLAP = 0
N=4, M=4, L=1 : NO FOCK STATE
N=4, M=4, L=0 : CF=[0,2,5,7][0,2,5,7] : OVERLAP = 0
```

Table 5.4: Best simple state overlaps, $(N, M) = (3, 5)$ and $(4, 4)$, $L \leq M$.

5.6 Conclusions for $L \leq M$

Based on the data and discussions presented in the previous section we can now make some general statements for the suitability of CF wave functions in the Papenbrock-Reimann-Kavoulakis range of angular momenta.

1. For a given N, M, L we can either find a set of (non-vanishing) simple states, or a set of states obtained from simple states at other values of $M - N$ by spin lowering.

2. If simple states can be found at the given N, M, L, the state with the highest overlap is the state that "looks the most like" the state given for $N = M = L$, Eq. (5.2.2). That is, Φ_z will have the form $[0, 2, \ldots, 2(N-1)]$ and Φ_w must be chosen to give the correct angular momentum L. The other simple states will either reproduce this wave function or a wave function with lower overlap.

3. Any non-vanishing simple state will be equal to the exact state if the angular momentum L is low enough. For $N + M = 8$ (and possibly higher), the statement holds if $L < \min(2N, M)$. In some cases, the simple state also equals the exact ground state if $L = 2N < M$ or $L = M < 2N$.

4. The maximum overlaps one can achieve by taking linear combinations of simple states, regardless of L, are very good, typically higher than 99% for the systems sizes we have studied.

The second statement is simply an observation we have made from producing the lists of overlaps for different combinations of N, M, L. If one does not require the highest precision available when calculating quantities based on these wave functions, we argued in the last section that one can choose to take only the state with the highest overlap as a good approximate wave function, instead of a linear combination. The second statement allows us to find this state without the need of computing all the simple states and comparing their overlaps.

The third statement is again an observation made from computing the lists of overlaps. The abrupt transition from Fock states with many different overlaps to trial wave functions

with either 0 or 1 overlap at $L < 2N$ leads us to believe that this is a systematic feature rather than a coincidence due to small system size. We have found that all the states from Chapter 3 can be reproduced by linear combinations of CF states that are not necessarily simple. We realize that if the dimension of the subspace of unique, non-zero CF states is 1, then the simple state equals the exact state trivially. We believe this is the cause for the transition; at angular momenta as low as $L < \min(2N, M)$, the CF subspace becomes one-dimensional, and contains only one simple state that equals the exact ground state. One normally perceives such low angular momentum states as far beyond the scope the CF formalism, because we are very far away from the quantum Hall regime. We have shown here that the opposite is true: CF trial wave functions work extraordinarily well in this regime. We return to this discussion in the final section of this chapter.

5.7 Higher angular momenta $M < L \leq A$

As we have now analyzed the application of CF trial wave functions to ground states in the angular momentum range $0 \leq L \leq M$, we turn to higher angular momenta $M < L \leq A$. Since we do not know expressions for the eigenstates in this angular momentum regime, we turn to exact numerical diagonalization of the interaction to produce the wave functions and energies. By applying the general CF prediction procedure described in Section 5.3, we find that we are *not* able to achieve complete overlap with the eigenstates of the interaction in this range of angular momenta. Additionally, higher angular momenta means a larger Hilbert space, making the general procedure computationally difficult. But we can still choose to work with simple CF states, and this is the approach we take also in this section. The details of the algorithm that was used are discussed in Appendix A.

As we go to higher L, more and more configurations are available for the bosons, and the coefficients in the ground state polynomial become highly non-trivial. The ground state energies are also no longer given by simple fractions as was the case in the previous section. Therefore one might suspect that the overlaps would start to worsen in this range of angular momenta. However, we find that it is possible to obtain quite good overlaps also in this range. An important difference from $L \leq M$ is that rule number 2 from the last section fails in this higher angular momentum range: to give an example, $[0, 2, 5] \times [0, 2, 3, 4, 5]$ has higher overlap than $[0, 2, 4] \times [0, 2, 3, 4, 6]$. Apart from this, there are no fundamental changes to the way one creates simple states or in their overlaps. To illustrate the combined discoveries from this chapter, we proceed to plot the energies of the simple Fock states with the best overlaps, along with their pseudospin lowered states. These are plotted together with the full energy spectrum that one finds from exact diagonalization, neglecting center-of-mass excitations. The interaction has been taken to be a contact interaction in these plots, that is, we have used

$$v_m = \frac{(-1/2)^m}{m!} \tag{5.7.1}$$

in the interaction defined in Section 3.1. We remember that the details of the repulsive interaction affect the energies, but not the states, and therefore, not the overlaps. The overlaps written below the ground state candidates are the overlaps between single simple states (not linear combinations) and the exact ground states. Remembering that it was possible to improve the overlaps somewhat by taking linear combinations of other simple states at the same N, M, L, we interpret the quoted overlaps as lower bounds on the overlap one can achieve. The plots are seen in Figures 5.7.1, 5.7.2. We use different colors to signify different values of the spin quantum number $\mathcal{S}$ in all plots, as described in the plot insets.

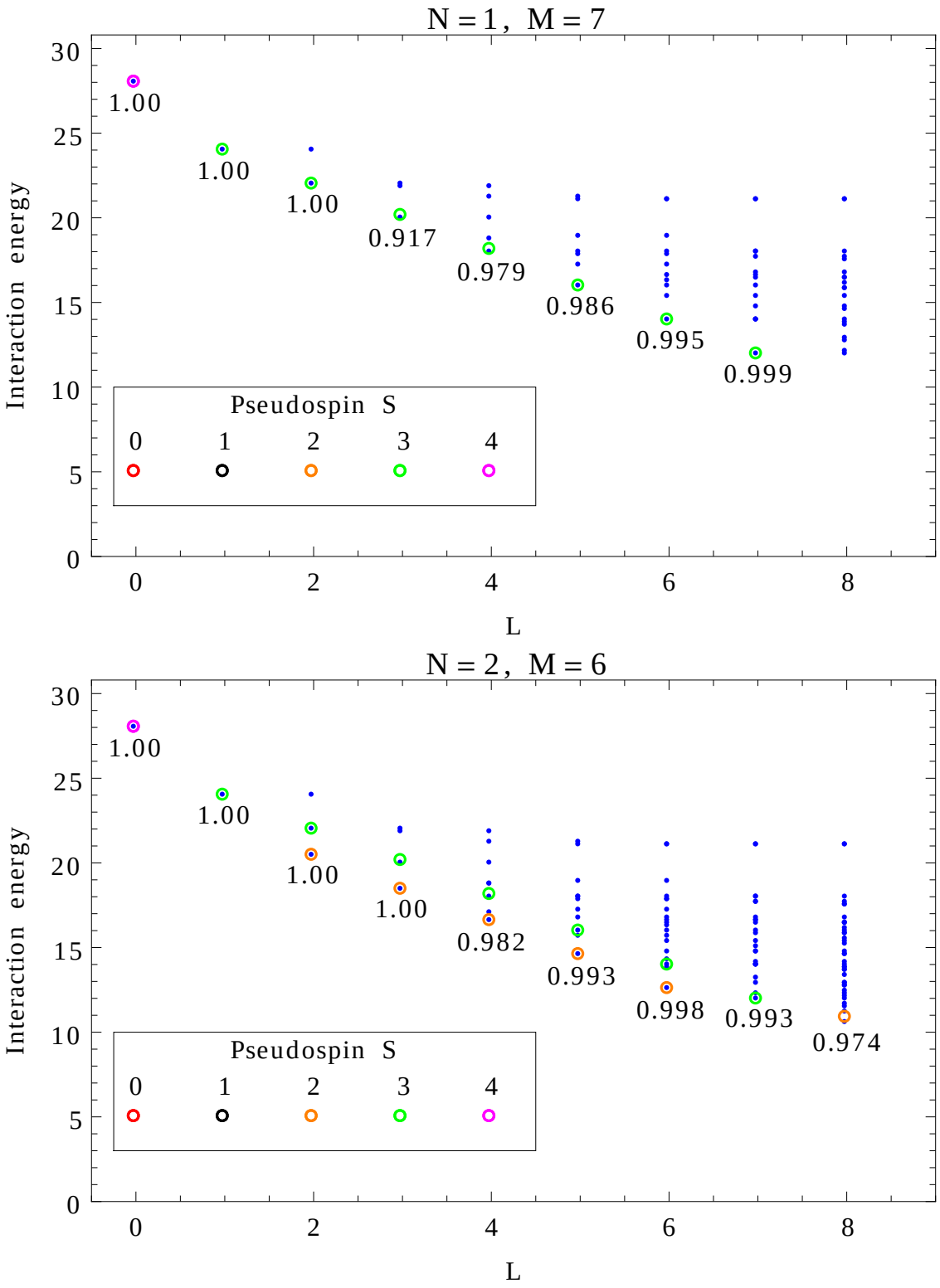

Figure 5.7.1: Plots of simple states and states lowered from simple states, $N = 1$, $M = 7$ and $N = 2$, $M = 6$ particles.

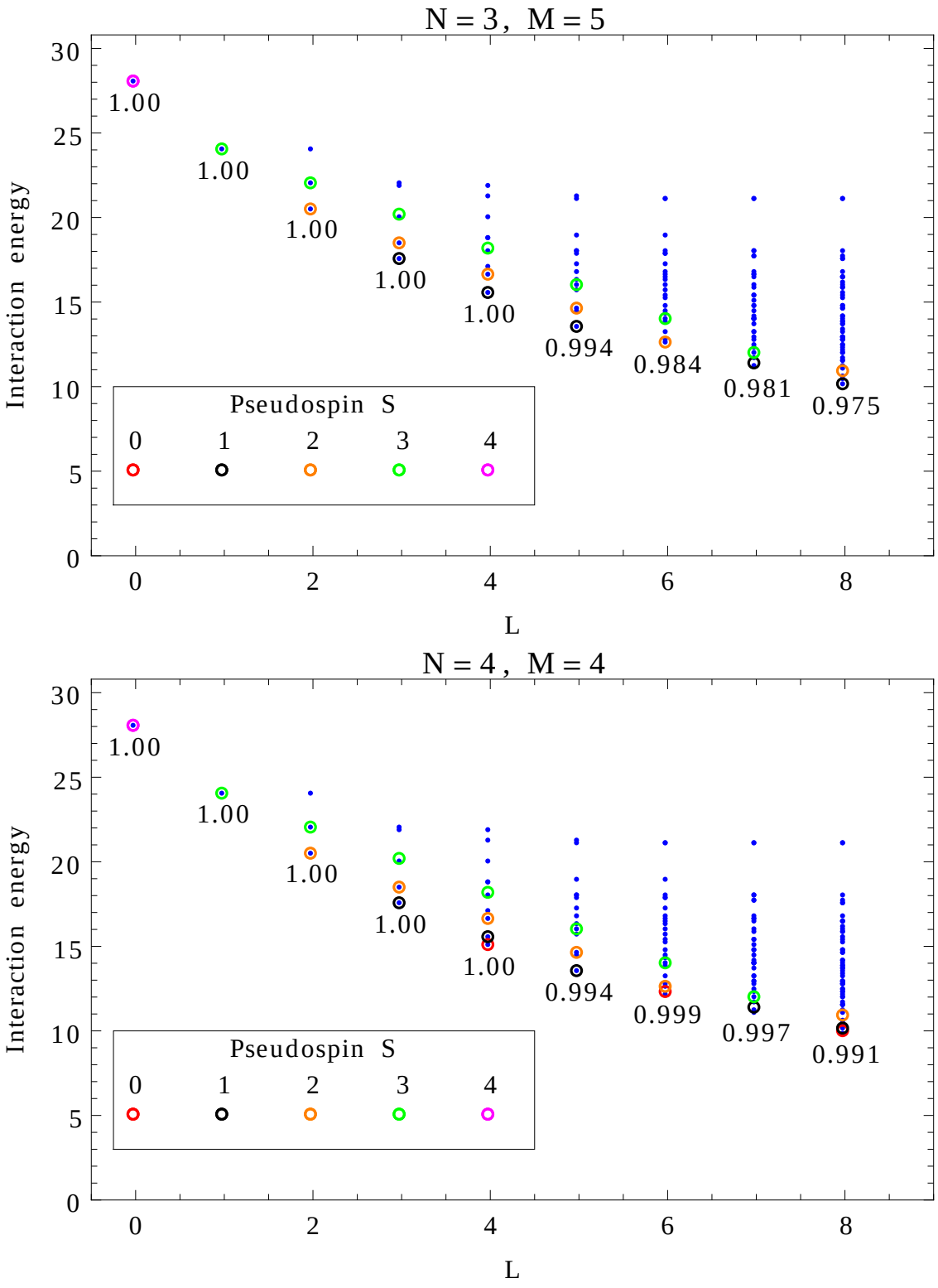

Figure 5.7.2: Plots of simple states and states lowered from simple states, $N = 3$, $M = 5$ and $N = M = 4$ particles.

We are very pleased to see that for all $M - N$ in the multiplet $N + M = 8$ and all $0 \leq L \leq N + M$, there are states given by a simple product of two Slater determinants with very high overlaps with the exact ground states. We also see that spin lowering produces some of the low-lying excitations as well. As already stated, the ground state candidates are either simple states or states lowered from simple states, with *one* exception, which we give special attention. This is the ground state at $N = M = 4$, $L = 7$. One can quickly figure out that it is not possible to create a pair of similar Slater determinants that give $L = 7$ here. A pair of Slaters at $N = M$ adds or subtracts an even amount of angular momentum from the Jastrow factor, and we know that L_J is even for $N = M = 4$. Therefore we would normally assume that its spin is $\mathcal{S} > \mathcal{S}_z$, and use spin lowering from another part of the multiplet. The natural choice is to lower the state $[0, 2, 5] \times [0, 2, 3, 4, 5]$, which has the highest overlap for $N = 3$, $M = 5$, to the state $[0, 2, 4, 5] \times [0, 2, 3, 5]$. But this state actually has an overlap of less than 0.40. To investigate, we look at the energies from the exact diagonalization: they reveal that this is a $\mathcal{S} = 0$ state, so the state must satisfy the Fock condition! The answer comes from creating a linear combination of lowered states:

$$\Phi = [0, 2, 3, 5] \times [0, 2, 4, 5] - [0, 2, 4, 5] \times [0, 2, 3, 5] \tag{5.7.2}$$

This looks very much like a spin singlet state

$$|\uparrow\downarrow\rangle - |\downarrow\uparrow\rangle \tag{5.7.3}$$

known from the two-level system of elementary quantum mechanics. This state satisfies the Fock condition, because the terms resulting from antisymmetrization of a z with respect to the w's of the first pair cancel the ones from the second pair. Therefore it is a Fock state, but indeed a more complicated one than those we have been dealing with until now. This state has 0.997 overlap, as seen in Figure 5.7.2. This result may implicate that Fock states that are not just a pair of determinants could become important in describing the states at $L > M$ for larger systems. We will not consider this however, because it complicates matters to such an extent that using trial wave functions seems almost pointless compared to exact diagonalization.

5.8 Occupancy of Λ-levels

We have now seen that the exact ground states can be modeled to impressive precision by composite fermion wave functions that only have singly occupied Λ-levels. Can we explain why we get such good results when only considering these simple trial wave functions? In the lowest angular momentum regime that we studied in Chapter 3, almost all CF states with more than one CF in each Λ-level actually vanish. We understand this by remembering that a CF in Λ-level n entails differentiation of the Jastrow factor n times with respect to one coordinate. Since the Jastrow factor has the form

$$x^0 x^1 \cdots x^{A-1} \tag{5.8.1}$$

where all the x are different z_i and w_k, we see that there is a maximum number of differentiations with respect to any coordinate we can have before the Jastrow vanishes completely. On the other hand, we need to differentiate it quite a bit in order to reduce the angular momentum down to the low values we are considering in this thesis. That is, as we approach lower angular momenta for a given N, M, there are less and less options for single-particle occupancies. It seems that the limit for placing two CFs in any same level is reached when

L becomes less than $\min(2N, M)$. Consider the case $N = 2$, $M = 6$, $L = 4$. Obviously $L = \min(2N, M)$. The simple state with the highest overlap here, about 98%, is given by determinants

$$[0, 2] \times [0, 2, 3, 4, 6, 7] \tag{5.8.2}$$

But there *are* non-zero states with more than one CF per level. In this case there is only one unique such state, and it is given by (for instance)

$$\{\{0, 0\}, \{2, -2\}\} \times \{\{0, 0\}, \{2, -2\}, \{4, -4\}, \{5, -5\}, \{5, -4\}, \{7, -7\}\} \tag{5.8.3}$$

What would happen if we tried to lower the angular momentum of these two CF states? We obviously need to increase the number of differentiations that act on the Jastrow factor. If we go to $L = 3$, where $L < \min(2N, M)$, we can easily manipulate the former state appropriately: we get for instance

$$[0, 2] \times [0, 2, 3, 5, 6, 7] \tag{5.8.4}$$

Table 5.3 shows that the overlap is 1 for this state. The state (5.8.3) is a different story. There is simply no way to get a non-vanishing wave function by rearranging this state so that we keep two CFs in the same Λ-level and get the correct L: the cost of two CFs in the same level is that we need to move another CF into a higher level, destroying the Jastrow factor. We verify this using the Fock state generation code in Appendix A, sorting out the candidates with multiply occupied levels. We plot the number of candidate Fock states and the number of states that have two or more CFs in the same level for the $(N, M) = (2, 6)$ system in Figure 5.8.1. We can easily see that there are no multiply occupied levels at $L < \min(2N, M) = 4$. We have not been able to prove this trend analytically however, mostly because there are generally very many states to consider. Therefore there might exist larger systems that also allow multiply occupied Λ-levels for some $L < 2N$. However, we believe that multiply occupied levels will be frozen out for all system sizes, for sufficiently small $L > 0$.

At higher L, we have seen that it is not possible to get complete overlaps with the exact states, even when taking states with multiply occupied levels into account. However, we have shown that we get very high overlaps even when only considering simple states. That means that, as we raise L, the states that are not simple states start to give significant contributions to the wave functions. But the most important parts (overlap-wise) still come from the states that are simple CF wave functions. This is perhaps the most important result in this thesis.

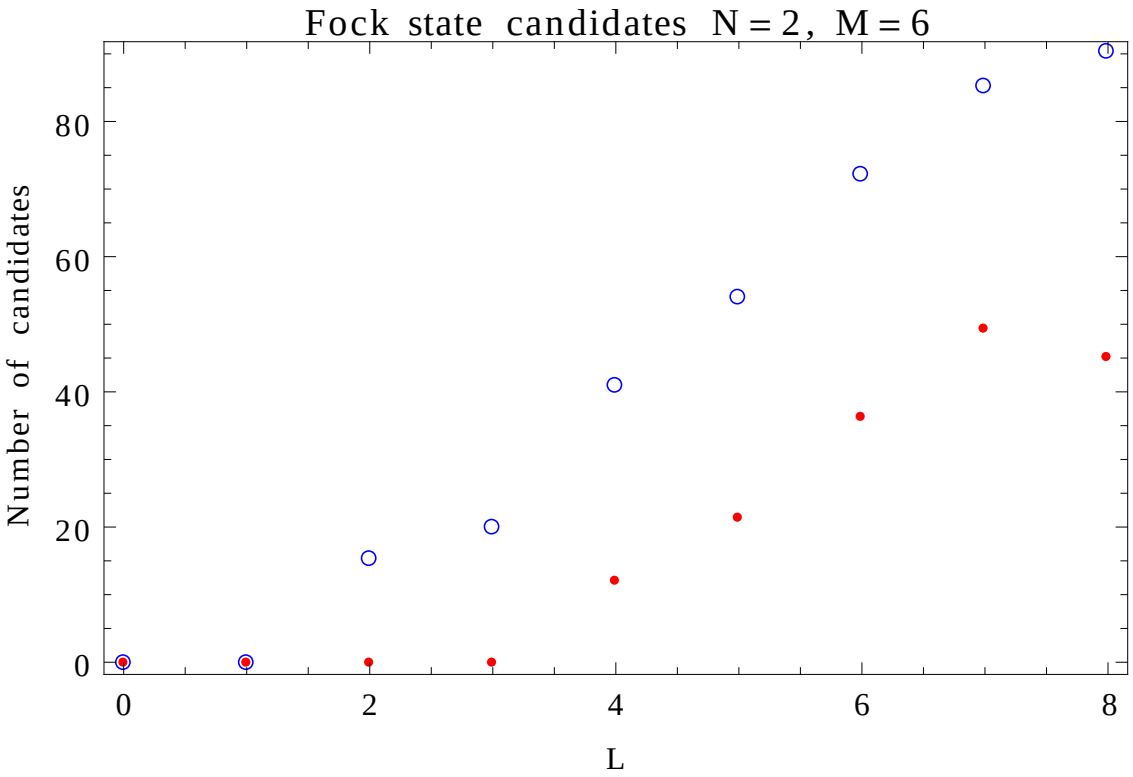

Figure 5.8.1: Numbers of unique Slater determinant configurations. The blue rings represent all allowed Fock states. The red disks represent Fock states with at least one multiply occupied Λ-level.

Chapter 6

Inhomogeneous interaction

In this chapter we will give a brief discussion on the case of inhomogeneous interaction. This is a highly relevant generalization of the homogeneous interaction we have been studying up to this point, because in most experimental situations, the mixture of two species of bosons will not interact completely uniformly. It has been studied very recently by Furukawa and Ueda [28], but in torus geometry and for rotations in the quantum Hall regime. On the other hand, letting the interaction become inhomogeneous breaks many of the symmetries that allowed the analytical derivation of states in Chapter 3, and so the expectations for analytical results in this regime and/or applicability of CF trial wave functions are lower. Therefore, we will not study the case of completely inhomogeneous interaction, but focus on a special case, and also limit the discussion to a certain well-known parameter range.

6.1 The interaction

We will continue to consider pairwise contact interactions modeled by simple delta function potentials as we did in the previous chapters. We will assume that the intra-species interactions are still equal in strength for the two species, but we will allow the inter-species interaction to have a different strength. That is, we will consider the interaction operator

$$V = \sum_{m=0}^{L} v_m(g_1 A_m + g_1 B_m + g_2 C_m) \tag{6.1.1}$$

where the operators A_m, B_m, C_m are still defined as in Section 3.1. We will allow the inter-species interaction strength g_2 to vary from 0 to g_1 continuously. There are two reasons for this choice: the first is that the two species have equal intra-species coupling strength: that makes it very unlikely that they should couple stronger to bosons of the other species than to bosons of the same species. The other reason is that the behavior is well known in the two limits $g_2/g_1 = 0$ and $g_2/g_1 = 1$. The latter is of course what we have been studying in the other chapters of this thesis. The former case simply means that the two species are *independent* of one another, meaning that the total wave function is a simple product of two wave functions, one for each species! For this reason, the goal of this chapter is to test an interpolation scheme where we use CF trial wave functions to interpolate between the two known limits. If we factor g_1 out of the sum in the interaction and set it as the unit of energy, the expression for the interaction becomes

$$V = \sum_{m=0}^{L} v_m(A_m + B_m + g C_m) \tag{6.1.2}$$

where $g = g_2/g_1 \in [0, 1]$. We will use $v_m = (-1/2)^m/m!$ corresponding to a simple delta function interaction as before.

6.2 Ground states in the two known limits

We showed in the previous chapter that linear combinations of CF wave functions satisfying the Fock condition give the exact ground states for $N \leq L \leq M$, and that the ground states at $L < N$ can be found by spin lowering of Fock states "higher up" in the multiplet. We want to take the simplest possible (non-trivial) starting point for our interpolation scheme, and choose to study the states where $N = M = L$. In the limit $g = 1$, we know that the ground state is given exactly by the CF state with Slater determinants

$$[0, 2, 4, \ldots, 2(L-1)] \times [0, 2, 4, \ldots, 2(L-1)] \tag{6.2.1}$$

This can be expressed in terms of symmetric polynomials as

$$\Psi_{L,L,g=1}(z, w) = \sum_{\lambda=0}^{L} c_\lambda^{(L)} e_\lambda(z) e_{L-\lambda}(w) \tag{6.2.2}$$

where we remember that projection P_0 is not necessary (Section 3.5). The coefficients can be found from the formula [8]

$$c_\lambda^{(L)} = (-1)^\lambda \frac{(M-N+\lambda)!(N-\lambda)!}{(M-L)!N!} \tag{6.2.3}$$

which for $N = M = L$ gives the very simple result

$$c_\lambda^{(L)} = (-1)^\lambda \frac{\lambda!(L-\lambda)!}{L!} = (-1)^\lambda \left(\frac{L!}{\lambda!(L-\lambda)!}\right)^{-1} = (-1)^\lambda \binom{L}{\lambda}^{-1} \tag{6.2.4}$$

This gives a formula for the ground state wave function:

$$\Psi_{L,L,g=1}(z, w) = \sum_{\lambda=0}^{L} (-1)^\lambda \binom{L}{\lambda}^{-1} e_\lambda(z) e_{L-\lambda}(w) \tag{6.2.5}$$

What about the other limit, $g = 0$? The total wave function should be a simple product of two *one-species* wave functions:

$$\Psi_{N,M,L,g=0}(z, w) = \Psi_{N,L_1}(z) \Psi_{M,L_2}(w) \tag{6.2.6}$$

where $L_1 + L_2 = L$. These one-species wave function have been studied in great detail in the literature [13,14,19] and are known to be given by

$$\Psi_{N,L}(z) = e_L(z - Z) \tag{6.2.7}$$

where Z is the center of mass for the species z,

$$Z = \frac{1}{N} e_1(z) \tag{6.2.8}$$

The same obviously holds for the other species w. The ground state is degenerate when $g = 0$, and the states with the lowest energy are

$$\Psi(z, w) = e_\lambda(z - Z) e_{L-\lambda}(w - W) \tag{6.2.9}$$

where $\lambda = 0, 2, 3, 4, \ldots, L-3, L-2, L$. The reason $\lambda = 1$ and $\lambda = L-1$ do not appear is simply because the wave functions will vanish in these cases:

$$e_1(z - Z) = \sum_{i=1}^{N} (z_i - Z) = \sum_{i=1}^{N} \left(z_i - \frac{1}{N}(z_1 + \cdots + z_N) \right) = 0 \tag{6.2.10}$$

Any normalized linear combination of these states will also be a state with the ground state energy, so it will be up to us to decide what such combination the interpolation should give in this limit. We would like the total wave function to satisfy the Fock condition, based on the results in Chapter 5. Note that for g in the range $(0, 1)$, the interaction eigenstates will in general not be eigenstates of the pseudospin operators at all, so it is not obvious that we should demand that the CF candidates satisfy the Fock condition. We choose this form simply because the CF candidate that give the exact ground state at $g = 1$ has this form, and because the interaction still treats the two species in a somewhat symmetric manner, leading us to believe that the ground states are highest weight states.

6.3 Trial wave functions at $g = 0$

The CF predictions in this limits are also products of two one-component wave functions. To find a CF trial wave function for the states (6.2.9) we produce CF candidates for the one-component functions

$$e_\lambda(z - Z) \quad \text{and} \quad e_{L-\lambda}(w - W) \tag{6.3.1}$$

We mentioned the one-component CF wave functions in Chapter 4, and we show the way they are created for the z species. The CF wave functions are

$$\Psi_{CF}(z) = \mathcal{P}_{LLL} \left(\Phi_{z,\lambda} J_N \right) \tag{6.3.2}$$

where $\Phi_{z,\lambda}$ is a Slater determinant resulting in $\Psi_{CF}(z)$ having angular momentum λ, and

$$J_N = \prod_{1 \le i < j \le N} (z_i - z_j) \tag{6.3.3}$$

for bosons. Since this Jastrow factor carries $L_J = N(N-1)/2 = L(L-1)/2$ we need to make a determinant Φ with angular momentum

$$L_\Phi = \lambda - L_J = \lambda - \frac{1}{2} L(L-1) \tag{6.3.4}$$

To accomplish this, we begin by placing one composite fermion each in the Λ-levels $n = 0, 1, \ldots, N-1 = 0, 1, \ldots, L-2$. This determinant would have carried negative angular momentum $L_\Phi = -(L-1)(L-2)/2$. We need to figure out in which Λ-level to place the final composite fermion. The available states for this last CF are $(n, -n+1)$ for $n = 0, 1, \ldots, L-2$ and $(n, -n)$ for $n \ge L-1$. Placing it in a state $(n, -n+1) = (1-m, m)$ gives us $L_\Phi = -(L-1)(L-2)/2 + m$, and we get the equation

$$\lambda - \frac{1}{2} L(L-1) = -\frac{1}{2}(L-1)(L-2) + m \tag{6.3.5}$$

The solution is

$$m = \lambda + 1 - L \tag{6.3.6}$$

That is, to get the correct angular momentum λ, we place the last CF in the single-particle state $(L-\lambda, \lambda+1-L)$. To make a compact state, we see that this expression only holds if

$$\begin{aligned} L-\lambda &\leq L-2 \\ \lambda &\geq 2 \end{aligned} \tag{6.3.7}$$

We have seen that $\lambda = 1$ does not occur, and $\lambda = 0$ corresponds to the exponent notation $[0, 1, 2, \ldots, L-1]$. This last CF state is simply equal to 1 after normalization, matching perfectly $e_0(z - Z) = 1$.

What about other sets of single-particle states? We know already that different choices will generally give different wave functions. To check this, we use a modified version of the Fock state generation code in Appendix A. For the angular momenta $L = 3, 4, 5, 6$ we find that they all reduce to the same wave functions or vanish. This makes matters simpler for us. Indeed, we know from the previous chapter that this was also the case for $g = 1$, and so we anticipated that it might also happen at $g = 0$. A few diagrams make the process easier to visualize. We display the diagrams of single-particle states for $\Phi_{z,\lambda}$ at $N = M = 6$ for $\lambda = 0, 3, 5$:

$\lambda = 0$

	5	♦	–	–	–	–	–	–	–
	4		♦	–	–	–	–	–	–
	3			♦	–	–	–	–	–
	2				♦	–	–	–	–
n	1					♦	–	–	–
	0						♦	–	–
				−3	−2	−1	0	1	2
						m			

$\lambda = 3$

	5	–	–	–	–	–	–	–	–
	4		♦	–	–	–	–	–	–
	3			♦	♦	–	–	–	–
	2				♦	–	–	–	–
n	1					♦	–	–	–
	0						♦	–	–
				−3	−2	−1	0	1	2
						m			

$\lambda = 5$

	5	–	–	–	–	–	–	–	–
	4		♦	–	–	–	–	–	–
	3			♦	–	–	–	–	–
	2				♦	–	–	–	–
n	1					♦	♦	–	–
	0						♦	–	–
				−3	−2	−1	0	1	2
						m			

(6.3.8)

We mentioned in Chapter 5 that the one-component CF wave function is known to equal the symmetric polynomial $e_L(z - Z)$ when $L = 2, 3$. This means that for a total angular momentum larger than $2 \cdot 3 = 6$, the product of two CF trial wave functions will *not* equal the exact ground state. It has been shown [12,13] that the overlaps with the exact ground state seem to increase with N. Therefore we do not expect the trial wave functions to give the ground states exactly when $g < 1$. Out goal will be to create an interpolation process to approximate the ground states at $g \in (0, 1)$ which has the states discussed in the last two sections as limits when $g = 0$ or 1.

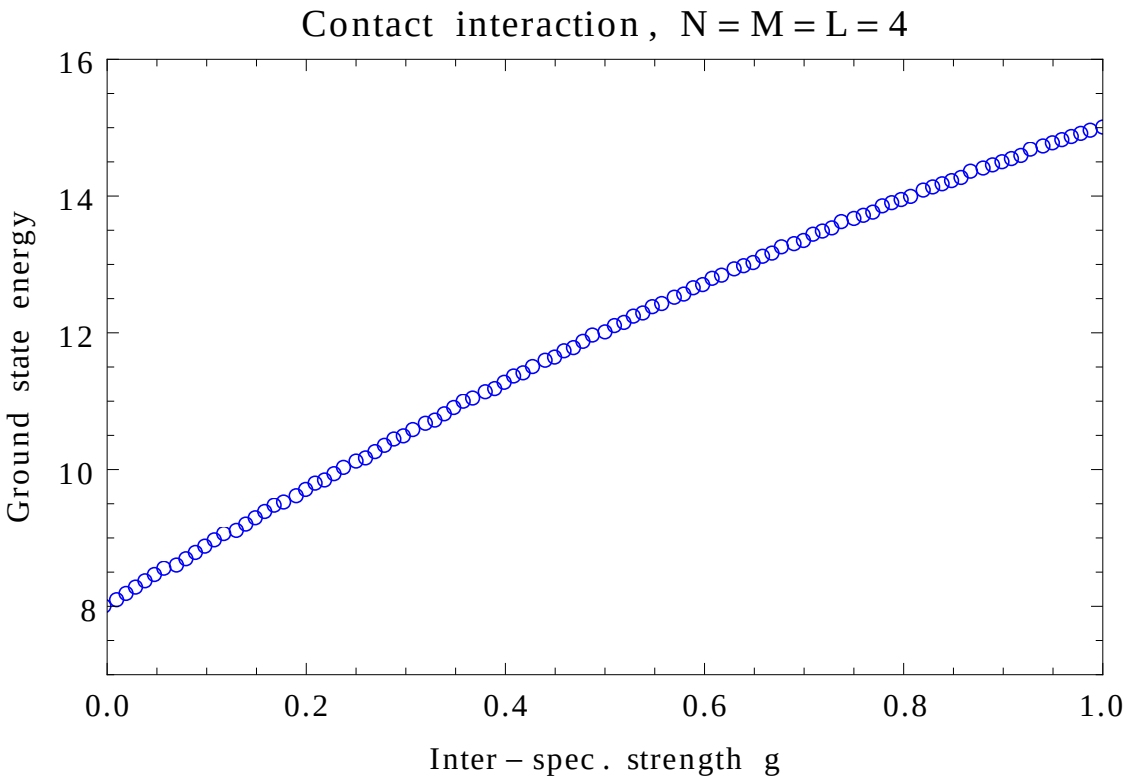

Figure 6.4.1: Ground state energy vs. g from exact diagonalization, calculated for 100 values of $g \in [0, 1]$.

6.4 Exact ground state energies

Before giving the interpolating trial wave functions, we would like to know something about how the ground states vary as a function of g. We choose to calculate and plot the ground state energies for various values of g in the range $[0, 1]$ using exact diagonalization. We made a script that runs the diagonalization code in Appendix A with $g = i/100$, $i = 0, 1, \ldots, 100$. The ground state energies were then plotted against the values of g. Figure 6.4.1 shows the result.

We see that the energy varies rather smoothly with g and seems to be parabolic. We let Mathematica find a least-squares quadratic fit, and we get

$$E(g) = 7.96276 + 9.0732g - 2.01899g^2 \tag{6.4.1}$$

with $R^2 = 0.999999$. The statistic R^2 measures how well $E(g)$ fits the data, and is given by

$$R^2 = 1 - \frac{\sum_i (E_i - E(g_i))^2}{\sum_i (E_i - \overline{E})^2} \tag{6.4.2}$$

where E_i is the computed energy expectation value at $g = g_i$ and

$$\overline{E} = \frac{1}{N} \sum_i E_i \tag{6.4.3}$$

is the mean value of the calculated expectation values. We see that a perfect fit, e.g. $E(g_i) = E_i$ entails $R^2 = 1$, meaning that (6.4.1) is a very good fit to the calculated

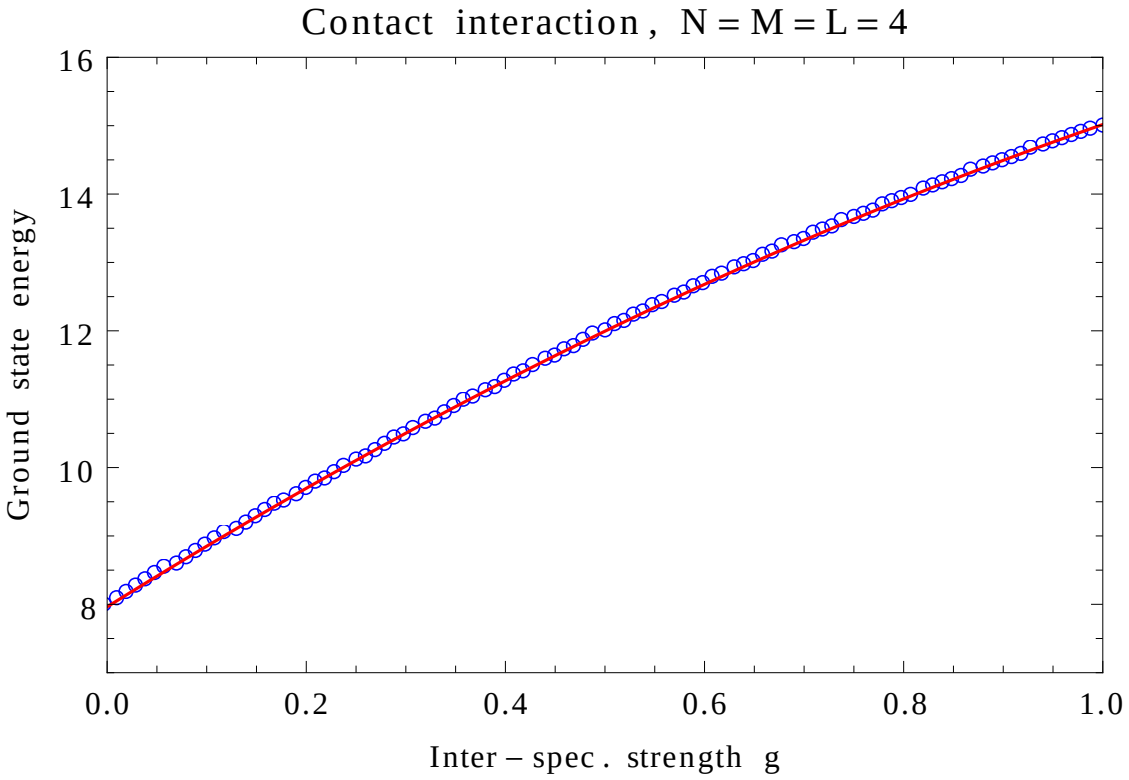

Figure 6.4.2: Quadratic fit to the ground state energies.

data. The function $E(g)$ is plotted together with the data points in Figure 6.4.2. When creating the trial wave functions in the next sections, comparison with these plots will be an important way of checking the validity of the trial functions.

6.5 A naive interpolation

The simplest interpolation we can think of is based on the energy distribution in Figure 6.4.1. To reproduce this plot, we naively interpolate the ground states at intermediate g by a linear combination of the states we already know, namely the states at $g = 0$ and $g = 1$:

$$\Psi_g(z, w) = f(g)\Psi_{g=0}(z, w) + h(g)\Psi_{g=1}(z, w) \tag{6.5.1}$$

The state at $g = 0$ is chosen to be the state in the degenerate set of ground states (6.2.9) that distributes the angular momentum most equally between the two species. That is, we choose

$$\Psi_{g=0}(z, w) = e_{L/2}(z - Z)e_{L/2}(w - W) \tag{6.5.2}$$

for even L and

$$\Psi_{g=0}(z, w) = e_{(L+1)/2}(z - Z)e_{(L-1)/2}(w - W) + e_{(L-1)/2}(z - Z)e_{(L+1)/2}(w - W) \tag{6.5.3}$$

for odd L. We also normalize the wave functions $\Psi_{g=1}$ and $\Psi_{g=0}$. We demand that the known states are reproduced by this formula, meaning that

$$\begin{aligned} f(0) &= 1 \quad h(0) = 0 \\ f(1) &= 0 \quad h(1) = 1 \end{aligned} \tag{6.5.4}$$

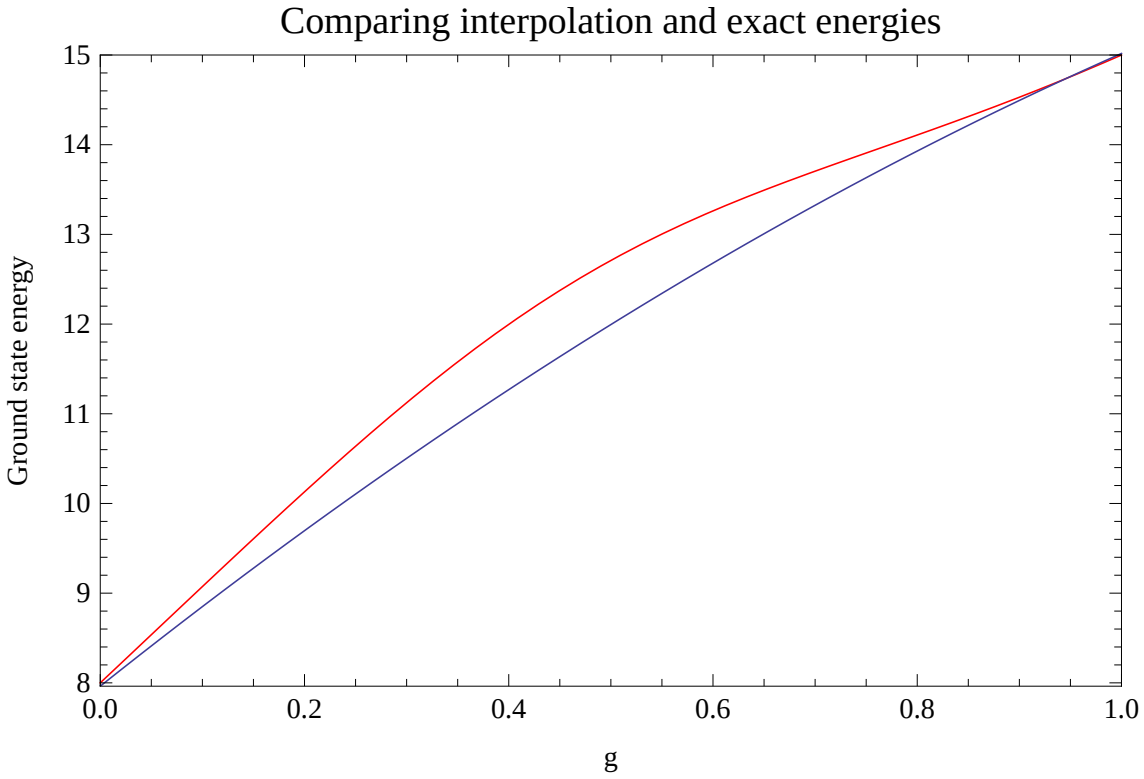

Figure 6.5.1: Expectancy of interaction energy of the naive interpolating function $(1-g)\Psi_{g=0}+g\Psi_{g=1}$. The blue line is the quadratic fit in (6.4.1).

Since we do not (yet) know the physics precisely in the intermediate g-regime, we propose a linear transition from $\Psi_{g=0}$ to $\Psi_{g=1}$ as g grows. This means that

$$\Psi_g(z,w) = (1-g)\Psi_{g=0} + g\Psi_{g=1} \tag{6.5.5}$$

The expectation value of the interaction energy is found in Mathematica for $N=M=L=4$, and we plot it in Figure 6.5.1. We see that the energy approaches the exact ground state energies in the two limits, as we demanded, but does a relatively poor job of approximating the exact energies in the interior region of the plot. Considering the very naive approach we have utilized here, this is to be expected. How about overlaps with exact states? Even if the energy of the state (6.5.5) had a very similar structure to the exact energies, the overlaps might have been good, or they might have been terrible. Of course, the energy is only one out of many observables, and any wave function certainly contains much more information than what its energy is. Calculating the overlap between the state (6.5.5) and the exact ground states for a few values of g results in some overlaps of about 60-70%, and some overlaps that are almost zero. The overlap of order 10^{-12} at $g=0.4$ makes us realize that this method is indeed too simple, and completely unreliable. We therefore discard it, and move on to the next attempt at an interpolating scheme, where the difference between the forms of the CF constructions in the two limits leads to a recipe for interpolation.

6.6 The improved interpolating wave functions

We are now ready to present a more carefully planned interpolation process. When examining the form of the CF wave functions at $g = 1$

$$\Psi_{CF,g=1} = \mathcal{P}_{LLL}\left(\Phi_z \Phi_w J_{N,M}\right) \tag{6.6.1}$$

and at $g = 0$

$$\Psi_{CF,g=0} = \mathcal{P}_{LLL}\left(\Phi_z J_N \Phi_w J_M\right) \tag{6.6.2}$$

we see that the main structural difference is in the Jastrow factor(s). Since Φ_w does not act on J_N in the last equation, we can move it to the right and write out the factors of J explicitly. We get

$$\begin{aligned}
\Psi_{CF,g=1} &= \mathcal{P}_{LLL}\left(\Phi_z \Phi_w \prod_{i<j}(z_i - z_j) \prod_{k<l}(w_k - w_l) \prod_{i,k}(z_i - w_k)\right) \\
\Psi_{CF,g=0} &= \mathcal{P}_{LLL}\left(\Phi_z \Phi_w \prod_{i<j}(z_i - z_j) \prod_{k<l}(w_k - w_l)\right)
\end{aligned} \tag{6.6.3}$$

The products run over the same indices as in previous chapters. The difference is obvious: the factors that correlate pairs of z's and w's are completely absent at $g = 0$, and fully present at $g = 1$. Based on this, we choose the interpolation to be a gradual attachment of factors of the form $(z_i - w_k)$ when raising g from 0 to 1. The way to do this while preserving the symmetry required by the bosonic statistics is to attach *elementary symmetric polynomials* in the *coordinate differences* to $\Psi_{CF,g=0}$: we define a set

$$\mathcal{A} = \{(z_i - w_k) \mid 0 \leq i \leq N, 0 \leq k \leq M\} \tag{6.6.4}$$

and attach the factors

$$e_k(\mathcal{A}) \tag{6.6.5}$$

The two limits $g = 1$ and $g = 0$ correspond to $k = N \cdot M$ and $k = 0$ respectively. The limits are reproduced nicely because

$$\begin{aligned}
e_0(\mathcal{A}) &= 1 \\
e_{N\cdot M}(\mathcal{A}) &= \prod_{i,k}(z_i - w_k)
\end{aligned} \tag{6.6.6}$$

To be able to construct Fock state CF wave functions at $N = M = L$, we notice that the Jastrow-like part of the wave function needs to carry an even number of angular momentum units. Therefore we let k take values $k = 0, 2, 4, \ldots, N \cdot M$. We will be interested in determining what values of k correspond best to what values of g. The fact that the energy of the ground state does not grow linearly in g suggests that the correspondence between k and g is non-trivial.

When lowering the value of k, we obviously need to adjust what single-particle states we place in the determinants in order for the angular momentum to remain L. Since we lower k in steps of 2, we correct for this by moving the composite fermion at $(L - \lambda, \lambda + 1 - L)$, mentioned in the last section, down one Λ-level in both Φ_z and Φ_w. If we have only one CF in each Λ-level, we begin by moving the CF in the highest level to the level below it. Working this way, we are able to find CF candidates for all the cases $k = 0, 2, \ldots N \cdot M$. We

begin at $k = N \cdot M$ where we know that the CF wave function given by $[0, 2, 4, \ldots, 2(L-1)]$ equals the exact ground state. Then, as we lower k to $N \cdot M - 2$, we move the highest level CF down one level in each determinant, i.e. $[0, 2, 4, \ldots, 2(L-1)-1]$. The procedure continues in this manner. In the next section we show the interpolation procedure explicitly for a choice of L.

6.7 The case $N = M = L = 4$

We focus our efforts on this case and show explicitly how to create the interpolating wave functions when $k = 0, 2, \ldots, 16$. We will use both explicit and exponent notation for determinants in this section. We begin at $k = 16$. The starting point for the interpolation is the exact ground state at $g = 1$, given by

$$\Psi_{CF,k=16}(z, w) = (\Phi_{z,2}\Phi_{w,2}) \prod_{i<j}(z_i - z_j) \prod_{k<l}(w_k - w_l) \prod_{i,k}(z_i - w_k) \tag{6.7.1}$$

where $[\Phi_{z,2}] = [\Phi_{w,2}] = [0, 2, 4, 6]$. The state of course corresponds to $g = 1$, and we can calculate the energy using formula in Chapter 3; the energy is $E_{k=16} = 15$. It is interesting however to let Mathematica treat g as a variable, and instead calculate the energy as a function of g. The result is

$$E_{16}(g) = \langle \Psi_{CF,k=16} \,|\, V \,|\, \Psi_{CF,16=0} \rangle = 10 + 5g \tag{6.7.2}$$

We may compare this result to what we get for other values of k and see if there is a systematic behavior. The next step is $k = 14$. The CF trial wave function is

$$\Psi_{CF,k=14}(z, w) = (\Phi_{z,2}\Phi_{w,2}) \prod_{i<j}(z_i - z_j) \prod_{k<l}(w_k - w_l) e_{14}(\mathcal{A}) \tag{6.7.3}$$

where the determinants now have the form $[0, 2, 4, 5]$. The energy is

$$E_{14}(g) = \langle \Psi_{CF,k=14} \,|\, V \,|\, \Psi_{CF,14=0} \rangle = 10.9602 + 4.33243g \tag{6.7.4}$$

We continue to lower k and adjusting the determinants in this fashion. We use the Fock state generator code to check how many unique trial wave functions there are at each k; for $k = 16, 14$ there are only the states we have quoted, but at $k = 12$ there are two distinct states, namely $[0, 2, 3, 5]$ and $[0, 1, 4, 5]$. These have somewhat different energy dependence on g: we will list them in Table 6.1 in what follows. For $k = 10$, the first candidate with more than one CF in a Λ-level appears. The three candidates are $\{\{0, 0\}, \{0, 1\}, \{4, -4\}, \{5, -5\}\}$, $[0, 2, 3, 4]$ and $[0, 1, 3, 5]$. There are generally very few Fock states to choose from, and at most three unique wave functions, for $N = M = L = 4$.

The final state at $k = 0$ deserves special mention, because we remember that there was *a priori* no preference to which of the degenerate ground state basis states (6.2.9) the interpolation should take us to. Table 6.1 shows us that the interpolation gives an energy of exactly 8 at $g = 0$, which is the energy for the states (6.2.9). Upon inspection, the CF state at $k = 0$, which is given by determinants $\{\{0, 0\}, \{0, 1\}, \{2, -2\}, \{3, -3\}\}$, is seen to be exactly equal to the state

$$e_2(z - Z)e_2(w - W) \tag{6.7.5}$$

which is of course an exact ground state. It is delightful to see that the interpolation, whose form was mostly based on the known ground state at $g = 1$, reproduces the known

k	16	14	12	10	8
$E_k(g)$	$10+5g$	$10.96+4.33g$	$10.93+4.38g$ $10.76+4.40g$	$8+10.44g$ $11.00+4.41g$ $10.77+4.42g$	$8+10.44g$ $10.81+4.40g$

k	6	4	2	0
$E_k(g)$	$8+10.44g$ $10.79+4.41g$	$8+10.44g$ $10.79+4.41g$	$8+10.44g$	$8+10.44g$

Table 6.1: Energies as function of g for $k = 16, 14, \ldots 2, 0$. Multiple lines for a given k corresponds to unique Fock states.

lower limit $g = 0$. As mentioned, for $L > 6$, the interpolation would not give the *exact* ground state in the limit $g = 0$, but we see that we would get that CF state which is known to have the highest overlap.

The entries in Table 6.1 are somewhat peculiar. For example, the energy $8+10.44g$ appears at all $k < 12$. These correspond to Fock states with more than one CF in a Λ-level. The adjustment of the determinants apparently cancels the change of the Jastrow-like factor as k is varied; these are all the same wave function! We see that this is not the case for the other energies, which correspond to Fock states with only one CF in any level. We know that the exact ground state energy falls off monotonically as g goes from 1 to 0; from the entries at $k = 12, 10, 8$, it seems that we might need to take linear combinations of the unique states in order to not overshoot the energy of the states we are trying to approximate. A plot will make this point clearer.

We plot the two energy expressions at $k = 8$ together with the quadratic fit of the exact energies. Intuitively, $k = 8$ could correspond to $g = 1/2$ as it is the middle value of the two limits. We see from Figure 6.7.1 that both the interpolating functions give energies that are too large in the middle region of the plot. We choose to investigate this point by calculating some overlaps in the region $g \in [0.4, 0.6]$. We choose the trial wave function to be a linear combination of the two states at $k = 8$, that is,

$$\Psi_{trial}(z, w) = c_1\Psi_1 + c_2\Psi_2 \tag{6.7.6}$$

where

$$\begin{aligned} \Psi_1 &: \{\{0,0\},\{0,1\},\{4,-4\},\{5,-5\}\} \\ \Psi_2 &: [0,1,3,4] \end{aligned} \tag{6.7.7}$$

The calculations show that, for $g < 0.5$ (we chose values 0.40, 0.43, 0.45, 0.48) the overlaps are in fact as bad as they were with the naive approach. The maximum overlap one can achieve by varying c_1, c_2 are of order 10^{-10}. For $g = 0.5$, the situation changes radically. The exact ground state is actually degenerate, with two eigenstates of minimum energy, and the best overlap in the subspace of these two states is 58%. As we let g take even larger values (0.53, 0.55, 0.58, 0.60) the ground state is again non-degenerate, and the best overlap increases monotonically. The weight of the function Ψ_{trial} gradually shifts more and more to Ψ_2 as we raise g, which is to be expected. But the fact remains that, at $g < 0.5$, the trial wave functions at $k = 8$ failed to produce good overlaps with the exact ground state.

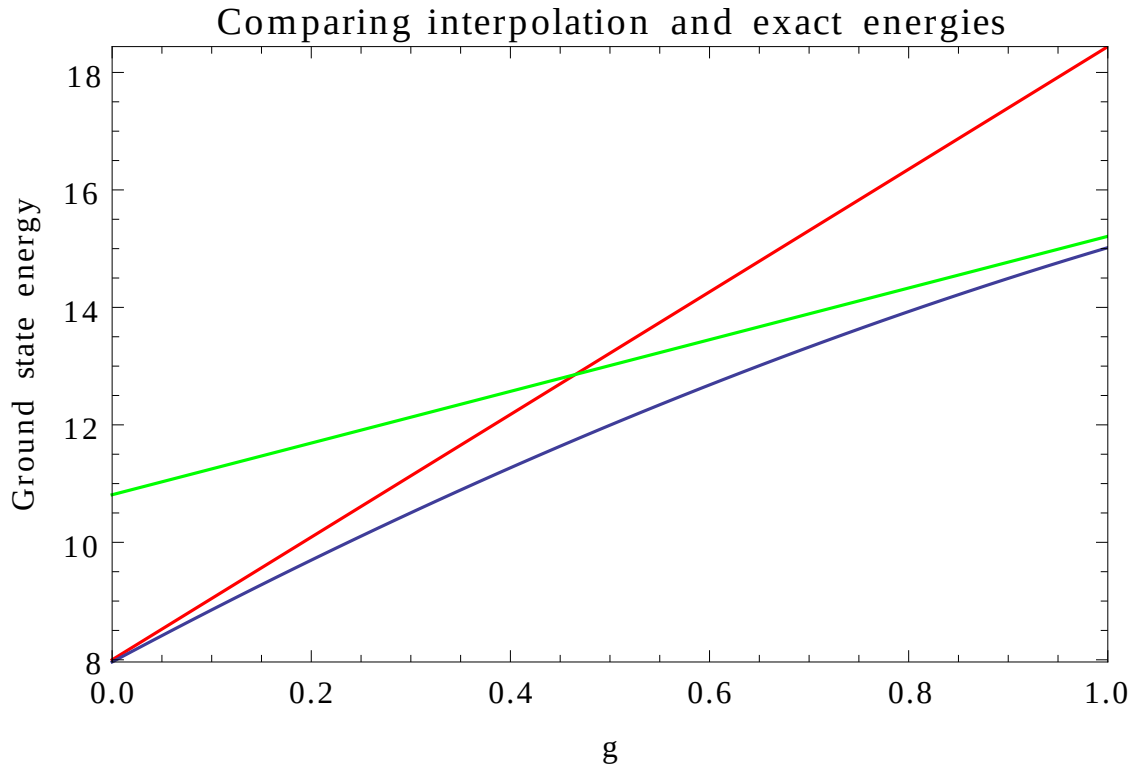

Figure 6.7.1: Comparing exact energies and the two expressions at $k = 8$. The red line is $8 + 10.44g$, the green line is $10.81 + 4.40g$ and the blue line is the quadratic fit (6.4.1)

6.8 Concluding remarks

How can we understand the fact that our interpolation recipe fails so miserably just below $g = 0.5$, while it does a better, but not near satisfactory, job at higher values? We choose to inspect the form of the wave functions to see if we can find a clue to answer this question. We know that the ground state at $g = 1$ only has single-particle angular momenta $l = 0, 1$. That is, all terms in the polynomial are of the form

$$Cx_{i_1}x_{i_2}x_{i_3}x_{i_4} \tag{6.8.1}$$

for $N = M = L = 4$. The x are either z's or w's. When removing factors $(z_i - w_k)$ from $J_{N,M}$ and adjusting the determinants accordingly, we introduce terms with higher single-particle angular momenta. However, the coefficients of these terms are significantly lower than those for $l = 0, 1$, so we can say that contributions to the overlap with another wave function of similar form will still mainly come from the terms (6.8.1). On the other hand, we have seen that all the wave functions with two CF's in the same Λ-level are in fact equal, regardless of k. By inspection, we find that these wave functions have comparable coefficients on all terms, and the terms have single-particle angular momenta $l = 0, 1, 2$.

The exact ground states are not like this for g slightly less than 0.5. In fact, the largest coefficients here are for terms of the form

$$x_{i_1}^2 x_{i_2}x_{i_3}, \quad x_{i_1}^2 x_{i_2}^2 \tag{6.8.2}$$

and also some terms with $l = 3, 4$. On the contrary, the coefficients of terms (6.8.1) are almost zero! This helps explain the almost vanishing overlaps. If we compare with *excited*

states instead, the overlaps actually improve; the overlap with the second excited state at $g = 0.45$ is as high as 0.87. We are therefore forced to make the following conclusion. The interpolation recipe we have designed here is not suitable for approximating the ground states at g far from the limits $g = 0$, $g = 1$. For values of g close to but less than 0.5, a new type of ground state seems to emerge, where configurations of the form (6.8.1) seem to be unfavorable, energetically. Indeed, the interpolation we have developed might somewhat describe excited states in this g-regime. In any case, the interpolation does not fulfill the goals we set, namely to give decent approximations to the ground states, and to establish a connection between the values of g and k. We have, however, been able to see hints of possibly new physics at g slightly less than 0.5. It would be interesting to study the exact ground states in further detail, for instance calculating pseudospin properties, correlation functions or similar observables. With this information at hand one could possibly design better interpolation schemes. This is beyond the scope of this thesis, and is left for future work on the subject.

Chapter 7

Conclusions

In this thesis we have explored the rotational properties of a two-species Bose gas rotating in a harmonic trap. We have used analytical and numerical methods to study the eigenstates of a perturbatively weak repulsive interaction. For a homogeneous interaction, we have derived exact analytical expressions for eigenstates and -energies in a subspace $\mathcal{M}$ of Hilbert space. We showed that linear combinations of trial wave functions from the composite fermion formalism reproduce both these states *and* many of the more excited states, as long as we considered sufficiently low angular momenta $0 \leq L \leq M$. For higher angular momenta $M < L \leq N + M$, the procedure gave good but not exact wave functions and energies. The lowest-lying states were further approximated by very simple CF states, which we showed had good overlaps with exact states also outside the subspace $\mathcal{M}$, i.e. at all L in the range $0 \leq L \leq N + M$. Many ideas were formulated in the language of pseudospin, which is the natural language to use both when understanding the structure of the subspace $\mathcal{M}$, and also when applying the two-component CF formalism.

The fact that the CF wave functions produce exact or nearly exact states *could* be interpreted as a support for the idea that the bosons "capture" vortices and become composite fermions in order to minimize the interaction. In this sense the bosons could be seen to turn into composite fermions in order to take advantage of the combined effects of Pauli exclusion and vortex screening. However, there is some controversy associated with this literal interpretation of the composite fermion ideas. Also, we must remember that the Jastrow factor representing the vortices bound to the bosons is *heavily* manipulated by differential operators as we construct the trial wave functions. In particular, the origin of the exactness of wave functions for $L \leq M$ is not perfectly clear. Since the dimension of Hilbert space decreases with L, it may be a mathematical peculiarity (that we are unaware of) causing such low values of the angular momentum to force the CF predictions to become exact.

For a certain inhomogeneous interaction, we showed that we are somewhat able to predict interaction energies by using an interpolation scheme, but that the wave functions derived from this scheme are poor representation of the exact wave functions. Our results hint at physics that is not captured by the CF wave functions, at least in the manner utilized in Chapter 6, in the intermediate inter-species interaction regime. The inhomogeneous case might be interesting to study further, both because of the possibly novel phases in this situation, and because of the relevance to experiments. We leave this for future work.

In total, the conclusion we can draw from this thesis is that the CF method of making trial wave functions is well suited for two-component rotating bosons with homogeneous

interaction. At the angular momenta we have studied, we have identified certain simple CF wave functions, representing singly occupied Λ-levels. These were shown to be the major contributors to the large overlaps with exact states.

Appendix A

Algorithms and Mathematica code

In this Appendix I will explain the algorithms and display the Mathematica code that was used in the calculations in this thesis. The first sections will contain descriptions of the algorithms that have been used, while the actual pieces of code will be collected in the final section. I have divided the code into smaller parts for two reasons. The first reason is readability, as I hope the ideas behind the algorithms and their implementation will be clearer when separated in this fashion. The second reason is that many calculations were made by combining these smaller code parts into larger pieces of code and/or making small adjustments to the parts, and considering each part at a time therefore reduces repetition.

There are two main reasons that I chose to use Mathematica as the programming language for this thesis. Both reasons stem from the fact that Mathematica is a *symbolic programming language*, meaning that it is able to represent and do operations on mathematical variables without the need to assign numeric values to these variables. The first reason is that the main objects of study in this thesis are polynomials in $N + M$ variables. The symbolic nature of Mathematica lets us input these polynomials as we would write them with pen and paper, and compare, add, subtract, multiply and differentiate (among other operations) these polynomials without the need of representing them as lists of numerical coefficients. This is particularly handy when constructing the CF wave functions, as we shall see. Mathematica also comes with some very useful functions specifically suited to handle polynomials in their symbolic form. For example, the function `PolynomialReduce` will write any polynomial as a linear combination of a given set of basis polynomials. The second reason is that the symbolic nature of Mathematica allows it to represent fractions, radicals and powers of integers *exactly*, without converting them to floating point numbers with a given precision in each sub-calculation. This feature is important to us because we find that some CF wave functions are *exactly* equal to the analytic ground state in the $L \leq M$ regime. Mathematica allows us to be sure that this conclusion is not caused by limited floating point precision.

A note is in order regarding efficiency of the code in this appendix. I am not experienced with symbolic programming or Mathematica beyond the work with this thesis, but I have made some small effort in optimizing the code, beyond it being able to complete the desired computations in a reasonable amount of time. This has involved the use of sparse matrices instead of dense matrices where appropriate, to conserve system memory, and certain exploitations of symmetries instead of "brute force" computations (see Section A.5). The code could probably be optimized to run faster than it does in the current form, but this has been of negligible interest in this thesis as we primarily wanted to bring out the physics and structure of the system.

Comments have been added to the code in places where built-in Mathematica functions have been used, unless the name of the function or its context in the code makes the meaning relatively obvious. The reader is encouraged to use the excellent Mathematica documentation found online to complement the explanations in this appendix.

A.1 Defining variables and quantities

The first code snippet is simply a piece of code that initializes the parameters of the problem and creates variables that will be used in the other pieces of code. When creating CF trial wave functions, all the information about the parameters of the problem is stored in the contents of the Slater determinants. These are normally expressed in exponent notation in the code. When allowing more than one particle in any Λ-level, we use the explicit notation instead, modifying the code that generates Slater determinants accordingly: the difference is discussed in the CF code section. The initialization code can be seen in Algorithm A.1. In the case where we do not compute CF wave functions, for example when computing the Papenbrock-Reimann-Kavoulakis ground states or when doing exact diagonalization of the interaction, we simply remove the definitions of `expolist1`, `expolist2` from the code and manually input `Nn,M,L`. Note that Mathematica reserves the symbol `N` to signify that numerical methods should be used instead of symbolic computation. Therefore the number of particles of the first species is called `Nn` throughout.

A.2 Analytical wave functions

In this section, we implement the results from [8,18], derived in Chapter 3. Algorithm A.2 essentially backtraces the derivations we made: first the β_k are calculated by equating coefficients of powers of λ in the recurrence relation

$$\begin{aligned}&(N\lambda + M(L-\lambda) + 2\lambda(L-\lambda) - \varepsilon_n)\, c_\lambda^{(n)} \\ &+(N-\lambda)(L-\lambda)c_{\lambda+1}^{(n)} + \lambda(M-L+\lambda)c_{\lambda-1}^{(n)} = 0\end{aligned} \tag{A.2.1}$$

using the power series ansatz

$$c_\lambda^{(n)} = \sum_{k=0}^{n} \beta_k \lambda^k \tag{A.2.2}$$

From these, the coefficients $c_\lambda^{(n)}$ are calculated, and the ground state wave function is computed and given the name `phi`.

A.3 Exact diagonalization

Algorithm A.3 was created to find an exact diagonalization of the two-body contact interaction. We start by defining the interaction as it was formulated in Section 31, using the coefficients v_m appropriate for the delta function interaction. Then we create the basis for the Hilbert space,

$$e_{\lambda_1}(z)e_{\lambda_2}(z)\cdots e_{\lambda_k}(z)e_{\mu_1}(w)e_{\mu_2}(w)\cdots e_{\mu_l}(w) \tag{A.3.1}$$

where the degrees of the polynomials λ_i, μ_j must satisfy

$$\sum_{i=1}^{k} \lambda_i + \sum_{j=1}^{l} \mu_j = L \tag{A.3.2}$$

All the sets $\{\lambda\} \cup \{\mu\}$ that satisfy (A.3.2) can be found by letting

$$\sum_{i=1}^{k} \lambda_i = L' \quad \Rightarrow \quad \sum_{j=1}^{l} \mu_j = L - L' \tag{A.3.3}$$

where $L' = 0, 1, \ldots, L$. For a given L', the possible values of λ equal the integer partitions of L', as mentioned in Section 3.2. That is, for $L' = 5$ the possible values of $\{\lambda\}$ are

$$\begin{array}{c} \{5,0,0,0,0\} \\ \{4,1,0,0,0\} \\ \{3,2,0,0,0\} \\ \{3,1,1,0,0\} \\ \{2,2,1,0,0\} \\ \{2,1,1,1,0\} \\ \{1,1,1,1,1\} \end{array} \tag{A.3.4}$$

In our code, the integer partitions are generated with the command `IntegerPartitions`. The number of partitions of a natural number n, $p(n)$, is not a known function in closed form: one must solve a recurrence relation to determine it. Therefore, the dimension of Hilbert space is not straight forward to calculate, and we choose to simply count the number of basis states generated by the above algorithm.

After creating the basis polynomials, they are sorted using Mathematica's `Sort` function, and represented by a set of elementary unit vectors. Then, the action of the interaction operator on each basis polynomial is computed, and the result is projected onto the vector basis using the built-in command `PolynomialReduce`. These projected vectors form the columns of the matrix representation of the interaction operator. This matrix is diagonalized exactly. The function `Eigensystem` yields the eigenvalues and eigenvectors of the matrix, and the numbers are represented *exactly*: note however that finding the eigenvalues E of a $m \times m$ matrix V is equivalent to solving the characteristic equation $\det(V - EI_m) = 0$ where I_m is the $m \times m$ identity matrix. This equation is of degree m, and because of the Abel-Ruffini theorem the exact eigenvalues may not be represented by radicals when $m \geq 5$. Mathematica handles this by representing these eigenvalues as objects called `Root[polynomial,n]` , meaning the `n`'th solution to the equation `polynomial`=0. Using the function `N` one may obtain these eigenvalues as floating point numbers.

When the dimension of Hilbert space becomes somewhat large (say, larger than 30) the diagonalization using exact representation of numbers begins to take a good deal of time. Since there is little use in knowing the exact form of the energies and coefficients beyond visually comparing with the analytical results on a case by case basis, one may very well tell Mathematica to represent the interaction matrix using floating point numbers. This speeds up the diagonalization tremendously, and we have done just this in most calculations. Normally we are most interested in the ground state, and we store the polynomial form of this in the variable `phi`. If needed, one can also export the full spectra to files. This was done for instance when plotting the yrast spectra in Chapters 3 and 5. These are commented by default.

A.4 Generating Fock states

We now turn to the computation of the CF wave functions. These first two pieces of code create all possible pairs of Slater determinants that are compact and satisfy the Fock condition. The first code Algorithm A.4 was used for most of the calculations in Chapter 5, and only considers those states that have singly occupied Λ-levels. Therefore, the Slater determinants in the code are expressed in exponent notation. The code tries all combinations of singly occupied Λ-levels, and returns the ones that satisfy the Fock condition and give the correct angular momentum for a given N, M, L. Note that the highest Λ-level we can possibly occupy without completely eradicating the Jastrow factor is $A - 1$.

The second code, Algorithm A.5 was written to also include multiply occupied levels, in order to more closely examine the exact ground states of both homogeneous and inhomogeneous interaction. The notation here is different: we use the explicit notation, specifying the quantum numbers (n, m) of all occupied single-particle states. Instead of trying all possible combinations of single-particle states, this code fills the Λ-levels in Φ_z from "below", only making compact states. Then the result is copied over to Φ_w, and this is filled with the remaining particles in the same manner. This ensures that the product state obeys the Fock condition. The code then returns the states that end up with the correct angular momentum. In addition to only occupy Λ-levels $n \leq A - 1$, we impose another constraint on the candidates. We recall that the Jastrow factor contains terms of the form

$$x^0 x^1 \cdots x^{A-1} \tag{A.4.1}$$

We know of course that it vanishes if differentiated more than once by a differential operator ∂_x^{A-1}. If we have no such operators in the Slater determinants, it vanishes if acted upon more than *twice* by operators ∂_x^{A-2}; if we have one operator ∂_x^{A-1} then we can only have one ∂_x^{A-2}. In any case, the number of differential operators of degree larger than or equal to $A-2$ is two. The same reasoning applies to all the lower degrees $A-p$: we can have at most p differential operators of degree larger than or equal to $A-p$. The last condition in the final `If`-statement guarantees this. A familiar result can be produced from this code, namely that for all systems with $N = M = L$, the only state returned by the code is the known exact state

$$[0, 2, 4, \ldots, 2(L-1)] \tag{A.4.2}$$

A.5 Computing CF wave functions

Here we explain the code used to actually generate the CF wave functions. It is split in two and displayed in Algorithms A.6 and A.7. Algorithm A.6 displays the code that sets up variables and definitions used during the calculations, and this part does not depend on the specific choice of Slater determinants. First, the Jastrow factor is constructed from definition. Then, a function `MakeSlater` is defined to create Slater determinants from specifications in either explicit or exponent notation. We show the explicit version here, as the exponent version is a simplified case. Finally, lists of all the possible permutations of the particles of each species, and the Mathematica rules one would apply to perform the permutations, are generated. The reason for this is discussed in a moment.

Algorithm A.7 shows the procedure for acting on the Jastrow factor with the operators in the determinants. We explain the method here. The most direct way of computing the wave functions would have been to simply expand the determinants and then

let all terms in the expansion act on the Jastrow factor one by one, adding up the result. However, both the number of factors in the Jastrow and the number of terms in the expanded determinants grow very quickly with N and M, making this method quite time consuming. However there is a clever way about it that exploits the symmetry between particles of the same species. We realize that, for a given set of single-particle states $\{\{n_1, m_1\}, \{n_2, m_2\}, \ldots, \{n_N, m_N\}\}$ to put in the determinant Φ_z, all terms in the expanded determinant will have the form

$$\varepsilon(i_1, \ldots i_N) z_{i_1}^{n_1+m_1} \partial_{z_{i_1}}^{n_1} \cdots z_{i_N}^{n_N+m_N} \partial_{z_{i_N}}^{n_N} \tag{A.5.1}$$

where all permutations of the indices are allowed. The factor $\varepsilon(i_1, \ldots, i_N)$ is the Levi-Civita symbol, giving the sign of the permutation. The same is of course true for the other determinant Φ_w. So instead of letting all these similar terms act on the Jastrow factor, we let the representative term

$$\Phi_z^{rep} = z_1^{n_1+m_1} \partial_{z_1}^{n_1} \cdots z_N^{n_N+m_N} \partial_{z_N}^{n_N} \tag{A.5.2}$$

together with the corresponding term from Φ_w, Φ_w^{rep}, act on the Jastrow factor:

$$\Psi_{CF}^{rep} = \Phi_z^{rep} \Phi_w^{rep} \prod_{i,j} (z_i - z_j) \prod_{k,l} (w_k - w_l) \prod_{i,k} (z_i - w_k) \tag{A.5.3}$$

We then sum up all permutations of z's and w's in Ψ_{CF}^{rep}, and this gives us the complete CF wave function Ψ_{CF}. We actually do not need to worry about the signs ε coming from the permutations here: the sign coming from the permutations of the operator part of the expression will always equal the overall sign induced when permuting the Jastrow factor. That is, the sign from permuting z's will always be the same in the operator part and in the Jastrow part $\prod_{i,j}(z_i - z_j)$, and likewise for permutations of w's. The permutations do not affect the sign of the $(z_i - w_k)$ part of the Jastrow factor. Finally, we divide out any overall constant factor in the wave function. We have chosen to write this code as a function instead of a procedure, because we will need to generate CF wave functions repeatedly when investigating linear combinations of Fock states. If needed, one may change the lines of code that divide out the overall factor to normalize the wave functions instead, if one needs to work with normalized states. The normalization code can be copied from the code that calculates overlaps, see the next section.

A.6 Overlap between states

To compare CF and exact wave functions, we will calculate what is known as the overlap [14] between a pair of wave functions. The overlap O is defined as the inner product of two normalized wave functions ψ_a, ψ_b; in bra-ket notation

$$O = \langle \psi_a \,|\, \psi_b \rangle \tag{A.6.1}$$

If the wave functions are not normalized, we take care of this by remembering that the normalization factor $\mathcal{N}$ of a wave function ψ is given by

$$|\mathcal{N}|^2 = \langle \psi \,|\, \psi \rangle \tag{A.6.2}$$

so the overlap becomes

$$O = \frac{\langle \psi_a \,|\, \psi_b \rangle}{\sqrt{\langle \psi_a \,|\, \psi_a \rangle \langle \psi_b \,|\, \psi_b \rangle}} \tag{A.6.3}$$

We are working with wave functions that, in configuration space, are homogeneous symmetric polynomials of a given degree L times an exponential function. This allows us to write down a formula for the overlap in terms of the coefficients and powers in the polynomial part of the wave function. Let

$$\begin{aligned}\psi_a(z,w) &= F(z,w)\exp\left(-\tfrac{M\omega}{2\hbar}\left(\textstyle\sum_{i=1}^{N}|z_i|^2+\sum_{j=1}^{M}|w_j|^2\right)\right)\\ \psi_b(z,w) &= G(z,w)\exp\left(-\tfrac{M\omega}{2\hbar}\left(\textstyle\sum_{i=1}^{N}|z_i|^2+\sum_{j=1}^{M}|w_j|^2\right)\right)\end{aligned} \tag{A.6.4}$$

Here F and G are the polynomial parts of the wave functions. We have

$$\langle\psi_a\,|\,\psi_b\rangle = \int_{\mathbb{C}^{N+M}} \overline{\psi_a(z,w)}\psi_b(z,w)\; dz_1\cdots dz_N dw_1\cdots dw_M \tag{A.6.5}$$

in configuration space, so inserting (A.6.4) results in the equation

$$\langle\psi_a\,|\,\psi_b\rangle = \int \overline{F(z,w)}G(z,w)\exp\left(-\frac{M\omega}{\hbar}\left(\sum_{i=1}^{N}|z_i|^2+\sum_{j=1}^{M}|w_j|^2\right)\right)\; d^{N+M}\mathbf{x} \tag{A.6.6}$$

where $d^{N+M}\mathbf{x} = dz_1\cdots dz_N\; dw_1\cdots dw_M$. Let

$$\{x\} = x_1,\ldots,x_N,x_{N+1},\ldots x_{N+M} = z_1,\ldots,z_N,w_1,\ldots,w_M \tag{A.6.7}$$

and $\{y\} = \{\overline{x}\}$. The product $\overline{F(z,w)}G(z,w)$ contains terms of the form

$$C(p_1,\ldots,p_{N+M})C(q_1,\ldots,q_{N+M})\prod_{i,j=1}^{N+M} y^{p_i}x^{q_i} \tag{A.6.8}$$

where $\sum_{i=1}^{N+M} p_i = \sum_{i=1}^{N+M} q_i = L$. That is, we will only be calculating overlaps of wave functions of the same angular momentum. The real numbers $C_F(p_1,\ldots,p_{N+M})$, $C_G(q_1,\ldots,q_{N+M})$ are the coefficients of the terms in $\overline{F(z,w)}$ and $G(z,w)$ respectively.

Consider the integral

$$I = \int_{\mathbb{C}} \overline{x}^n x^m \exp(-\frac{M\omega}{\hbar}|x|^2)\; dx \tag{A.6.9}$$

where $n,m\in\mathbb{Z}$. Changing to polar coordinates $x = re^{i\theta}$ gives

$$I = \int_0^{2\pi}\int_0^{\infty} r^{n+m}e^{i(m-n)\theta}e^{-M\omega r^2/\hbar}\; dr\; rd\theta \tag{A.6.10}$$

At once we see that the integral over θ gives a factor $2\pi\delta_{n,m}$ where $\delta_{n,m}$ is the Kronecker delta. The integral over r can be looked up or computed with successive integrations by parts. The result is

$$I = 2\pi\delta_{n,m}2^n n! \tag{A.6.11}$$

This tells us that only the terms (A.6.8) that satisfy $p_i = q_i$ survive the integration. That is, when the terms (A.6.8) are inserted into (A.6.6), the result is

$$\langle\psi_a\,|\,\psi_b\rangle = \sum_{\{p\}} C_F(\{p\})C_G(\{p\})(2\pi)^{N+M}2^L\prod_{i=1}^{N+M} p_i! \tag{A.6.12}$$

This is the desired formula for the inner product. The sum runs over all sets of powers $\{p\}$ in the polynomial F. Inserted into (A.6.3) we find

$$O = \frac{\sum_{\{p\}} C_F(\{p\}) C_G(\{p\}) \prod p_i!}{\sqrt{\sum_{\{p\}} C_F(\{p\})^2 \prod p_i! \sum_{\{q\}} C_G(\{q\})^2 \prod q_i!}} \tag{A.6.13}$$

which is the formula we sought. Notice that the factors $(2\pi)^{N+M}$ and 2^L were divided out in the fraction.

Using Mathematica to compute overlaps using (A.6.13) is now rather straightforward. We assume that the two polynomials $F(z,w)$ and $G(z,w)$ are stored in the variables `psi` and `phi`. The built-in Mathematica function `CoefficientList` returns a matrix of all coefficients in the argument, assumed to be a polynomial. The coefficient $C(p_1,\ldots,p_{N+M})$ as defined above is stored in the position $[[p_1+1, p_2+1, \ldots, p_{N+M}+1]]$. Note that this will result in a $(N+M)\times(N+M)$ matrix, and normally there will be very many elements that are zero. Working with sparse arrays therefore has advantages both when system memory and computation time is concerned. A function `f` produces the inner product coefficients $\prod p_i!$ The squared normalization factors are calculated for both wave functions, and finally the overlap is computed. Algorithm A.8 contains the code that was used.

A.7 Calculating interaction energy

This is really just a mixture of the code for overlap calculation and the code that models the interaction. We calculate the expected value of the interaction energy of a state ψ,

$$E = \langle \psi \,|\, V \,|\, \psi \rangle \tag{A.7.1}$$

by first normalizing the wave function. We store the coefficients in the variable `newpsilist`. Then we let the interaction, modeled as in the exact diagonalization code, act on the normalized state, store the resulting wave function in a variable `VPsi`, find its coefficients using `CoefficientList`, and finally we take the inner product with this and the normalized state, using the algorithm for the inner product developed above. The code is displayed in Algorithm A.9. In the displayed code we have added a variable `g` to the interaction model, needed for the calculations in Chapter 6. For homogeneous interaction this is set to 1 as discussed in that chapter.

A.8 Plotting energies

This last pieces of code take care of plotting energy spectra and overlaps together in nice figures. The code is split in two, visible in Algorithm A.10 and A.11. We describe them both here. First we choose what values of N and M to consider, and we import lists of energies generated from CF diagonalization of the interaction that are stored in text files in the working directory. The format of the data in the text files are

$$\{N, M, L, \text{energy}\} \tag{A.8.1}$$

separated by line shifts. As these files may contain data for complete pseudospin multiplets (all $M - N \geq 0$ for a given $N + M$), we first select only the ones matching out choice for

N, M. Then the energies of states "higher up" in the multiplet (larger values of $M - N$) gets taken into account, because these have the same energies as spin lowered states, which we want to include. The data are stored in lists called `CFplotlist[S]` where the number `S` is the spin quantum number $\mathcal{S}$ of the states in that list.

The code then repeats this procedure for the energies from the full diagonalization. These are stored in text files as well, with the same format as above. After importing the data, we proceed to remove center-of-mass excitations. In Chapter 3, we argued that states of the form

$$R^l \Psi_L(z, w) \tag{A.8.2}$$

has angular momentum $L + l$ and the same energy as Ψ_L. Naturally, such states will show up in the full diagonalization spectrum. The code removes these from the lists of data point by comparing any given energy at angular momentum L with all the energies at higher angular momenta $L + l$, $l > 0$.

Finally, we create scatter plots for exact and simple CF state energies, and show them in the same figure. This code was used for the energy diagrams in Chapters 3 and 5. In Chapter 5, we add lines of code that sets up plot markers of different colors corresponding to different spin quantum numbers, and to plot a legend inset describing the colors. We have included the lines of code that accomplishes this in Algorithm A.11. It also reads overlaps between CF candidates and exact ground states from lists and presents these as text in the figures. The overlaps are stored in two lists, `overlaplist.txt` and `remaining-overlaps.txt` containing overlaps of Fock states and pseudospin lowered states respectively.

A.9 Pieces of code

Algorithm A.1 Parameters and variables for CF

```
Clear["Global`*"]
SetDirectory[NotebookDirectory[]];

(* Slater determinants exponent notation *)
expolist1 = {0, 2, 4, 6};
expolist2 = {0, 2, 4, 6};

Nn = Length[expolist1];
M = Length[expolist2];
tot = Nn + M;
L = 1/2*tot*(tot - 1) - Total[expolist1] - Total[expolist2];
n = Min[L, Nn]; (* Ground state parameter in PRK (10) *)

(* Lists of coordinates *)
zcoor = {}; Do[AppendTo[zcoor, Subscript[z, i]], {i, Nn}];
wcoor = {}; Do[AppendTo[wcoor, Subscript[w, i]], {i, M}];
coor = Flatten[{zcoor, wcoor}];
R = Sum[coor[[i]], {i, tot}]/tot; (* Center of mass *)
zred = zcoor - R;
wred = wcoor - R;
SP[k_, vars_] := SymmetricPolynomial[k, vars]
```

Algorithm A.2 Papenbrock-Reimann-Kavoulakis wave functions

```
(* Compute the beta coefficients *)
epsilon = (Nn + M)(L - n) + n(n - 1); (* Eigenvalue parameter *)
lambdapoly[l_] :=
    (L*M + l(2L + Nn - M - 2l) - epsilon)*Sum[B[k]*l^k, {k, 0, n}]
    + (Nn - l)(L - l)*Sum[B[k]*(l + 1)^k, {k, 0, n}]
    + l(M - L + l)*Sum[B[k]*(l - 1)^k, {k, 0, n}]; (* Recurrence relation *)

Blist = Array[B[# - 1] &, n]; (* List of beta coefficients, not including B[n] *)

(* Gather up the equations needed to find the B[k] in terms of B[n]*)
equationlist = {};
Module[{i, l},
    For[i = n - 1, i >= 0, i--,
        If[i != 0,
            AppendTo[equationlist, Coefficient[lambdapoly[l], l^i] == 0],
            AppendTo[equationlist, CoefficientList[lambdapoly[l], l][[1]] == 0]
        ]
    ]
];

rules = Solve[equationlist, Blist];
AppendTo[Blist, B[n]]; Blist = Blist /. Flatten[rules];

(* Choose a normalisation so that we only get integer betas *)
Blist = Blist /. B[n] -> LCM[##] & @@ Denominator[Blist];

(* Compute the Papenbrock wave function *)
coff[l_] :=
    If[l != 0,
        Sum[Blist[[k + 1]]*l^k, {k, 0, n}],
        Blist[[1]]
    ];

If[L <= M,
    phi = Sum[coff[l]*SymmetricPolynomial[l, zred]
        *SymmetricPolynomial[L - l, wred], {l, 0, n}]
];
```

Algorithm A.3 Exact diagonalization of the interaction.

```
(* Interaction model *)
A[z_,m_,psi_] :=
  Sum[
    If[j > i,
      (z[[i]] - z[[j]])^m * Sum[
        Binomial[m, k] * (-1)^k * D[psi,{z[[i]],m - k},{z[[j]], k}],
        {k, 0, m}
        ],
      0
    ], {i, 1, Nn - 1}, {j, 2, Nn}
  ]; (* Papenbrock et al (4) *)

B[w_,m_,psi_] :=
  Sum[
    If[j > i,
      (w[[i]] - w[[j]])^m * Sum[
        Binomial[m, k] * (-1)^k * D[psi,{w[[i]],m - k},{w[[j]], k}],
        {k, 0, m}
        ],
      0
    ], {i, 1, M - 1}, {j, 2, M}
  ]; (* Papenbrock et al (5) *)

Cc[z_,w_,m_,psi_] :=
  Sum[
    (z[[i]] - w[[j]])^m * Sum[
      Binomial[m, k] * (-1)^k * D[psi,{z[[i]],m - k},{w[[j]], k}],
      {k, 0, m}
    ], {i, 1, Nn}, {j, 1, M}
  ]; (* Papenbrock et al (6) *)

v[m_] := (-1/2)^m/(m!);
vPsi[z_, w_, psi_] :=
  Sum[v[m]*(A[z, m, psi] + B[w, m, psi] + Cc[z, w, m, psi]), {m, 0, L + 1}];

(* Create a Hilbert space basis *)
basis = {};
Do[iparts = IntegerPartitions[I]; jparts = IntegerPartitions[L - I];
  Do[If[(Max[iparts[[i]]] <= Nn) && (Max[jparts[[j]]] <= M),
    AppendTo[basis,
      Product[SP[ii, zcoor], {ii, iparts[[i]]}] *
      Product[SP[jj, wcoor], {jj, jparts[[j]]}]
    ]
  ], {i, Length[iparts]}, {j, Length[jparts]}
], {I, 0, L}];

sortbasis = Union[basis];
dim = Length[sortbasis];

(* Create the interaction matrix *)
Velem = {};
Do[AppendTo[Velem,
  PolynomialReduce[vPsi[zcoor, wcoor, sortbasis[[i]]], sortbasis, coor][[1]]
  ], {i, dim}
];
Vmat = Transpose[Velem];
{energies, states} = Eigensystem[N[Vmat]];
phi=states[[-1]].sortbasis;

(* Export[StringInsert[ToString[100*Nn+10*M+L],"-energies.txt",-1],energies]; *)
(* Export[StringInsert[ToString[100*Nn+10*M+L],"-states.txt",-1],states]; *)
(* Export[StringInsert[ToString[100*Nn+10*M+L],"-basis.txt",-1],sortbasis]; *)
```

Algorithm A.4 Simple Fock states.

```
(* Degree of Slater determinants *)
Ls = 1/2*tot*(tot - 1) - L;

vars = Array[If[# <= Nn, a[#], b[# - Nn]] &, tot];
iterators = Flatten[
   {Array[If[# == 1,
      {vars[[#]], 0, tot - 1},
      {vars[[#]], vars[[# - 1]] + 1, tot - 1}] &, Nn
      ],
    Array[If[# == Nn + 1,
      {vars[[#]], 0, tot - 1},
      {vars[[#]], vars[[# - 1]] + 1, tot - 1}] &, M, Nn + 1]
   },
1];

focklist = {};
Do[
   If[
      DeleteDuplicates[vars[[;; Nn]]] == vars[[;; Nn]] &&
      DeleteDuplicates[vars[[Nn + 1 ;;]]] == vars[[Nn + 1 ;;]] &&
      Total[vars] == Ls &&
      (And[##] & @@ Array[MemberQ[vars[[Nn + 1 ;;]], a[#]] &, Nn]),
      AppendTo[focklist, {vars[[;; Nn]], vars[[Nn + 1 ;;]]}]
   ], ##
] & @@ iterators;
```

Algorithm A.5 All compact Fock states.

```
(* Degree of Slater determinants *)
Ls = L - 1/2*tot*(tot - 1);

iterators = Array[If[# == 1,
   {n[#], 0, tot - 2},
   {n[#], n[# - 1], tot - 2}] &, Nn
];
additerators = Array[If[# == Nn + 1,
   {nn[#], 0, tot - 1},
   {nn[#], nn[# - 1], tot - 1}] &, M - Nn, Nn + 1
];

focklist = {};
Do[
   zpropose = {{n[1], -n[1]}};
   maxm = -n[1];
   Do[
      m[i] = -n[i] + Count[Array[n[#] &, i - 1], n[i]];
      If[n[i] == 0 || maxm >= m[i],
         AppendTo[zpropose, {n[i], m[i]}];
         If[m[i] > maxm, maxm = m[i];];
      ], {i, 2, Nn}
   ];
   wpropose = zpropose;
   Do[nn[i] = n[i], {i, Nn}];
   Do[
      m[i] = -nn[i] + Count[Array[nn[#] &, i - 1], nn[i]];
      If[nn[i] == 0 || maxm >= m[i],
         AppendTo[wpropose, {nn[i], m[i]}];
         If[m[i] > maxm, maxm = m[i];];
      ], {i, Nn + 1, M}
   ];
   If[
      Length[zpropose] == Nn &&
      Length[wpropose] == M &&
      Total[Map[Last, Flatten[{zpropose, wpropose}, 1]]] == Ls &&
      (And[##] & @@ Array[
         Length[Cases[Map[First, Flatten[{zpropose, wpropose}, 1]],
         x_ /; x >= tot - #]] <= # &, tot
      ]),
      AppendTo[focklist, {zpropose, wpropose}];
   ], ##
] & @@ Flatten[{iterators, additerators}, 1];
```

Algorithm A.6 Computing the CF wave functions, part 1

```
jastrow = 1;
Do[
   If[Unequal[i, j] && i < j,
      jastrow *= (coor[[i]] - coor[[j]])
   ], {i, 1, tot}, {j, 1, tot}
];

derop[a_, n_] := D[#, {a, n}] &;
timesop[a_, n_] := Times[a^n, #] &;
MakeSlater[x_, explist_] :=
   Module[{slat, l, n, m},
      slat = {};
      l = Length[explist];
      Do[
         {n, m} = explist[[i]];
         AppendTo[slat,
          Array[Composition[timesop[x[[#]], n + m], derop[x[[#]], n]] &, l]
         ], {i, 1, l}
      ];
   Return[slat]
];

zperms = Permutations[zcoor];
wperms = Permutations[wcoor];

zpermrules = {};
Do[
   AppendTo[zpermrules,
    {Array[zcoor[[#]] -> a[#] &, Nn],
     Array[zperms[[i, #]] -> zcoor[[#]] &, Nn],
     Array[a[#] -> zperms[[i, #]] &, Nn]
    }
   ], {i, Length[zperms]}
]

wpermrules = {};
Do[
   AppendTo[wpermrules,
    {Array[wcoor[[#]] -> b[#] &, M],
     Array[wperms[[i, #]] -> wcoor[[#]] &, M],
     Array[b[#] -> wperms[[i, #]] &, M]
    }
   ], {i, Length[wperms]}
]
```

Algorithm A.7 Computing the CF wave function, part 2

```
makeCF[expolist1_, expolist2_] := (
slat1 = MakeSlater[zcoor, expolist1];
slat2 = MakeSlater[wcoor, expolist2];

(* The next lines expands the Slater determinants *)
(* and makes a representative operator called compdet *)
Siglist1 = LeviCivitaTensor[Nn];
Siglist2 = LeviCivitaTensor[M];
Looplist1 = Drop[Map[First, ArrayRules[Siglist1]], -1];
Looplist2 = Drop[Map[First, ArrayRules[Siglist2]], -1];

ii = Looplist1[[1]];
detlist1 = Array[slat1[[#, ii[[#]]]] &, Nn];

jj = Looplist2[[1]];
detlist2 = Array[slat2[[#, jj[[#]]]] &, M];

compdet = Composition[##] & @@ Flatten[{detlist1, detlist2}];

psibase = Expand[compdet @ jastrow];

(* Add up all permutations of variables corresponding to *)
(* different operators from expanded Slater terms *)
psi = Sum[
   Fold[#1 /. #2 &,
      Fold[#1 /. #2 &,
         psibase, Array[zpermrules[[i, #]] &, 3]
      ], Array[wpermrules[[j, #]] &, 3
   ]
   ], {i, Length[zperms]}, {j, Length[wperms]}
];

(* Divide out any overall numerical factor *)
If[
   ! IntegerQ[psi],
   psi = psi/First[FactorTerms[psi]];
];

Return[Expand[psi]]
)
```

Algorithm A.8 Calculating the overlap between two wave functions.

```
dimlist = ConstantArray[tot, tot];
psilist = SparseArray[CoefficientList[psi, coor], dimlist];

(* List of positions of non-zero coefficients *)
psiposlist = Drop[Map[First, ArrayRules[psilist]], -1];

(* f constructs inner product coefficients *)
f[l_] := Module[{i, y},
   For[i = 1; y = 1, i <= Length[l], i++, y = y*(l[[i]] - 1)!];
   Return[y]
];

(* psifactlist contains necessary inner product coefficients
for psi *)
psifactlist = SparseArray[psiposlist -> Map[f, psiposlist, 2], dimlist];

(* psinorm is the squared normalization factor for psi *)
(* equal to the inner product of psi with itself *)
psinorm = Total[Drop[Map[Last, ArrayRules[psilist*psilist*psifactlist]], -1]];

philist = SparseArray[CoefficientList[phi, coor], dimlist];
phiposlist = Drop[Map[First, ArrayRules[philist]], -1];
phifactlist = SparseArray[phiposlist -> Map[f, phiposlist, 2], dimlist];
phinorm = Total[Drop[Map[Last, ArrayRules[philist*philist*phifactlist]], -1]];

If[psinorm == 0,
    overlap = 0,
    overlap = N[Total[Drop[Map[Last,
        ArrayRules[psilist*philist*phifactlist]], -1]]/Sqrt[phinorm*psinorm]
    ]
]
```

Algorithm A.9 Calculating the interaction energy expectation value for a state.

```
(* Interaction model *)
A[z_,m_,psi_] :=
   Sum[
      If[j > i,
         (z[[i]] - z[[j]])^m * Sum[
            Binomial[m, k] * (-1)^k * D[psi,{z[[i]],m - k},{z[[j]], k}],
            {k, 0, m}
            ],
         0
      ], {i, 1, Nn - 1}, {j, 2, Nn}
   ]; (* Papenbrock et al (4) *)

B[w_,m_,psi_] :=
   Sum[
      If[j > i,
         (w[[i]] - w[[j]])^m * Sum[
            Binomial[m, k] * (-1)^k * D[psi,{w[[i]],m - k},{w[[j]], k}],
            {k, 0, m}
            ],
         0
      ], {i, 1, M - 1}, {j, 2, M}
   ]; (* Papenbrock et al (5) *)

Cc[z_,w_,m_,psi_] :=
   Sum[
      (z[[i]] - w[[j]])^m * Sum[
         Binomial[m, k] * (-1)^k * D[psi,{z[[i]],m - k},{w[[j]], k}],
         {k, 0, m}
      ], {i, 1, Nn}, {j, 1, M}
   ]; (* Papenbrock et al (6) *)

v[m_] := (-1/2)^m/(m!);
vPsi[z_, w_, psi_] :=
   Sum[v[m]*(A[z, m, psi] + B[w, m, psi] + g * Cc[z, w, m, psi]), {m, 0, L + 1}];

(* Calculate interaction energy *)
psi = psi/Sqrt[psinorm];
newpsilist = SparseArray[CoefficientList[ psi, coor], dimlist];
VPsi = vPsi[zcoor, wcoor, psi];
VPsilist = SparseArray[CoefficientList[ VPsi, coor], dimlist];

energy = N[Total[Drop[Map[Last, ArrayRules[newpsilist*VPsilist*psifactlist]], -1]]]
```

Algorithm A.10 Plotting energy spectra, part 1.

```
SetDirectory[NotebookDirectory[]]

(* CF energies and overlaps *)
energylist = ReadList["CFenergylist.txt"];
overlaps = Map[Last, ReadList["overlaplist.txt"]];

Nn = 4; M = 4; tot = Nn + M;

thismultiplet = Cases[energylist, {Nn, M, _, _}];
theseoverlaps =
   Flatten[Map[overlaps[[#]] &, Position[energylist, {Nn, M, _, _}]], 1];
Do[CFplotlist[i] = {}, {i, (M - Nn)/2, tot/2}] (* Indices in brackets are spin *)
CFplotlist[(M - Nn)/2] = Map[#[[3 ;; 4]] &, thismultiplet];

Do[{a, b, c, d} = energylist[[i]];
   If[b > M,
      AppendTo[CFplotlist[(b - a)/2, {c, d}]
   ], {i, Length[energylist]}
]

overlapplotlist =
   Array[{thismultiplet[[#, 3]], theseoverlaps[[#]]} &, Length[theseoverlaps]];
remoplist = ReadList["remaining-overlaps.txt"];
thisremoplist = Cases[remoplist, {Nn, M, _, _}];
overlapplotlist =
   Sort[Flatten[{overlapplotlist, Map[#[[3 ;; 4]] &, thisremoplist]}, 1]];

(* Energies from exact diagonalization *)
f = FileNames[ToString[Nn] <> ToString[M] <> "*-energies.txt"];
Do[en[i] = ReadList[f[[i + 1]]], {i, 0, tot}];

(* Remove center-of-mass excitations from the plot *)
Do[
   If[
      Count[Chop[en[j] - en[i][[k]]], 0] >= Count[en[i], en[i][[k]]],
      en[j] = Delete[en[j], Position[Chop[en[j] - en[i][[k]]], 0][[1, 1]]]
   ], {i, 0, tot}, {j, i + 1, tot}, {k, Length[en[i]]}
]
Do[
   list[i] = {};
   Do[
      AppendTo[list[i], {i, en[i][[j]]}]
   , {j, Length[en[i]]}
   ], {i, 0, tot}
]
enplotlist = Flatten[Array[list[#] & , tot + 1, 0], 1];
```

Algorithm A.11 Plotting energy spectra, part 2.

```
totplotlist = {enplotlist};
Do[
   AppendTo[totplotlist, CFplotlist[i]]
   , {i, (M - Nn)/2, tot/2}
]
spinplotmarkers = {
  {Graphics[{Red, Thickness[Medium], Circle[]}], 0.03},
  {Graphics[{Black, Thickness[Medium], Circle[]}], 0.03},
  {Graphics[{Orange, Thickness[Medium], Circle[]}], 0.03},
  {Graphics[{Green, Thickness[Medium], Circle[]}], 0.03},
  {Graphics[{Magenta, Thickness[Medium], Circle[]}], 0.03}
};

(* Make plot of energies. Colored CF markers are defined above, the exact *)
(* energies are given blue dot markers in the line below *)
plot1 =
   ListPlot[totplotlist,
      PlotMarkers -> Flatten[
         {{{Graphics[{Blue, Disk[]}], 0.015}}, spinplotmarkers[[1 + (M - Nn)/2 ;;]]}
      , 1],
      PlotRange -> {{-0.5, tot + 1}, {0, Max[en[0]] + 0.1*Max[en[0]]}},
      Frame -> True, FrameLabel -> {"L", "Interaction energy"},
      PlotLabel -> "N=" <> ToString[Nn] <> ", M=" <> ToString[M],
      Axes -> False
   ];

overlaplabels =
   Array[Graphics[Text[
      ToString[
         SetPrecision[Last[overlapplotlist[[#]]], 3]
      ],
      {overlapplotlist[[#, 1]],
       Min[Map[Last, Cases[enplotlist, {overlapplotlist[[#, 1]], _}]]] - 1
      }
      ]] &, Length[overlapplotlist]
   ];

spinlegend = {
   Graphics[Text["Pseudospin S", {2, 9}]],
   Array[Graphics[Text[ToString[#], {#, 7}]] &, 5, 0],
   ListPlot[Array[{{#, 5}} &, 5, 0], PlotMarkers -> spinplotmarkers]
};

legendbox = {Graphics[{
   Thin,
   Line[{{-0.25, 3}, {-0.25, 10}, {4.5, 10}, {4.5, 3}, {-0.25, 3}}]
}]};

Show[plot1, overlaplabels, spinlegend, legendbox]
```

Bibliography

[1] S. Viefers, *Quantum Hall physics in rotating Bose-Einstein condensates*, J. Phys.: Condens. Matter **20** (2008)

[2] A. L. Fetter & C. J. Foot, *Bose gas: Theory and Experiment*, Preprint **arXiv:1203.3183 [cond.mat-quant.gas]** (2012)

[3] N. R. Cooper & N. K. Wilkin, *A Composite Fermion Description of Rotating Bose-Einstein Condensates*, Phys. Rev. B **60**, R16279 (1999)

[4] K. Kasamatsu, M. Tsubota & M. Ueda *Vortices in multicomponent Bose-Einstein condensates*, Int. J. Mod. Phys. B **19**, 1835 (2005)

[5] M. R. Matthews, B. P. Anderson, P. C. Haljan, D. S. Hall, C. E. Wiemann & E. A. Cornell, *Vortices in a Bose-Einstein Condensate*, Phys. Rev. Lett. **83**, 2498-2501 (1999)

[6] J. Christensson, S. Bargi, K. Kärkkäinen, Y. Yu, G. M. Kavoulakis, M. Manninen & S. M. Reimann, *Rotational properties of a mixture of two Bose gases*, New J. Phys. **10**, 033029 (2008)

[7] M. H. Anderson, J. R. Ensher, M. R. Matthews, C. E. Wiemann & E. A. Cornell, *Observation of Bose-Einstein Condensation in a Dilute Atomic Vapor*, Science **269**, 198-201 (1995)

[8] T. Papenbrock, S. M. Reimann & G. M. Kavoulakis, *Condensates of p-Wave Pairs Are Exact Solutions for Rotating Two-Component Bose Gases*, Phys. Rev. Lett. **108**, 075305 (2012)

[9] J. K. Jain, *Composite Fermions,* Cambridge: Cambridge University Press (2007)

[10] J. K. Jain, *The Composite Fermion: A Quantum Particle And Its Quantum Fluids*, Phys. Today **53**, 39-45 (2000)

[11] S. Viefers, T. H. Hansson & S. M. Reimann, *Bose condensates at high angular momenta*, Phys. Rev. A **62**, 053604 (2000)

[12] M. N. Korslund & S. Viefers, *Composite-fermion description of rotating Bose gases at low angular momenta*, Phys. Rev. A **73** 063602 (2006)

[13] S. Viefers & M. Taillefumier, *Asymptotically exact trial wave functions for yrast states of rotating Bose gases*, J. Phys. B: At. Mol. Opt. Phys. **43**, 155302 (2010)

[14] N. Regnault, C. C. Chang, Th. Jolicoeur & J. K. Jain, *Composite fermion theory of rapidly rotating two-dimensional bosons*, J. Phys. B: At. Mol. Opt. Phys. **39** 89-99 (2006)

[15] J. M. Leinaas & J. Myrheim, *On the Theory of Identical Particles*, Il Nuovo Cimento B **37** 1-23 (1977)

[16] J. P. Sethna, *Entropy, Order Parameters, and Complexity*, Oxford: Oxford University Press (2006)

[17] C. J. Pethick & H. Smith, *Bose-Einstein Condensation in Dilute Gases*, Cambridge: Cambridge University Press (2008)

[18] T. Papenbrock, S. M. Reimann & G. M. Kavoulakis, *Universal analytical solutions for mixtures of rotating Bose-Einstein condensates*, version 1 of [8], **arXiv:1107.4517v1 [cond.mat-quant.gas]** (2011)

[19] T. Papenbrock & G. F. Bertsch, *Exact solutions for interacting boson systems under rotation*, J. Phys. A **34** (2001)

[20] N. Gemelke, E. Sarajlic & S. Chu, *Rotating Few-body Atomic Systems in the Fractional Quantum Hall Regime*, Preprint **arXiv:1007.2677 [cond.mat-quant.gas]** (2010)

[21] S. A. Trugman & S. Kivelson, *Exact results for the fractional quantum Hall effect with general interaction*, Phys. Rev. B **31** (1985)

[22] S. Bargi, J. Christensson, G. M. Kavoulakis & S. M. Reimann, *Mixtures of Bose gases under rotation*, Phys. Rev. Lett. **98** 130403 (2007)

[23] T. Ando, Y. Matsumoto & Y. Uemura, *Theory of Hall Effect in a Two-Dimensional Electron System*, J. Phys. Soc. Jpn. **39** 279-288 (1975)

[24] K. v. Klitzing, G. Dorda & M. Pepper, *New Method for High-Accuracy Determination of the Fine-Structure Constant Based on Quantized Hall Resistance*, Phys. Rev. Lett. **45** 494-497 (1980)

[25] D. C. Tsui, H. L. Stormer & A. C. Gossard, *Two-Dimensional Magnetotransport in the Extreme Quantum Limit*, Phys. Rev. Lett. **48** 1559-1562 (1982)

[26] R. B. Laughlin, *Anomalous Quantum Hall effect: An Incompressible Quantum Fluid with Fractionally Charges Excitations*, Phys. Rev. Lett. **50**1395-1398 (1983)

[27] S. Börm & C. Mehl, *Numerical Methods for Eigenvalue Problems*, Berlin: Walter de Gruyter (2012)

[28] S. Furukawa & M. Ueda, *Quantum Hall states in rapidly rotating two-component Bose gases*, Phys. Rev. A **86** 031604(R) (2012)

[29] Y. Wu & J. K. Jain, *Quantum Hall Effect of Two-Component Bosons at Fractional and Integral Fillings*, Preprint **arXiv:1304.7553 [cond.mat-str.el]** (2013)